Macroscopic Equations for Flow in Unsaturated Porous Media

Marc Rene Hoffmann

Macroscopic Equations for Flow in Unsaturated Porous Media

Abstract

Hoffmann, M.R., 2003. *Macroscopic Equations for Flow in Unsaturated Porous Media*. Dissertation, Wageningen University, The Netherlands.

This dissertation describes averaging of microscale flow equations to obtain a consistent description of liquid flow in unsaturated porous media on the macroscale. It introduces a new method of averaging the pressure term and a unit cell model capable of describing unsaturated flow.

Starting from the description of liquid flow through individual pores, a macroscopic equation for flow of a liquid in a porous medium in the presence of a gas is derived. The flow is directly influenced by phase interfaces, i.e. solid-liquid or gas-liquid. By including these pore scale phenomena in a continuum description of fluid transport in porous media, equations for liquid flow on the macroscale are obtained.

The unit cell model is based on a simplified geometric representation of a porous medium. It allows for the modeling of the important characteristics of a porous medium for unsaturated flow.

Through the use of volume averaging and direct integration macroscale momentum and mass balance equations are derived from the microscale momentum and mass balance equations, resulting in a novel form of the macroscale pressure term. The macroscale flow of liquids in unsaturated porous media can be written proportional to a driving force, which is proportional to the difference of the inverse area averaged liquid pressures across an averaging volume. In principle the flow is driven by gradients in liquid pressure, but due to the nonlinear coupling between capillary forces and liquid pressure the driving force becomes nonlinear.

Two dynamic terms were derived by simplifying the flow dynamics in a porous medium. They remain to be tested quantitatively and still have considerable uncertainty concerning their exact form and/or magnitude.

Comparison of the newly proposed macroscale equations with the Buckingham-Darcy equation shows that, using reasonable assumptions, the newly proposed macroscale equations can be written in a form similar to the Buckingham-Darcy equation. The newly proposed macroscale equations are compared to an experiment and satisfactory agreement between experiment and calculations was observed.

keywords: momentum balance, nonlocal equations, porous media, upscaling, unsaturated flow, volume averaging.

Contents

Nomenclature

symbol	description
a	fraction characterising pore opening (–)
A	area (m^2)
$\mathcal{A}$	area in pore (corner) occupied by fluid (m^2)
$A(h)$	adsorptive component in AYL (eq. (2.19)) (m^2/s^2)
$\mathcal{A}_c$	liquid area in corner, perpendicular to flow (m^2)
A_p	pore area normal to flow (m^2)
A_{svl}	Hamacker constant, for quartz sand $-1.9 * 10^{-19}$ (J)
b	factor characterising if pore is open (2), or closed (1) (–)
Bo	Bond number, (eq. (2.11)) (–)
$c_{1,2,3,4}$	factors defined by equations (5.46), (5.47), (5.48), (5.49) (–)
C	factor depending on x, curvature (1/m); positive for an interface concave outward from the liquid
Ca	Capillary number, (eq. (2.37)) (–)
C_c	capillary component in eq. (2.19) (m^2/s^2)
d	microscopic characteristic length (RUC) (m)
f	Fanning friction factor for fully developed flow (–)
f	function describing geometric components, (eq. (4.40)) (–)
f	function $f(x,t)$ in eq. (3.12)
F	conductance factor (–)
F_v	conductance factor two-phase flow 1.7 (–)
g	gravity acceleration (m/s^2)
G	Gibbs partial specific free energy (J)
h	hydraulic head, film thickness in AYL equation (m)
H	slit spacing, characteristic height of liquid in corner (m)
i	index number (–)
j	number of corners in RUC (–)
k_D	saturated hydraulic conductivity (m/s)
k_r	relative hydraulic conductivity (–)
Kn	Knudsen number (–)

1

symbol	description
l_g	flow length in RUC (m)
l_p	penetration length in Lucas-Washburn equation (eq. (2.4)) (m)
L	characteristic length (m)
$\mathcal{L}$	length (m)
n_l	liquid saturation (–)
$\mathbf{N}$	macroscopic unit vector (–)
N_l	characteristic liquid saturation (–)
p	pressure (kg/ms^2)
p_c	capillary pressure (kg/ms^2)
p_{lc}	critical pressure drainage for liquid (kg/ms^2)
P	generic Pressure (kg/ms^2)
$\mathcal{P}$	wetted perimeter (m)
$\mathbf{q}$	volumetric flow rate (m^3/s)
r	radius of curvature of gas-liquid interface (m)
r_c	critical radius of curvature of gas-liquid interface during drainage (m)
r_h	hydraulic radius (m)
r_i	critical radius of curvature of gas-liquid interface during imhibition (m)
R_1, R_2	principal radii of curved surface (m)
Re	Reynolds number (–)
$\mathcal{S}$	surface (m^2)
$\mathbf{s}$	unit vector tangent to surface (–)
S	saturation (m^3/m^3)
t	time (s)
T	characteristic time (s)
U	characteristic velocity (m/s)
$\mathbf{v}$	velocity (m/s)
v	velocity (m/s)
$\mathcal{V}_l$	volume of liquid in averaging volume (m^3)
$\mathcal{V}_p$	volume of pores in averaging volume (m^3)
$\mathcal{V}_s$	volume of solid in averaging volume (m^3)
$\mathcal{V}_0$	volume of averaging volume (m^3)
$\mathbf{w}$	velocity of surface (m/s)
x, y, z	space coordinates (m)
α	half opening angle of corner (rad)
γ	surface (interfacial) tension at interface (kg/s^2)
ϵ	porosity (m^3/m^3), V_p/V_0

symbol	description
θ	contact angle liquid - solid (rad)
μ	dynamic viscosity (kg/ms)
$\boldsymbol{\nu}$	unit normal vector on $\mathcal{S}$ (–)
ρ	density (kg/m^3)
τ	proportionality factor in dynamic term (kg/ms)
$\tau_{\mathcal{S}_{sl}}$	cross-sectional average wall shear stress (kg/ms^2)
$\boldsymbol{\Psi}$	generalized variable
$\langle\ \rangle$	average of quantity over volume of RUC, except when superscript given
$(\ \dot{\ }\ )$	deviation from mean
$\vert\ \vert$	magnitude
subscripts:	
0	boundary of RUC (averaged quantity, entrance)
1	boundary of RUC (averaged quantity, exit)
D	as subscript for specific discharge, also "Darcy" velocity
a	air
c	mean inside corner
d	dynamic
f	fluid (gas or liquid)
g	gas
l	liquid
m	mean
p	mean inside pore
s	solid, static
tot	total
w	water

Vector notation follows Bird et al. (1960).

1   Introduction

This dissertation describes averaging of the microscale flow equations to obtain a consistent description of liquid flow in unsaturated porous media on the macroscale. It introduces a new method of averaging the pressure term and a unit cell model capable of describing unsaturated flow.

1.1   What is it about?

This dissertation is about unsaturated flow in porous media. More specifically it is about mathematical modeling of two-phase flow through rigid porous media. The two phases considered are a wetting liquid and a gas. In practice one can think of a sandy soil partially saturated with water, partially with air. Strictly speaking, the flow of the liquid phase is treated as single-phase flow in the presence of an inviscid gas phase. However, the gas phase directly influences the liquid flow through surface forces and the resulting flow is called two-phase flow or unsaturated flow in this dissertation.

Starting from the description of fluid flow through individual pores, an equation for flow of a liquid in a porous medium in the presence of a gas is derived. This flow is directly influenced by phase interfaces e.g. solid-liquid or gas-liquid. By explicitly including these pore scale phenomena in a continuum description of fluid transport in porous media, a consistent theoretical description of fluid flow on the macroscale is obtained.

1.2   Problem Description

Groundwater flow, flow in lungs, flow inside the catalytic converter of a car and wind blowing through a forest are all examples of flow in porous media.

Examples where two-phase flow plays an important role are drainage and irrigation of agricultural lands, groundwater pollution, nuclear waste storage, oil and gas winning, and the drying of food materials.

Current equations describing fluid transport in porous media are based on (semi)empirical equations derived in the 19th century (Darcy, 1856) for single-phase flow and in the 20th century for multi-phase flow (Buckingham, 1907; Washburn, 1921; Richards, 1931; Buckley and Leverett, 1942). The current standard equations used in soil physics are called the Buckingham-Darcy equation and Richards equation. These equations try to describe the "average" behavior of a mixture of a porous medium and one or more fluids. They have since then been put on a firm basis by theoretical investigations of Hubbert (1956), Anderson and Jackson (1967), Whitaker (1966, 1969), Slattery (1967, 1969), and Gray and Hassanizadeh (1991a). The theoretical work by Whitaker (1977) confirmed the general nature of Richards equation, if considerable assumptions are made. Theoretical work of Gray and Hassanizadeh (1991a), and experimental work of Alemán et al. (1989) and Grant and Salehzadeh (1996) showed that there is still a considerable gap between the theory and experiments, and Richards equation. The main problems lie in the nature of the average capillary or liquid pressure and the interplay between the parameterization of constitutive relations and the average liquid pressure. These difficulties are in part due to the averaged nature of Richards equation. Averaging smoothes discontinuities, leading to smoothed macroscale equations. Another difficulty arises when Richards equation is applied in practice. In order to find a solution, constitutive relations are needed between water content and pressure head, and relative hydraulic conductivity and water content. At very low water contents, often unrealistic solutions are obtained due to the form of the constitutive relations used (Fuentes et al., 1992). Due to the nonlinear character of Richard's equation only a limited number of analytical solutions are known. Usually one resorts to numerical solution techniques, which normally involve discretisation and integration. In mathematical terms Richards equation is a partial differential equation that is defined with local point support, but in physical terms Richards equation is seen as a description on the cm scale. These interpretations somewhat conflict when discretisation is applied (Nitsche and Brenner, 1989, p. 240). This is due to the fact that when discretisation is applied, always interpolation is needed. In practice this interpolation is different from the assumptions made in deriving Richards equation. For example the constitutive relations commonly used are based on the assumption of gradient independence.

At the end of the last millennium Gray and Hassanizadeh (1991a), and Has-

sanizadeh and Gray (1997, 1993) proposed more general, theoretically obtained equations to describe multi-phase flow in porous media. These equations were derived by volume averaging and thermodynamics. Volume averaging has been used in the last decennia, mostly for single-phase flow in porous media, although examples of multi-phase flow are described in Bear and Bensabat (1989) and Hassanizadeh and Gray (1997). Despite enormous theoretical developments, practical applications of volume averaging have been limited due to the so called closure problem. A closure problem, or closure, refers to a step in volume averaging where terms containing microscale variables are expressed in terms containing macroscale variables. Different possibilities exist to solve this closure problem: numerical methods (Quintard and Whitaker, 1990), approximations based on empirical equations (Whitaker, 1980) and analytical solutions for Representative Unit Cells (RUC's) (du Plessis and Masliyah, 1988; du Plessis and Diedericks, 1997). The difficulty in applying the volume averaging theory lies in the development of a practical solvable closure problem.

Volume averaging starts with a description of fluid flow on the pore or microscale. Through the averaging process we replace the microscale variables by macroscale variables, for example we change from the description of the actual liquid configuration in pore to the average liquid content on the macroscale. The term scale refers to a "typical" measurement scale. A spatial scale is a representative length unit through which we want to describe flow. The magnitude is usually the diameter of an averaging volume. On the microscale or pore-scale this would be tenth of mm, on the macroscale or continuum scale cm's. It is also possible that the term scale refers to a typical time unit which captures the characteristics of the flow.

1.3 Relevance

Flow in porous media is difficult to be accurately modeled quantitatively. Richards equation can give good results, but needs constitutive relations. These are usually empirically based and require extensive calibration (van Genuchten, 1980; Pullan, 1990). The parameters needed in the calibration are amongst others: capillary pressure and pressure gradient, volumetric flow, liquid content, irreducible liquid content, and temperature (Bachmann et al., 2002). In practice it is usually too demanding to measure all these parameters.

In the model introduced in this dissertation no constitutive relations per se are used, but a description of flow in terms of physical parameters of the porous

medium and the fluids. These parameters are amongst others: viscosity, porosity, and interfacial tensions. The concept of a Representative Unit Cell (RUC) implicitly replaces part of the constitutive relations, because it defines the geometry of the pore space. The newly derived mathematical model can be used in drainage modeling and in the following applications where the Buckingham-Darcy or Richards equation are not directly applicable, e.g. gravity free flow of fluids in porous media in space for plant growth (Scovazzo et al., 2001), (inverse) determination of structural porous media properties from fluid flow measurements (Montillet et al., 1992; Roberts and Knackstedt, 1996). Note that these properties depend on the specific porous medium model chosen.

In their present form the newly derived equations are not suited for infiltration models, for the description of fingering flow, for flow of non-Newtonian fluids, and for flow with drag along the fluid-fluid interfaces. The model can be extended to include additional processes like vapor diffusion, heat transport, and electrical conductivity, by directly averaging these processes with the aid of the RUC approach.

1.4   Objectives and Approach

The objective of this dissertation is to develop a macroscopic model for the movement of a wetting liquid in a rigid porous medium in the presence of a gas phase. This dissertation uses the method of spatial averaging to change scales in the description of flow in porous media. The starting point is a description of the fluid flow on the pore- or microscale. By coarsening the description of the microscale, solid and fluid phases start to form a continuum. This new imaginary continuum has all the properties of the small scale system on "average". The averaged properties are derived through a closure method based on the Representative Unit Cell (RUC) concept developed by professor J. P. du Plessis (du Plessis and Masliyah, 1988). It is extended to allow unsaturated flow, and phase interfaces are explicitly included.

By making different choices in the volume averaging procedure, a different form of the equations than the traditional one (Whitaker, 1986b) is obtained. The work presented in this dissertation introduces:

1. A new way of handling the liquid pressure term.

2. A unit cell model for unsaturated flow.

1.5 Outline of Dissertation

Chapter 2 gives an overview of the historical development of the study of flow and transport in porous media. Chapter 3 describes the method of spatial averaging as used in this dissertation, and states the basic equations, assumptions and conditions. In chapter 4 a geometric model for a porous medium is developed together with the pore scale flow equations. The results of chapters 3 and 4 are used in chapter 5 to derive averaged equations that describe unsaturated flow in porous media. A comparison of the newly derived equations with the Buckingham-Darcy equation and an experiment is given in chapter 6. Chapter 7 contains an overall discussion, recommendations and conclusions.

2 Overview and Review

This chapter provides an overview and gives a historical perspective of the study of flow in porous media. Single-phase and two-phase flow at the pore scale are described, basic equations are introduced, and concepts of the different flow mechanisms are explained. Thereafter different methods for upscaling to a continuum description of flow in porous media are introduced and the basics of volume averaging are explained.

2.1 Introduction

Flow in porous media plays an important role in many areas of science and engineering. Examples of the application of porous media flow phenomena are as diverse as flow in human lungs or flow due to solidification in the mushy zone of liquid metals. Table 2.1 lists other areas where flow in porous media plays an important role. The description of the behavior of fluids in porous media is based on knowledge gained in studying these fluids in pure form. Flow and transport phenomena are described analogous to the movement of pure fluids without the presence of a porous medium. The presence of a permeable solid influences these phenomena significantly. The individual description of the movement of the fluid phases and their interaction with the solid phase is modeled by an upscaled porous media flow equation. The concept of upscaling from small to large scales is widely used in physics. Statistical physics translates the description of individual molecules into a continuum description of different phases, which in turn is translated by volume averaging into a continuum porous medium description.

2.1.1 Definition of a porous medium

The definition of a porous medium used in this dissertation is based on the objective of describing flow in porous media. A porous medium is a heteroge-

Hydrology	Groundwater flow, salt water intrusion into coastal aquifers, soil remediation
Agriculture	Irrigation, drainage, contaminant movement in soils, soil-less cultures
Geology	Petroleum reservoir engineering, geothermal energy
Chemical engineering	Packed bed rectors, filtration, fuel cells, drying of granular materials
Mechanical engineering	Solar cell design, wicked heat pipes, heat exchangers, porous gas burners
Industrial materials	Rubber foam, glass fiber mats, concrete, brick manufacturing

Table 2.1: Areas where flow in porous media plays an important role.

neous system consisting of a rigid and stationary solid matrix and fluid filled voids. The solid matrix or phase is always continuous and fully connected. A phase is considered a homogeneous portion of a system, which is separated from other such portions by a definitive boundary, called an interface. The size of the voids or pores is large enough such that the contained fluids can be treated as a continuum. On the other hand, they are small enough that the interface between different fluids is not significantly affected by gravity.

The topology of the solid phase determines if the porous medium is permeable, i.e. if fluid can flow through it, and the geometry determines the resistance to flown and therefore the permeability. The most important influence of the geometry on the permeability is through the interfacial or surface area between the solid phase and the fluid phase. The topology and geometry also determine if a porous medium is isotropic, i.e. all parameters are independent of orientation, or anisotropic if the parameters depend on orientation. In multiphase flow the geometry and surface characteristics of the solid phase determine the fluid distribution in the pores, as does the interaction between the fluids. A porous medium is homogeneous if its average properties are independent of location, and heterogeneous if they depend on location. An example of a porous medium is sand. Sand is an unconsolidated porous medium, and the grains have predominantly point contact. Because of the irregular and angular nature of sand grains, many wedge-like crevices are present. An important quantitative aspect is the surface area of the sand grains exposed to the fluid. It determines the amount of water which can be held by capillary forces against the action of gravity and influences the degree of permeability.

The fluid phase

The fluid phase occupying the voids can be heterogeneous in itself, consisting of any number of miscible or immiscible fluids. If a specific fluid phase is connected, continuous flow is possible. If the specific fluid phase is not connected, it can still have bulk movement in ganglia or drops. For single-phase flow the movement of a Newtonian fluid is described. For two-phase immiscible flow, a viscous Newtonian wetting liquid together with a non-viscous gas are described. In practice these would be water and air. Other fluid phase compositions are not considered in this dissertation.

2.1.2 History

One of the first successful attempts to describe flow through porous media was by the French engineer Henry Darcy (Darcy, 1856). He was a civil engineer responsible for the drinking water supply of the city of Dijon. The drinking water was cleaned by percolation through sand columns. Darcy wanted to know the relation between specific discharge and head gradient in the sand columns. He found the following relation, commonly called Darcy's law, by experiment and written in modern notation:

$$v_D = -k_D \, \frac{\Delta h}{\Delta x} \tag{2.1}$$

with v_D the specific discharge, k_D the hydraulic conductivity, x a space coordinate and h the hydraulic head. This equation has formed the basis for nearly all models describing the creeping flow of fluids through porous media up to the end of the 1960's, when it was also derived theoretically (Hubbert, 1956) and alternative models were proposed (Bear and Bachmat, 1990, p. 122, 161). In Darcy's law, the head drop is entirely due to viscous dissipation, induced by the solid-liquid interface. This implies that Darcy's law becomes invalid when inertial effects play a role, or when the solid surface area (porosity) becomes very small (large) (Carman, 1956).

A major contribution to the description of flow in unsaturated soils was made by Buckingham (1907). He introduced a flux law for the movement of water in unsaturated soils, which is a modification of Darcy's law:

$$v_D = -k_D k_r(S) \, \frac{\partial h}{\partial x} \tag{2.2}$$

with $S = S(h)$ the liquid saturation, and $k_r(S)$ the relative hydraulic conductivity.

Richards (1931) combined the Buckingham flux law together with the mass balance equation (Richards equation):

$$\frac{\partial \epsilon S(h)}{\partial t} = -\nabla \cdot [k_D k_r(S) \nabla h] \tag{2.3}$$

with ϵ the porosity. The above two equations form the basis for most of the current studies of flow in unsaturated soils. In order to solve these equations constitutive relations between k_r and S, and S and h are necessary. The constitutive relations in Richards equation are commonly described by empirical parametric formulas, for example the formulas of Leverett (1941) and Corey (1994) from petroleum engineering, and the formulas of van Genuchten (1980) and Pullan (1990) from agricultural engineering. They contain fitting parameters which are calibrated by experiments.

Lucas (1918) and Washburn (1921) described the kinetics of wetting in capillaries by the following equation:

$$v(t) = \frac{\partial}{\partial t} \, l_p(t) = \frac{r\gamma_{gl} \cos\theta}{4\mu_l \, l_p(t)} \tag{2.4}$$

with $v(t)$ the penetration velocity , r the radius of the capillary, γ_{gl} the interfacial tension between gas and liquid, θ the contact angle between liquid and solid, μ_l the liquid viscosity, and $l_p(t)$ the penetration length of the liquid. This equation can be directly integrated, yielding:

$$l_p(t)^2 = \frac{\gamma_{gl} r \cos\theta}{2\mu_l} \, t \tag{2.5}$$

It describes the translation of the gas-liquid interface as it penetrates a capillary porous solid. Washburn (1921) applied this equation to charcoal as an example of a porous medium. It is one of the few equations which explicitly takes into account the kinetics of the wetting fluid movement. In this dissertation the kinetics of wetting fluid movement are taken into account in the closure modeling.

In 1956 Miller and Miller were the first researchers to describe explicitly the different force balances at micro- and macroscales in a porous medium. They derived similarity scaling laws based on capillary forces (surface tension) and

characteristic length scales. Morrow (1970) extended the description of two-phase flow by thermodynamic considerations, i.e. by taking into account pore level gas-fluid-solid configurations and interfacial energies.

This short account of the historical developments shows a continuous improvement made in the modeling of flow through porous media. In the next section the different flow mechanisms are explained and more recent developments included. Additional background information can be found in the excellent reviews of Hilfer (1996), and Adler and Brenner (1988).

2.2 Flow at the Pore Scale

Flow at the pore scale is governed by the specific geometry of the solid phase, which determines the boundary with the fluid phases. This boundary exerts a viscous drag on a moving fluid. If multiple fluid phases are present, their interaction gives rise to a phenomenon called capillarity. Capillarity is a manifestation of the interaction between the fluids and the solid, and the cohesion in the fluids, called surface tension. This overview mainly deals with quasi steady flow at the pore scale, which can still give rise to unsteady phenomena at the continuum scale.

2.2.1 Single-phase flow

In single-phase flow, one fluid phase is present in the voids of the porous medium. When the fluid starts moving, friction develops at the fluid solid interface and inside the fluid. For an incompressible Newtonian fluid with no other body forces than gravity, motion is described by the momentum balance equations (Navier-Stokes equations) (Bird et al., 1960; Fourie, 2000):

$$\rho \left(\frac{\partial \mathbf{v}}{\partial t} + \nabla \cdot (\mathbf{v}\mathbf{v}) \right) = -\nabla p + \mu \nabla^2 \mathbf{v} + \rho \mathbf{g} \tag{2.6}$$

with ρ the density, $\mathbf{v}$ the velocity, t time, p the pressure, μ the dynamic viscosity, and $\mathbf{g}$ the gravitational acceleration. Together with the mass balance equation (Bird et al., 1960):

$$\nabla \cdot (\rho \mathbf{v}) = 0 \tag{2.7}$$

which for incompressible flow becomes:

$$\nabla \cdot \mathbf{v} = 0 \tag{2.8}$$

a consistent set of equations with variables p and v is obtained. This system
of equations describes the temporal and spatial evolution of the fluid move-
ment. It is still under-determined without initial and boundary conditions.
Initial conditions are the starting configuration of the fluid at $t = t_0$, and the
boundary conditions describe the space-time boundaries of the flow domain.
Assuming steady state flow, the boundary conditions reduce to a specification
of the interfacial conditions at the fluid-solid interface and the fluid entrances
and exits. The boundary condition at the fluid-solid interface is:

$$\text{B.C.} \quad \mathbf{v}(x, t) = 0 \quad \text{at fluid-solid interface} \tag{2.9}$$

The above boundary condition is called a no-slip condition. It is appropriate
if the Knudsen number Kn $= d/\lambda_0 > 10$, with λ_0 the molecular mean free
path length and d a characteristic distance (Helmig, 1997, p. 86). For low
values of the Reynolds number, i.e. slow viscous flow at low Reynolds numbers,
equations (2.6) reduce to (Hilfer and Øren, 1996):

$$-\rho\mathbf{g} + \nabla p = \mu\nabla^2\mathbf{v} \tag{2.10}$$

These equations are called the Stokes equations and model slow viscous domi-
nated flow in the pores of a porous medium. It is important to recognize that
the absolute pressure level p plays no role in equations (2.6) and (2.10) because
of incompressibility. Only differences in pressure affect the fluid flow. This im-
plies that flow at a high pressure level in deep groundwater is exactly the
same than flow at an atmospheric pressure level, if the same pressure gradient
applies.

2.2.2   Two-phase flow

Two-phase flow in porous media is in effect flow in a three-phase system:
the solid phase and two fluid phases. Moving interfaces in two-phase flow
will give rise to effects not observed in single-phase flow. The interaction
between the different fluids and the solid surface at the pore scale determines
the fluid distribution and behavior (Buckingham, 1907). If the cohesive forces
in the fluids are larger than the adhesive forces between the fluids, they form

a sharp interface and are immiscible (Dracos, 1991). An example are water and air (possibly including water vapor), or oil and water. Miscible fluids, for example, are alcohol and water. The concept of miscibility depends on the thermodynamic state of the fluids. The examples given here are for standard conditions in soils [1].

At the pore, scale surface forces usually play a much more important role than gravity (through the density of the fluids). For example, for air and water, the Bond number related to the density difference is:

$$\text{Bo} = \frac{\text{gravitational force}}{\text{surface tension force}} = \frac{(\rho_w - \rho_a)gL^2}{\gamma_{wa}} \approx 10^{-2} \tag{2.11}$$

with $\gamma_{wa} \approx 10^{-2}$ kg/s^2 the interfacial tension between water and air, $L \approx 10^{-4}$ m the pore characteristic length scale, and $\rho_w \approx 10^3$ kg/m^3, $\rho_a \approx 1$ kg/m^3, the densities of water and air respectively. Gravitational and surface tension forces become comparable in magnitude in pores of approximately cm size. Due to the strong influence of surface forces, the fluid distribution is directly influenced by the fluid volume through the fluid surface area.

Surface Tension

The geometry of the interface between two fluids is determined by interfacial (surface) tension. This tension is defined as the amount of energy that is required to create a unit area of surface. It can also be seen as a force per unit length acting along an arbitrary line on the interface. The interfacial tension acts tangentially to the interface and minimizes the amount of interface, if no other forces prevent this (Pellicer et al., 1995). It is formally defined as the change of Helmholtz free energy per change in unit area A_i of the interface at constant temperature, volume and chemical composition (Sherwood, 1971). In this dissertation the interfacial tension is treated as constant. The interfacial tension gives rise to a difference in pressure across the interface at equilibrium (Pellicer et al., 1995):

$$\Delta p = p_g - p_l = \gamma_{gl} \frac{dA_i}{d\mathcal{V}_l} \tag{2.12}$$

with p_g the gas phase pressure, p_l the liquid phase pressure and $\mathcal{V}_l$ the liquid volume. It can also be expressed as (Young-Laplace equation) (de Gennes,

---

[1] Air phase at atmospheric pressure, temperature $\approx 10 - 20°$C

1985):

$$\Delta p = \gamma_{gl} \left(\frac{1}{R_1} + \frac{1}{R_2} \right) = \gamma_{gl} C \qquad (2.13)$$

with R_1 and R_2 the principal radii of the curved surface and C the curvature of the interface, which is positive for an interface concave outward from the liquid.

Wettability

When three phases are in contact with each other, they are separated by interfaces between each two phases and by contact lines where the three phases meet. If one of the surfaces is static (the solid surface) we can write (Pellicer et al., 1995):

$$\cos \theta = \frac{\gamma_{sg} - \gamma_{sl}}{\gamma_{gl}} \qquad (2.14)$$

which is called Young's equation and defines the contact angle θ. The smaller the contact angle, the larger the area of the solid surface wetted by a constant volume of fluid. If the contact angle goes to zero, the wetting fluid will tend to cover the surface of the solid completely. In soils most surfaces are rough, and an apparent contact angle develops (de Gennes, 1985), and θ is used to denote this apparent contact angle. A moving liquid will exhibit contact angle hysteresis, depending on direction and velocity with respect to the solid surface (de Gennes, 1985). Receding contact angles are usually smaller than advancing contact angles. If the solid surface is rough, jumps of the contact line can occur, causing sudden interface stretching and contraction. This is due to the "pinning" of the contact line (de Gennes, 1985). The interaction between the wetting state and the fluid-fluid interfacial tension results in a specific fluid configuration inside a pore.

Capillary Pressure

Capillary pressure is a term with different usage. Sometimes it is strictly related to interfacial tension (Mason and Morrow, 1991), sometimes it denotes a general potential driving transport processes (Nitao and Bear, 1996). In soil science water is usually assumed to be the wetting fluid and at lower pressure

than atmospheric pressure. The standard definition for capillary pressure in soil science is:

$$p_c = p_{\text{non wetting}} - p_{\text{wetting}} = p_g - p_l \qquad (2.15)$$

The non-wetting pressure is chosen as reference level and arbitrarily set to zero:

$$p_{\text{non wetting}} = 0 \qquad (2.16)$$

which implies that:

$$p_c = -p_l \qquad (2.17)$$

and, using equation (2.13):

$$p_l = -\gamma_{gl}\left(\frac{1}{R_1} + \frac{1}{R_2}\right) \qquad (2.18)$$

The above definition of a pressure reference level implies that p_l can become negative. This does not imply that absolute negative pressures exist, but that p_l is negative compared to $p_g = 0$. In soils, the liquid pressure at low water contents is usually measured by comparing the soil to some other material at a given potential (Koorevaar et al., 1983). In effect these "capillary pressure" measurements are thus potential measurements. These are often highly negative, below the bubbling pressure of pure water. The picture of capillary pressure as being a water pressure is highly simplified and not justifiable on physical grounds (Gray and Hassanizadeh, 1991a). It is possible to use p_c as a measure of the energy state of soil water, and so include effects of electrostatic forces and other not directly specified influences (Nitao and Bear, 1996). If the radius of the gas-liquid interface is calculated by using equation (2.13) from the average Δp on the macroscale, the result is highly questionable, if this radius is to represent the true radius of the gas-liquid interface (Gray and Hassanizadeh, 1991a). In order to overcome the difficulties related to the bubbling pressure of water, p_c can be defined as composed of a capillary component $C_c(C)$ and an adsorptive component $A(h)$. The adsorptive component accounts for water held by the solid porous medium matrix, usually in thin films, covering the solid phase. The geometry of these films follows the outer surface of the solid phase, and as such these films can be concave or convex. The Young-Laplace equation does not apply to these films. Written in terms of constant partial

specific Gibbs free energy, G, the Augmented Young-Laplace equation (AYL), which extends equation (2.13) by considering the gas-liquid interface as a liquid vapor interface and including adsorption effects (Nitao and Bear, 1996; Tuller et al., 1999), can be written as:

$$G = A(h) + C_c(C) \tag{2.19}$$

or in terms of capillary pressure:

$$p_c = \rho_l \left[A(h) + C_c(C) \right] \tag{2.20}$$

where h is the thickness of the adsorbed film. $C_c(C)$ can be expressed as (Tuller et al., 1999):

$$C_c(C) = \frac{\gamma_{gl}}{\rho_l} \left(\frac{1}{R_1} + \frac{1}{R_2} \right) \cos \theta \tag{2.21}$$

and $A(h)$ as:

$$A(h) = \frac{A_{svl}}{6 \pi \rho_l h^3} \tag{2.22}$$

with A_{svl} the Hamacker constant, a material property, and h the thickness of the liquid film. In principle the Hamacker constant is "constant" only for flat surfaces, but here it is used for order of magnitude estimation only. It can then be treated as a constant even if the surfaces are not perfectly flat. If the dimensionless ratio of the terms on the left hand side of equation (2.20) is of order 1, they are equally important. This ratio can be expressed as:

$$
\begin{aligned}
\frac{A(h)}{C_c(C)} &= \frac{\text{adsorption term}}{\text{capillary term}} \\
&= \frac{A_{svl}}{6 \pi h^3 \gamma_{gl} \left(\frac{1}{R_1} + \frac{1}{R_2} \right) \cos \theta}
\end{aligned} \tag{2.23}
$$

Assuming that $\lim_{R_2 \to \infty}$, i.e. the capillary meniscus is curved only due to R_1, and $\theta = 0$. In that case the terms are equally important if:

$$
\begin{aligned}
1 &\approx \frac{A_{svl} R_1}{6 \pi h^3 \gamma_{gl}} \\
h &\approx (10^{-19} \, R_1)^{1/3} \, \text{m}^{2/3}
\end{aligned} \tag{2.24}
$$
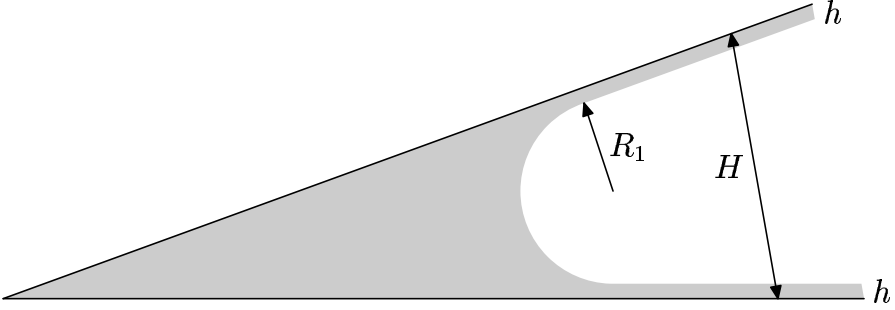
Figure 2.1: Schematic picture of adsorbed film and capillary meniscus in flat wedge (not to scale), symbols explained in text, gray area denotes liquid.

with $\gamma_{gl} \approx 0.07$ kg/s^2, $A_{svl} \approx 2 * 10^{-19}$ J and m$^{2/3}$ accounting for the units of the constants. For smaller values of h the adsorption term becomes more important. Figure 2.1 shows the geometry of the capillary meniscus and the adsorbed film inside a wedge. In thin slits the maximum thickness of the films before coalescence occurs is $h = H/3$ (Tuller et al., 1999). The following geometrical relation holds, with H the spacing of the solid phase:

$$
\begin{aligned}
2R_1 + 2h &= H \\
2R_1 + 2h &= 3h \\
R_1 &= \frac{1}{2}h
\end{aligned}
\tag{2.25}
$$

Combining equations (2.24) and (2.25) gives:

$$
\begin{aligned}
R_1 &\approx \frac{1}{2}(10^{-19}\, R_1)^{1/3}\, \text{m}^{2/3} \\
R_1 &\approx 10^{-10}\, \text{m}
\end{aligned}
\tag{2.26}
$$

and for smaller values of R_1 the adsorption term would be the important one. If the radius of the air water interface were so small, this would correspond to a pressure difference across the interface of about $-7 * 10^8$ Pa, which is about the (negative) pressure of a water column of 7 km height, or equivalent pF 6.8. At these high pF values, the porous medium is essentially dry and practically no water movement occurs in the liquid phase anymore. Once p_l becomes very low, the liquid films covering the solid surface become extremely thin. In these thin films viscosity and density of the liquid can not be

assumed constant any more (Gray and Hassanizadeh, 1991a; Tuller and Or, 2001, p. 261). The liquid viscosity and density then depend on the distance to the solid surface. This plays a role only in films thinner than 10^{-8} m (Tuller and Or, 2001). These effects can play an important role in fine textured soils, but are relative unimportant in sands (Tuller and Or, 2001) with their specific surface areas in the order of 10^4 m^2/m^3 (Hilfer, 1996). The amount of water held by adsorptive forces in sands at the above limit can be easily estimated as 10^{-10} m $*10^4 m^2/m^3 \approx 10^{-6} m^3/m^3$, which is indeed negligible for most practical purposes. The same conclusions can be drawn from capillary rise and drainage, and from flow in capillary groove experiments. Hence in these cases capillary bound water is more important than water bound by adsorptive forces (Lago and Araujo, 2001; Romero and Yost, 1996).

In conclusion, the assumption is justified that most water at low capillary pressure is held by capillary forces in sandy soils, and that these capillary forces are the major phenomena in determining the flow of liquid, in contrast to adsorptive forces that play only a minor role. From now on the adsorptive forces as such are not longer directly considered in this dissertation and it is assumed that practically all water is held by capillary forces.

In the last few paragraphs the contribution of the vapor phase on the liquid equilibrium was not considered (as is in the reminder of this dissertation). It should be kept in mind that mass transport through the vapor phase in very dry soils is more important than liquid flow. This subject would warrant at least another few years of research. However the movement of liquid in very dry soils is not further considered here.

Flow at the Pore Scale

The equations describing two-phase flow at the pore scale are very similar to the single-phase flow equations. The major difference is that two fluids are present and hence two momentum and mass balances need to be solved. Additionally the interfacial conditions between the two fluid phases need to be specified. The momentum balances (eqs. (2.6)) become:

$$\rho_g \left(\frac{\partial \mathbf{v}_g}{\partial t} + \nabla \cdot (\mathbf{v}_g \mathbf{v}_g) \right) = -\nabla p_g + \mu_g \nabla^2 \mathbf{v}_g + \rho_g \mathbf{g} \qquad (2.27)$$

$$\rho_l \left(\frac{\partial \mathbf{v}_l}{\partial t} + \nabla \cdot (\mathbf{v}_l \mathbf{v}_l) \right) = -\nabla p_l + \mu_l \nabla^2 \mathbf{v}_l + \rho_l \mathbf{g} \qquad (2.28)$$

with subscript g for the gas phase and l for the liquid phase. They are augmented by the mass balance equations:

$$\nabla \cdot (\rho_g \mathbf{v}_g) = 0 \tag{2.29}$$

$$\nabla \cdot (\rho_l \mathbf{v}_l) = 0 \tag{2.30}$$

with boundary conditions:

B.C.1	$\mathbf{v}_g = 0$	at gas-solid interface	(2.31)
B.C.2	$\mathbf{v}_l = 0$	at solid-liquid interface	(2.32)
B.C.3	$\mathbf{v}_g = \mathbf{v}_l$	at gas-liquid interface	(2.33)
B.C.4	$(p_l - p_g)(x,t) = -\gamma_{gl} C(x,t)$	at gas-liquid interface	(2.34)

B.C.1 and B.C.2 are the standard no-slip boundary conditions for the fluid-solid interface. B.C.3 states that there is no mass transfer across the gas-liquid interface. B.C.4 describes the pressure jump condition across the gas-liquid interface. This expression is a simplified form of the full stress balance at the gas-liquid interface (Hilfer, 1996). If the dynamics of the interface need to be taken into account, explicit balance equations can be derived (Gray and Hassanizadeh, 1991b). Additionally the boundary conditions at the entries and exits of the fluid domain need to be described. The above equations contain a self contradiction: B.C.1 and B.C.2 state no-slip at the solid interface. If the contact line between gas, liquid and solid moves, it must slip along the solid interface. This contradiction is not important in the following description of two-phase flow (Hilfer, 1996; Dussan V., 1979; de Gennes, 1985). Here the assumption is made that a thin, quasi stationary liquid film covers the solid at all times, and so the singularity at the contact line is removed.

It is a common assumption that the gas phase has atmospheric pressure everywhere and that the influence of gravity on the gas phase is negligible (Koorevaar et al., 1983). This implies that all gradients in the gas phase vanish:

$$\nabla p_g = 0 \tag{2.35}$$

A second common assumption is that the gas phase has "infinite" mobility, i.e. $\mu_g = 0$ (Bear, 1988). This implies that there is no viscous coupling at the gas-liquid interface (and hence the simple form of B.C.4). In any case, due to the high viscosity contrast of water and air ($\mu_w \approx 1 \times 10^{-3}$, $\mu_a \approx 2 \times 10^{-5}$),

viscous coupling only plays a role in high-speed flows. Capillary equilibrium, i.e. quasi static capillary forces can be assumed if (Dracos, 1991):

$$\left| \frac{(\mu_l - \mu_g)U}{\gamma_{gl}} \right| \ll 1 \tag{2.36}$$

with U a characteristic velocity. The above term is a modified capillary number (Ca), related to the viscosity contrast. The common definition for Ca is (Probstein, 1989):

$$\text{Ca} = \frac{\text{viscous force}}{\text{surface tension force}} = \frac{\mu U}{\gamma} \tag{2.37}$$

With the given assumptions, equations (2.27) essentially vanish, and equations (2.28) can be used without direct reference to equation (2.27). Using dimensional analysis and scaling arguments similar to single-phase flow (Hilfer and Øren, 1996), equations (2.28) reduce to:

$$- \rho_l \mathbf{g} + \nabla p_l = \mu_l \nabla^2 \mathbf{v}_l \tag{2.38}$$

whereby slow, viscous dominated low Reynolds number flow is assumed. As with single-phase flow this can be described as purely viscous, creeping flow. When the volume of liquid becomes small, it will tend to cover the solid with thin films. Because the flow resistance in thin films scales with approximately the film thickness to the power three (Bird et al., 1960), liquid movement becomes slower and slower as the thickness approaches zero. There are several examples in the literature which solve two-phase flow at the pore scale. Payatakes et al. (1973) and Sáez et al. (1986) use a periodically constricted pore model. Their model allows capillary effects to play only a small role, because their model is essentially two-dimensional. As they use the model also for high-speed flows, where capillarity is of less importance, their assumptions are reasonable. Ruan and Illangasekare (1999) developed a liquid flow model applicable to sandy soils based on a sheet flow model. Their model is based on quasi-spherical unit cells and allows a variety of flow phenomena to be modeled. A drawback of their approach is that no closed-form relationship for saturation-capillary pressure dependence is given. Tuller (Tuller and Or, 2001) used a combination of polygonal pores and slits to describe flow together with capillary and adsorption phenomena. The great advantage of their model is the accurate representation of adsorption, but the flow model is quite primitive in terms of the geometrical representation of the pore space. In effect their model is a two-dimensional model.

2.3 Upscaling to the Continuum Scale

The change of scale from the pore or microscale to the continuum or macroscale changes the form of the flow equations. For single-phase and multi-phase flow different techniques and assumptions are used that lead to different forms of the governing equations. An important quality of the upscaled equations is whether they are local or nonlocal (Cushman, 1990a). Local equations have a mathematical structure similar to the Navier-Stokes equations (eqs. 2.6) and depend on local point values only. Nonlocal equations also depend on long range interactions. Most theories describing flow in porous media use local equations. Notable exceptions are so called "pressure drop" correlations used in chemical engineering (Brodkey and Hershey, 1988), and the original form of Darcy's law (Darcy, 1856). These equations are nonlocal, because they depend on an external pressure drop directly. Central to the local versus nonlocal distinction is the definition of so called point values. The definition of what a mathematical point and a physical point in the upscaled equations is, is given by Nitsche and Brenner (1989, p. 240): *"a 'point' at the microscale does not strictly represent a mathematical point; instead, it has meaning only beyond a much smaller intermediate size (characteristic of the mesoscale), which is nevertheless so much greater than the pore scale that the macroscopic 'point' contains an appreciable, indeed representative, portion of the microstructure"*. The 'volume' associated with the macroscopic point is called a Representative Elementary Volume (REV).

The term upscaling is used in many contexts. Here it is used to denote an operation that describes a spatial transformation from the pore scale to the continuum scale or macroscale . At the continuum scale new parameters enter the flow equations and replace small-scale descriptions. On the macroscale the detailed description of interfaces and spatial distributions disappears and is replaced by macroscale parameters. Going from the pore to the continuum scale results in a loss of information (Cushman, 1990b). This lost information is commonly replaced by implicit (du Plessis and Masliyah, 1988; du Plessis, 1997)) or explicit constitutive relations (Bear and Bachmat, 1990). There are different methods for the upscaling process: heuristic and empirically based methods, stochastic methods, methods based on homogenization, mixture theories and space averaging theories.

These upscaling methods have the following definitions in common. Porosity is defined as:

$$\epsilon = \frac{\mathcal{V}_p}{\mathcal{V}_0} \tag{2.39}$$

with $\mathcal{V}_p$ the pore volume and $\mathcal{V}_0$ the averaging volume. The liquid saturation n_l is defined as:

$$n_l = \frac{\mathcal{V}_l}{\mathcal{V}_p} \tag{2.40}$$

with $\mathcal{V}_l$ the volume of the liquid phase in $\mathcal{V}_0$. The following constraints apply:

$$
\begin{aligned}
\mathcal{V}_s + \mathcal{V}_p &= \mathcal{V}_0 & (2.41) \\
\mathcal{V}_l + \mathcal{V}_g &= \mathcal{V}_p & (2.42) \\
n_l + n_g &= 1 & (2.43)
\end{aligned}
$$

with the subscript s indicating the solid phase and $\mathcal{V}_s$ the volume of the solid phase in $\mathcal{V}_0$.

In the following sections the main upscaling approaches are listed.

Heuristics and empirical descriptions, and stochastic methods

Heuristics and empirical descriptions are based on the direct description of experiments (van Genuchten, 1980), or an extension of Darcy's equation to two-phase flow (Richards, 1931). Modern methods use pore network modeling (Hassanizadeh et al., 2001) to obtain upscaled flow equations and/or parameters for constitutive relations, based on physical or computer models.

Stochastic upscaling methods are not often used in flow in porous media. Their main application area lies in transport theories, e.g. solute transport (Cushman, 1990a).

Homogenization

A third class of upscaling techniques is based on the method of homogenization. *"A more descriptive name of this method is 'an asymptotic method for the study of periodic media'."* (Ene, 1990). Homogenization deals with multiscale systems, i.e. systems in which the different scales are clearly separated. It is based on the study of periodic solutions of partial differential equations and the asymptotic behavior of these as the period tends to zero. The method is restricted to problems with periodic boundary conditions and structures. Due to these restrictions the method cannot be applied directly to multi-phase flow (Pride and Flekkøy, 1999), although attempts have been made (Hornung, 1997).

Mixture theories

Mixture theories are based on "mixing" of the description of different phases in a multi-phase medium. They were applied in the context of flow in porous media by Bowen (1984) and Wang and Beckermann (1993). Mixture theories result in simpler upscaled equations than the homogenization method or spatial averaging, because they do not describe the movement of the different fluid phases in porous media separately, but lumped (Bowen, 1984). A disadvantage is that the information regarding a specific phase is lost and that certain pore level phenomena (phase discontinuities, counter-current flow) can not be described easily.

2.3.1   Space averaging theories

Space averaging theories are widely used in the upscaling of processes in porous media (Nitsche and Brenner, 1989). Space averaging is called volume averaging if the averaging is carried out over a three-dimensional volume. This volume is called a Representative Elementary Volume (REV). The basis of volume averaging in porous media was derived by Whitaker (1966, 1967, 1969), Anderson and Jackson (1967), Slattery (1967, 1969), Gray (1975), and Blake and Garg (1976). Later contributions and extensions were made by: Hassanizadeh and Gray (1979a,b, 1980), Tosun and Willis (1980), Narasimhan (1980b), Drew (1983), Whitaker (1985), Crapiste et al. (1986), and Bear and Bachmat (1990). Basically, volume averaging is a very simple technique, based on the mean value theorem for integrals. It states that for a given function $f(x)$, a unique average value $\langle f \rangle$ can be determined. On the other hand, a given average value $\langle f \rangle$ can be the result of averaging different functions $f(x)$. Volume averaging considers two types of averages, the phase average, defined by:

$$\langle \boldsymbol{\Psi} \rangle = \frac{\int\limits_{\mathcal{V}_0} \boldsymbol{\Psi} d\mathcal{V}}{\int\limits_{\mathcal{V}_0} 1 d\mathcal{V}} = \frac{1}{\mathcal{V}_0} \int\limits_{\mathcal{V}_0} \boldsymbol{\Psi} \, d\mathcal{V} \tag{2.44}$$

with $\boldsymbol{\Psi}$ a generalized variable, and the intrinsic phase average defined by:

$$\langle \boldsymbol{\Psi} \rangle^i = \frac{\int\limits_{\mathcal{V}_i} \boldsymbol{\Psi} d\mathcal{V}}{\int\limits_{\mathcal{V}_i} 1 \, d\mathcal{V}} = \frac{1}{\mathcal{V}_i} \int\limits_{\mathcal{V}_i} \boldsymbol{\Psi} \, d\mathcal{V} \tag{2.45}$$

with $\mathcal{V}_i$ the volume of phase i. The intrinsic phase average is defined as an average in a specific phase i. In the above two formulas, the angular brackets $\langle\ \rangle$ denote the average defined by the integrals. The intrinsic phase average is commonly used to describe the liquid pressure, as this pressure is defined inside the liquid phase only and not inside the whole averaging volume.

The microscale transport equations contain spatial and time derivatives. In order to average the spatial derivatives, the need arises to interchange differentiation with spatial integration. The resulting theorem is called the spatial averaging theorem (Anderson and Jackson, 1967; Whitaker, 1967; Slattery, 1967; Gray, 1975; Gray and Lee, 1977). For a general variable (Gray et al., 1993):

$$\langle\nabla\mathbf{\Psi}\rangle = \nabla\langle\mathbf{\Psi}\rangle + \frac{1}{\mathcal{V}_0}\int_{\mathcal{S}_\mathbf{\Psi}}\boldsymbol{\nu}\mathbf{\Psi}\ d\mathcal{S} \tag{2.46}$$

with $\mathcal{S}_\mathbf{\Psi}$ the surface of the averaging volume occupied by $\mathbf{\Psi}$, and $\boldsymbol{\nu}$ an outward unit normal vector on $\mathcal{S}_\mathbf{\Psi}$. The above implies for the divergence operation:

$$\langle\nabla\cdot\mathbf{\Psi}\rangle = \nabla\cdot\langle\mathbf{\Psi}\rangle + \frac{1}{\mathcal{V}_0}\int_{\mathcal{S}_\mathbf{\Psi}}\boldsymbol{\nu}\cdot\mathbf{\Psi}\ d\mathcal{S} \tag{2.47}$$

Gray (1975) introduced a consistent decomposition of the average value of a variable in the local value and the local deviations from the spatial average:

$$\langle\mathbf{\Psi}\rangle = \mathbf{\Psi} - \dot{\mathbf{\Psi}} \tag{2.48}$$

whereby the dot denotes the deviations from the average. This decomposition together with the spatial averaging theorem makes it possible to derive macroscale equations in a mathematically well defined and traceable way (Diedericks, 1999, p. 29). These averaging theorems, although mathematically well defined for any (continuous) function, are physically meaningful only for additive functions. Additive functions are those which measure the extent or amount of a given property in the system (Sherwood, 1971).

Hassanizadeh and Gray (1979a) proposed a set of four criteria, which should, in their view, be satisfied in the averaging process. These criteria are based on physical reasoning and try to ensure consistent and physically meaningful macroscale equations:

criterion I *When an averaging operation involves integration, the integrand multiplied by the infinitesimal element of integration must be an additive quantity.*

Several authors violate this criterion and obtain physically questionable macroscopic balances (Kowalski, 2000; Hager and Whitaker, 2000, 2002a,b; Hsu and Cheng, 1988; Pride and Flekkøy, 1999), see also Narasimhan (1980a) and the response by W. G. Gray in Narasimhan (1980a). Hager and Whitaker (2002b) showed that in certain situations this criterion can be relaxed. If the integrand, written as a linear combination with a capacity function, is additive, then also non additive quantities can be the directly averaged.

criterion II *The macroscopic quantities shall exactly account for the total amount of the corresponding microscopic quantity.*

In effect criterion II is a balance statement, and could be paraphrased as: The "large" is "the sum of all small parts".

criterion III *The primitive concept of a physical quantity, as first introduced into the classical continuum mechanics, must be preserved by proper definition of the macroscopic quantities.*

Hassanizadeh and Gray (1979a) give an example for this criterion: *"..., heat is a mode of transfer of energy through a boundary different from work. The definition of macroscopic heat flux must also be a mode of energy transfer different from macroscopic work."*

criterion IV *The average value of a microscopic quantity must be the same function that is most widely observed and measured in a field situation or in the laboratory.*

Criterion IV is not based on physical reasoning, but on practical considerations. The question arises what exactly should be considered the "most widely observed and measured" quantity (see also the discussion about tensiometers in sect. 3.4.2).

In their work Hassanizadeh and Gray (1979a) and Gray and Hassanizadeh (1991b) show that volume integrals of quantities such as pressure, which are defined per unit area, can be transformed into area integrals. This is of special importance in multi-phase flow, where the area integrals are often evaluated over the fluid-fluid interfaces (Bear and Bachmat, 1990).

Closure

After volume averaging of the microscopic equations, the resulting macroscopic equations still contain microscopic quantities, usually in the form of integrals of microscale terms (Whitaker, 1980; Crapiste et al., 1986). The approximation of these integrals in terms of macroscopic quantities is called closure. Different methods can be found in the literature:

- Numerical methods: Quintard and Whitaker (1990, 1994), Fourie (2000).

- Empirical methods: Whitaker (1980), Bear (1988).

- Units cell concepts: du Plessis and Masliyah (1988, 1991), du Plessis and Roos (1994), Hsu and Cheng (1988), Diedericks and du Plessis (1997), Smit and du Plessis (2000), Hoffmann (2000b).

Here the unit cell concept is used. Up to now this concept has been applied mainly to single-phase flow, and the application to multi-phase flow developed here extends this concept to the use in unsaturated flow. The work presented here is parallel to the work of Hassanizadeh and Gray (1980). They use thermodynamic relationships to constrain the closure problem while this work directly approximates the closure problem.

2.3.2   Resulting theories

Once the flow description retains to the macroscale, a different terminology is applied to the description of this flow. From experiments we know that at different liquid saturations, different flow paths for the liquid exist. At low capillary pressures the liquid preferentially occupies the smaller pores and corners in the porous medium. The liquid permeability is then determined by the connectivity of the liquid phase and the amount of contact surface with the solid. Different authors put forward flow models describing unsaturated flow. Buckingham (1907) formulates his theory analogous to thermal and electrical conduction. Whitaker (1986b) uses an analogy to Darcy's law, and derives an equation similar to Richards equation, assuming static contact lines and using order of magnitude analysis. Bear and Nitao (1993) derive a macroscopic flux law including thermal effects and thermodynamic relations for three fluid phases. Recently Pride and Flekkøy (1999) derived a macroscopic flux law in the fixed contact line regime. Hassanizadeh and Gray (1997) criticize most

models for apparent paradoxes and propose general relations based on thermodynamic relationships. The results of all these authors reflect their choices during the averaging process. The derived macroscopic flux laws are often similar, but it is not clear which one is more generally applicable in practical calculations of unsaturated flow. Most of the proposed macroscopic equations disregard time dependence or dynamics in the momentum balance and introduce no dependence on average gradients.

3 Development of a Mathematical Model for Flow in Unsaturated Porous Media

3.1 Introduction

This chapter describes the development of upscaled unsaturated flow equations in porous media. In chapter 2 an overview of the different approaches to volume averaging was given. From now on this dissertation is mainly concerned with liquid movement. The gas phase is still assumed to be present and to influence the liquid behavior, but is not described explicitly any more. The main assumptions are listed in section 3.2. In section 3.3 the starting equations on the pore scale and the boundary and initial conditions are stated. These equations are volume averaged and the closure problem is developed in section 3.4. In chapter 4, a geometrical model for a Representative Unit Cell (RUC) is described and analyzed and a method to solve the two-phase flow problem inside an RUC is proposed.

The approach taken in here is based on the closure scheme developed by du Plessis and Masliyah (1988). This scheme is augmented with additional boundary conditions which are introduced due to fluid-fluid interfaces. Previous applications of du Plessis and co-workers described high Reynolds number flow in porous media (du Plessis, 1994, 1992) and flow in granular porous media (du Plessis and Masliyah, 1991; Knackstedt and du Plessis, 1996).

3.2 Assumptions

In this section the assumptions underlying the development of the unsaturated flow model are stated formally. These assumptions are sometimes stated in

the literature (Pride and Flekkøy, 1999), but more often they are implicitly assumed (Whitaker, 1986b, 1980). It may seem that these assumptions are too restrictive or too many, but they are less than the (implicit) assumptions commonly made (Whitaker, 1986b). If additional assumptions are made during the derivation of the equations, they will be clearly stated.

3.2.1   Assumptions regarding the fluids

Assumption 1 *The fluids are incompressible and the density ρ is constant.*

Incompressibility and constant density are reasonable for flow in unsaturated soils, provided pressure variations are not too large. As this work is mainly concerned with capillary held water, these variations are relatively small. Close to a solid surface the variation of density of the liquid phase is relatively large, but it is assumed that the liquid bound by adhesive forces does not contribute to the flow.

Assumption 2 *The viscosity μ is constant.*

This assumption is common in the soil physics literature (Koorevaar et al., 1983), but was questioned by Gray and Hassanizadeh (1991a). In sandy soils it is justified, because only a small fraction of the liquid is held by adsorptive surface forces close to the solid grains. In this small fraction density and viscosity are not constant, but this fraction does not significantly contribute to liquid flow (see sec. 2.2.2).

Assumption 3 *The fluids exert no interfacial drag on each other.*

Because the viscosity ratio between liquid and gas is very high (sec. 2.2.2), the gas phase can be assumed to exert virtually no drag on the solid phase:

Assumption 4 *The individual fluid phases remain continuous at all times. Sometimes this continuity is through a thin film, which essentially allows no flow.*

The above assumption is made in order to remove the discontinuity at the contact line between solid, liquid and gas. The assumption is reasonable, because solid surfaces are covered by a thin film of liquid, which often is deposited by vapor.

Assumption 5 *The gas phase is assumed to be at constant, atmospheric pressure.*

This assumption is identical to the gas phase pressure assumption made in deriving Richards equation (Bear, 1988).

3.2.2 Assumptions regarding the porous medium

Assumption 6 *The porous medium is non-oriented or isotropic in the sense that there is no natural direction associated with the pore structure inside an averaging volume.*

Unconsolidated porous media are often isotropic within a specific layer. Due to natural deposition and sedimentation patterns, a layered porous medium is not isotropic. Here it is assumed that modeling takes place within such an isotropic layer.

Assumption 7 *The solid phase is fixed in space and time.*

The solid phase is assumed to be incompressible and not moving relative to a fixed reference frame.

Assumption 8 *The porous medium is homogeneous on the averaging scale.*

This assumption implies that there are no macroscopic boundaries inside an averaging volume, and that there is no change of medium.

3.2.3 Assumptions regarding flow and capillarity

Assumption 9 *The flow is essentially inertia free (see section 2.2.2) and the liquid flow is governed by equations (2.38).*

Assumption 10 *The flow is isothermal, and thermal effects on the surface tension, as described in e.g. Grant and Salehzadeh (1996), play no role.*

Assumption 11 *During and after drainage of the wetting liquid a thin liquid film is left covering the solid surface. This implies an effective receding contact angle $\theta = 0$.*

Assumption 12 *Contact lines between liquid, gas, and solid can move. This movement is assumed to be relatively smooth.*

The last assumption requires some explanation. Haines (1927) already showed that, due to capillary forces and the geometry of the solid phase, rapid contact line movement can occur in soils and lead to "pressure jumps". These pressure jumps are of very small duration (Morrow, 1970), and are assumed to average out in an averaging volume. Assumption 4 already stated that the solid surface is always covered with a thin liquid film. Given this assumption, the present assumption could be read as: contact lines between capillary held liquid, gas, and solid covered with a thin liquid film can move.

Assumption 13 *Gravity forces are small compared to capillary forces at the pore scale.*

The basis of this assumption was discussed in section 2.2.2.

Assumption 14 *The profile of capillary pressure inside a pore perpendicular to the flow is not directly influenced by the flow (sec. 2.2.2, eq. 2.36).*

This assumption leads to a Poiseuille like description of the microscale flow in the pores.

Assumption 15 *Only movement of liquid held by capillary forces contributes to flow, liquid held by adsorptive forces is essentially immobile.*

The above assumption was explained in section 2.2.2.

3.2.4   Assumptions not made

It is also important to list some assumptions not made here, but that are common in the volume averaging literature on two-phase porous media flows:

1. There are no assumptions about the pressure gradients inside the averaging volume (in contrast with Alemán et al. (1989); Whitaker (1986a), see also Pride and Flekkøy (1999)), except the standard volume averaging length scale requirements (Crapiste et al., 1986). These state: microscopic length scale ≪ radius of averaging volume ≪ macroscopic length scale.

2. No assumptions are made regarding the saturation gradient inside an averaging volume, except the length scale constraints imposed by volume averaging (Crapiste et al., 1986).

3. Dynamic effects are allowed in the macroscopic momentum balance and not neglected as in Whitaker (1986b).

3.3   The Basic Interstitial Equations

At the pore or microscopic scale the momentum balance is described by the Stokes equations (assumption 9). A pore can be occupied by air and water simultaneously. The presence of a phase interface (air - water) and the geometric configuration of the solid influence the configuration of the fluid phases and their dynamic behavior (see section 2.2.2). The pressure is also influenced by the phase interfaces. A jump in pressure across the interface, refereed to as capillary pressure, is generated. The pressure is directly influenced by the three-phase contact line of the solid, liquid, and gas.

For the liquid phase, the microscopic momentum balance equations (2.38) are:

$$-\rho_l \mathbf{g} + \nabla p_l = \mu_l \nabla^2 \mathbf{v}_l$$

They are augmented by the mass balance equation (2.30):

$$\nabla \cdot (\rho_l \mathbf{v}_l) = 0$$

And with $\rho_l = $ constant, this can be written as:

$$\nabla \cdot \mathbf{v}_l = 0 \tag{3.1}$$

with boundary conditions (similar to equations (2.31)):

B.C.1	$\mathbf{v}_l = 0$	at solid-liquid interface	(3.2)
B.C.2	$\mathbf{v}_g = \mathbf{v}_l$	at gas-liquid interface	(3.3)
B.C.3	$p_l(x) = -\gamma_{gl} C$	at gas-liquid interface	(3.4)
B.C.4	$p_l = p_{l_{0,1}}$	at entrances and exits of averaging volume	(3.5)

with C denoting the curvature of the gas-liquid interface and $p_{l_{0,1}}$ the entry and exit liquid pressure of an averaging volume.

Although the flow equations on the microscale are quasi-steady, due to the boundary conditions, the flow can be unsteady. Formally:

$$p_{l_{0,1}} = p_{l_{0,1}}(x, y, z, t) \tag{3.6}$$
$$\mathbf{v}_{l,g} = \mathbf{v}_{l,g}(x, y, z, t) \tag{3.7}$$
$$C = C(x, y, z, t) \tag{3.8}$$

This dependence on the time evolution of the boundary conditions influences the solution of the closure problem directly and gives rise to dynamic effects in the volume averaged flow equations.

3.4   Volume Averaging

In section 2.3 volume averaging was explained. Due to the specific nature of the two-phase flow problem certain averaging identities are worked out in detail. Equations (3.1) and (2.38) are averaged term by term, using volume averaging rules and theorems from vector integral calculus.

In the literature several examples exist of the use of volume averaging in a porous medium with constant volume fractions of fluids inside an averaging volume (see chapter 2). Averaging with variable fluid fractions is not common and introduces extra terms in the averaged equations which are similar to the case when the porosity varies (Ma and Ruth, 1993; Kaviany, 1995). Interfaces between the different phases are taken into account and are modeled in the closure approximation. This closure approximation circumvents the use of constitutive equations, which conventionally parameterize for phase interface effects (Whitaker, 1986b).

Here the boundary conditions are averaged also. This is necessary to keep the volume averaged equations compatible with the boundary conditions. Many workers do not directly consider the boundary conditions (Gray and Hassanizadeh, 1991a; Narasimhan, 1980b), or recognize their importance but ignore them in the averaging process (Whitaker, 1986b; Crapiste et al., 1986). The averaging of boundary conditions is sometimes used in pore network modeling (Dahle et al., 2002) and in unit cell concepts (Ma and Ruth, 1993). The direct averaging of the boundary conditions as part of the volume averaging helps in making the volume averaged equations applicable to practical situations. If the boundary conditions are not in an averaged form they are incompatible with the averaged equations.

3.4.1 Averaging of the mass balance equation

In contrast with single-phase flow, the mass balance equation has a different macroscopic form than the microscopic one. This is due to the change of fluid contents caused by the divergence of the macroscopic flow. This section follows closely Whitaker (1980, 1986b). Starting with equation (3.1), averaging the right hand side gives:

$$\langle 0 \rangle = 0 \tag{3.9}$$

The flow is incompressible (assumption 3.2.1), and the average of the left hand side is given by:

$$
\begin{aligned}
\langle \nabla \cdot \mathbf{v}_l \rangle &= \nabla \cdot \langle \mathbf{v}_l \rangle + \frac{1}{\mathcal{V}_0} \int_{\mathcal{S}} \boldsymbol{\nu} \cdot \mathbf{v}_l \, d\mathcal{S} \\
&= \nabla \cdot \langle \mathbf{v}_l \rangle + \frac{1}{\mathcal{V}_0} \int_{\mathcal{S}_{sl}} \boldsymbol{\nu} \cdot \mathbf{v}_l \, d\mathcal{S} + \frac{1}{\mathcal{V}_0} \int_{\mathcal{S}_{gl}} \boldsymbol{\nu} \cdot \mathbf{v}_l \, d\mathcal{S} \quad (3.10) \\
&= \nabla \cdot \langle \mathbf{v}_l \rangle + \frac{1}{\mathcal{V}_0} \int_{\mathcal{S}_{gl}} \boldsymbol{\nu} \cdot \mathbf{v}_l \, d\mathcal{S} \quad (3.11)
\end{aligned}
$$

where $\mathcal{S}_{gl}$ is the gas-liquid interfacial area and $\mathcal{S}_{sl}$ is the solid-liquid interfacial area. Because the solid-liquid interface is fixed in space, surface integrals normal to the solid-liquid interface which in the integrand explicitly contains the fluid velocity, are zero (eq. (3.2)). By making use of the transport theorem (Gray et al., 1993, p. 136, eq. 7.4):

$$\int_{\mathcal{V}} \left. \frac{\partial f}{\partial t} \right|_x d\mathcal{V} = \frac{d}{dt} \int_{\mathcal{V}} f \, d\mathcal{V} - \int_{\mathcal{S}} \boldsymbol{\nu} \cdot \mathbf{w} f \, d\mathcal{S} \tag{3.12}$$

where $\mathbf{w}$ is the velocity of the interface. Setting $f = 1$, $\mathcal{V} = n_l \mathcal{V}_p$ (volume of fluid):

$$
\begin{aligned}
\int_{(n_l \mathcal{V}_p)} \left. \frac{\partial 1}{\partial t} \right|_x d(n_l \mathcal{V}_p) &= \frac{d}{dt} \int_{(n_l \mathcal{V}_p)} 1 \, d(n_l \mathcal{V}_p) - \int_{\mathcal{S}} \boldsymbol{\nu} \cdot \mathbf{w} 1 \, d\mathcal{S} \\
0 &= \frac{\partial n_l \mathcal{V}_p}{\partial t} - \int_{\mathcal{S}_{sl}} \boldsymbol{\nu} \cdot \mathbf{w} \, d\mathcal{S} - \int_{\mathcal{S}_{gl}} \boldsymbol{\nu} \cdot \mathbf{w} \, d\mathcal{S} \quad (3.13)
\end{aligned}
$$

$$0 = \frac{\partial n_l \mathcal{V}_p}{\partial t} - \int_{\mathcal{S}_{gl}} \boldsymbol{\nu} \cdot \mathbf{w} \, d\mathcal{S}$$

$$0 = \frac{\partial \epsilon n_l}{\partial t} - \frac{1}{\mathcal{V}_0} \int_{\mathcal{S}_{gl}} \boldsymbol{\nu} \cdot \mathbf{w} \, d\mathcal{S} \qquad (3.14)$$

with ϵ the porosity. Adding equation (3.14) to equation (3.11):

$$\langle \nabla \cdot \mathbf{v}_l \rangle = \nabla \cdot \langle \mathbf{v}_l \rangle + \frac{1}{\mathcal{V}_0} \int_{\mathcal{S}_{gl}} \boldsymbol{\nu} \cdot (\mathbf{v}_l - \mathbf{w}) \, d\mathcal{S} + \frac{\partial \epsilon n_l}{\partial t} \qquad (3.15)$$

Assuming no mass transport over the gas-liquid interface (immiscible) requires that $\mathbf{v}_l - \mathbf{w} = 0$ or $\mathbf{v}_l = \mathbf{w}$, so that the above equation reduces to:

$$\langle \nabla \cdot \mathbf{v}_l \rangle = \nabla \cdot \langle \mathbf{v}_l \rangle + \frac{\partial \epsilon n_l}{\partial t} \qquad (3.16)$$

This equation contains the time derivative of the liquid content. The time dependence enters the equation due to the time dependence of the microscopic boundary conditions, i.e. the movement of the gas-liquid interface, resulting in the non-zero divergence of the average velocity.

3.4.2   Averaging of the momentum balance equation

Like the mass balance equation, the momentum balance (eq. (2.38)) is averaged term by term.

Averaging of the body-force term

The components of the body force term are constant, and their treatment in volume averaged form is similar to the microscopic form (Whitaker, 1986b):

$$\langle -\rho_l \mathbf{g} \rangle = -\frac{1}{\mathcal{V}_0} \int_{\mathcal{V}_0} \rho_l \mathbf{g} \, d\mathcal{V} \qquad (3.17)$$

$$\langle -\rho_l \mathbf{g} \rangle = -\frac{1}{\mathcal{V}_0} \left[\int_{\mathcal{V}_l} \rho_l \mathbf{g} \, d\mathcal{V} + \int_{\mathcal{V}_0 - \mathcal{V}_l} \rho_l \mathbf{g} \, d\mathcal{V} \right] \qquad (3.18)$$

Because ρ_l is zero in $\mathcal{V}_0 - \mathcal{V}_l$, i.e. the volume not occupied by the liquid:

$$\langle -\rho_l \mathbf{g} \rangle = -\frac{1}{\mathcal{V}_0} \int_{\mathcal{V}_l} \rho_l \mathbf{g} \, d\mathcal{V} \tag{3.19}$$

$$\langle -\rho_l \mathbf{g} \rangle = -\frac{\mathcal{V}_l}{\mathcal{V}_0} \rho_l \mathbf{g} \tag{3.20}$$

$$\langle -\rho_l \mathbf{g} \rangle = -\epsilon n_l \rho_l \mathbf{g} \tag{3.21}$$

Averaging of the pressure term

The pressure term contains the liquid pressure gradient. It is the most problematic term in the averaging process. Different researchers treat this term in completely different manners (Whitaker, 1986b; Hassanizadeh and Gray, 1993; Hassanizadeh et al., 2002; Dahle et al., 2002). As described in chapter 2, the pressure is used to describe the capillary component of the liquid potential and it is assumed that this drives the flow and is responsible for the bulk liquid phase movement. The treatment is based on an incompressible liquid. No macroscopic volume average form for the phase average pressure is proposed. Instead a nonlocal formulation is developed in chapter 5. It is based on an areal averaged pressure. In essence, the pressure gradient term is part of the closure problem, and in this chapter simply written in integral form:

$$\langle \nabla p_l \rangle = \frac{1}{\mathcal{V}_0} \int_{\mathcal{V}_0} \nabla p_l \, d\mathcal{V} \tag{3.22}$$

Treatment of the gradient of the liquid pressure as part of the closure problem is not common, and the question arises why the more common treatment of the pressure as a volume averaged quantity as in Whitaker (1986b), or a thermodynamics based approach as in Hassanizadeh and Gray (1997) is not used. In appendix A the traditional method of averaging the liquid pressure term is worked out. The major problem with this method is that there are no instruments measuring a volume averaged pressure. All instruments (e.g. tensiometers) measure a force per unit area, i.e. pressure averaged over a representative area. A tensiometer measures the areal averaged pressure around its circumference. This measurement includes the effect of gravity on the measurement, but this effect is small when the tensiometer is small. A similar reasoning can be applied to a multi-step outflow experiment in a pressure cell. Here the boundary conditions are applied on ceramic plates, which cover the

entrance and exit of the porous medium, and thus apply a uniform areal averaged liquid pressure. Here the gradient of the volume average pressure is not used at the boundaries of the porous medium, and on the macroscopic scale no volume average pressure needs to be defined (criterion IV, p. 29). Instead of the gradient of the volume averaged liquid pressure used in the traditional equations, the average of the pressure term is expressed here as a nonlocal term, which can be called the "volume average difference of the area averaged liquid pressure". The treatment of measurements and calculations for flow inside a porous medium is further developed in chapters 5 and 6. Alemán et al. (1989) in effect use the pressure at the boundaries of an averaging volume to define a volume averaged liquid pressure. As such their treatment is similar to the one used here, but they make the additional simplifying assumption that no pressure gradient inside of the averaging volume exists. As shown earlier, this leads to the following paradox: Flow is due to a pressure gradient, and if there is flow inside an averaging volume, there must be a pressure gradient. But in order to conduct the volume averaging it is assumed that there is no pressure gradient, and this implies no liquid flow.

Averaging of the viscous term

The viscous term is averaged in a similar way as described by du Plessis and Diedericks (1997) and Whitaker (1986b). The major difference in the derivation is due to the influence of the time dependent gas-liquid boundary:

$$
\begin{aligned}
\langle \mu_l \nabla^2 \mathbf{v}_l \rangle &= \langle \mu_l \nabla \cdot (\nabla \mathbf{v}_l) \rangle \\
&= \mu_l \nabla \cdot \langle \nabla \mathbf{v}_l \rangle + \frac{\mu_l}{\mathcal{V}_0} \int_{\mathcal{S}_{slg}} \boldsymbol{\nu} \cdot (\nabla \mathbf{v}_l) \, d\mathcal{S} \\
&= \mu_l \nabla \cdot \left[\nabla \langle \mathbf{v}_l \rangle + \frac{1}{\mathcal{V}_0} \int_{\mathcal{S}_{slg}} \boldsymbol{\nu} \mathbf{v}_l \, d\mathcal{S} \right] + \frac{\mu_l}{\mathcal{V}_0} \int_{\mathcal{S}_{slg}} \boldsymbol{\nu} \cdot (\nabla \mathbf{v}_l) \, d\mathcal{S} \\
&= \mu_l \nabla^2 \langle \mathbf{v}_l \rangle + \frac{\mu_l}{\mathcal{V}_0} \left[\nabla \cdot \int_{\mathcal{S}_{slg}} \boldsymbol{\nu} \mathbf{v}_l \, d\mathcal{S} + \int_{\mathcal{S}_{slg}} \boldsymbol{\nu} \cdot (\nabla \mathbf{v}_l) \, d\mathcal{S} \right] \quad (3.23)
\end{aligned}
$$

Using the vector identity (Bird et al., 1960, eq. A.3-14):

$$
\nabla^2 \langle \mathbf{v}_l \rangle = \nabla (\nabla \cdot \langle \mathbf{v}_l \rangle) - \nabla \times (\nabla \times \langle \mathbf{v}_l \rangle)
$$

the above equation can be written as:

$$
\begin{aligned}
\langle \mu_l \nabla^2 \mathbf{v}_l \rangle &= \mu_l \left[\nabla(\nabla \cdot \langle \mathbf{v}_l \rangle) - \nabla \times (\nabla \times \langle \mathbf{v}_l \rangle) \right] \\
&\quad + \frac{\mu_l}{\mathcal{V}_0} \left[\nabla \cdot \int_{\mathcal{S}_{slg}} \boldsymbol{\nu} \mathbf{v}_l \, d\mathcal{S} + \int_{\mathcal{S}_{slg}} \boldsymbol{\nu} \cdot (\nabla \mathbf{v}_l) \, d\mathcal{S} \right]
\end{aligned}
\tag{3.24}
$$

This form of the volume averaged viscous term will be further used in the closure. It should be noted that the macroscopic velocity $\langle \mathbf{v}_l \rangle$ is non-zero if the liquid content inside an averaging volume changes due to inflow, even if there is no outflow or vice versa (Pride and Flekkøy, 1999). The term $\mu_l \nabla^2 \langle \mathbf{v}_l \rangle$ is usually called the Brinkman term (Brinkman, 1947, 1949; Kaviany, 1995).

3.4.3 Averaging of the boundary conditions

In order to keep the boundary conditions (eqs. (3.2), (3.3), (3.4), and (3.5)) compatible with the volume averaged equations, they too need to be averaged. The boundary conditions internal in an averaging volume have no analog on the macroscopic scale, and thus do not arise on this scale. They are accounted for in the closure. In effect only equations (3.5) exist on the macroscale, supplemented by other macroscale boundary conditions (see sec. 5.4). Equation (3.5) needs to be compatible with the averaged pressure gradient term, and as such is area averaged over the entrances and exits of an averaging volume:

$$
\begin{aligned}
\langle p_l|_0 \rangle &= \frac{1}{\mathcal{S}_0} \int_{\mathcal{S}_0} p_0 \, d\mathcal{S} \\
&= p_0 \tag{3.25} \\
\langle p_l|_1 \rangle &= \frac{1}{\mathcal{S}_1} \int_{\mathcal{S}_1} p_1 \, d\mathcal{S} \\
&= p_1 \tag{3.26}
\end{aligned}
$$

with the following definitions:

$$
p_{1,0} = \frac{1}{\mathcal{S}_{\text{exit, entry}}} \int_{\mathcal{S}_{\text{exit, entry}}} p_l \, d\mathcal{S}
\tag{3.27}
$$

That is, $p_{1,0}$ is the area averaged pressure at the exit c.q. entrance.

3.4.4   The combined averaged equations

The combined averaged mass balance equation becomes (eqs. (3.16), (3.9)):

$$\nabla \cdot \langle \mathbf{v}_l \rangle = -\frac{\partial \epsilon n_l}{\partial t} \tag{3.28}$$

The volume averaged momentum balance equations are obtained by combining equations (3.21), (3.22) and (3.24):

$$-\epsilon n_l \rho_l \mathbf{g} + \mu_l \left[-\nabla(\nabla \cdot \langle \mathbf{v}_l \rangle) + \nabla \times (\nabla \times \langle \mathbf{v}_l \rangle) \right]$$
$$= \frac{\mu_l}{\mathcal{V}_0} \nabla \cdot \int\limits_{\mathcal{S}_{slg}} \boldsymbol{\nu} \mathbf{v}_l \, d\mathcal{S} + \frac{\mu_l}{\mathcal{V}_0} \int\limits_{\mathcal{S}_{slg}} \boldsymbol{\nu} \cdot (\nabla \mathbf{v}_l) \, d\mathcal{S} - \frac{1}{\mathcal{V}_0} \int\limits_{\mathcal{V}_0} \nabla p_l \, d\mathcal{V} \tag{3.29}$$

These are the upscaled momentum balance equations valid at the macroscale. The terms on the left hand side only contain macroscopic variables, whereas the terms on the right hand side contain microscopic variables inside the integrals. These terms represent the closure problem. In chapter 5 these equations are further analyzed. The averaged boundary conditions are given by p_0 and p_1.

4 Closure Model

4.1 Introduction

This chapter describes the development of a Representative Unit Cell (RUC) model for the closure of the volume averaged equations derived in chapter 3, and the proposed solution for the local flow equations. In sections 4.2 and 4.3 the geometrical RUC model together with the capillary pressure model is explained. An RUC is similar to a Representative Elementary Volume (REV) in the sense that it is a three dimensional averaging volume, but the concept of an RUC also entails a detailed geometrical description. This description is to imagine a typical porous medium configuration in which the flow processes are modeled. The RUC should not be equated with a portion of a real porous medium, because not all features of a real porous medium are modeled. Its "average" behavior is assumed to mimic the behavior of a real porous medium. The emphasis is on those features which directly influence the flow processes on average. The RUC needs to accommodate the topology, geometry and capillary pressure relationship of a porous medium. As shown in chapter 2, capillarity plays a major role in unsaturated flow. The geometry of the RUC is expressed in terms of the macroscopic parameters porosity, ϵ, and the critical radius for drainage, r_c. Additionally three RUC parameters, a, b, and j, will be defined. In sections 4.4 and 4.5 the microscopic momentum equations are solved, based on a Poiseuille type flow model. The solution is then used in the closure of equations (3.29).

4.2 Description of the RUC

The RUC is made of a cubic unit cell. In this chapter no explicit relations are given for the stacking of RUC's, as we are concerned only with the local flow problem here. du Plessis and Diedericks (1997) show that for a variety of RUC configurations in single-phase flow, maximum staggering is the

$b = 1$ $b = 2$
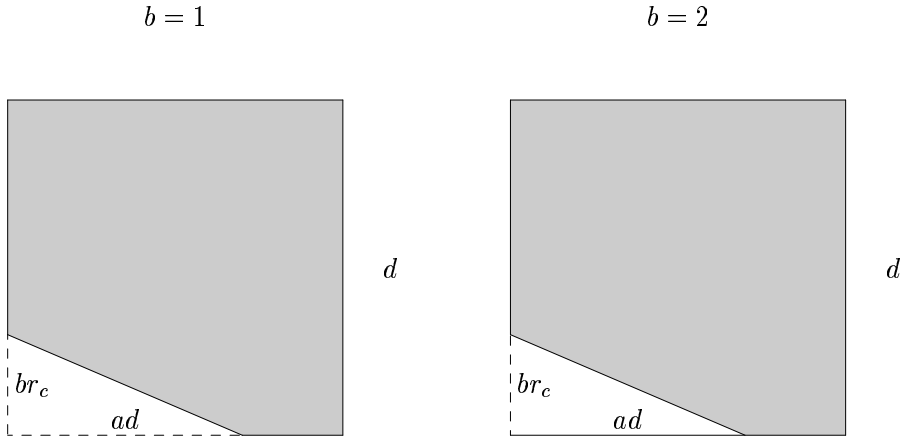
Figure 4.1: Two different RUC's, frontal view; dashed lines indicate opening to neighboring RUC; gray parts denote solid and white parts denote pore (symbols explained in text).

appropriate stacking configuration. For two-phase flow it is important to allow for continuity of the capillary held liquid phase, and thus corners should be assumed continuous across RUC's. The RUC's are assumed to model an isotropic porous medium, i.e. the configuration of the RUC's does not depend on direction (assumption 6, p. 35). The concept of an RUC is based on what a particle of liquid "sees" while flowing through a porous medium, and as such is similar to the definition of an REV.

4.2.1 Topology and geometry

The topology of the RUC allows for continuous corners and channels. If this were not the case, fluid could not flow, or capillary held fluid would be discontinuous, and two-phase flow would cease. To allow for a variety of different porous media to be modeled, an RUC can have open areas connecting to neighboring RUC's (fig. 4.1). The channels in the RUC follow a three-dimensional path, following three edges of the RUC cube. They are non-intersecting and continuous (fig. 4.2).
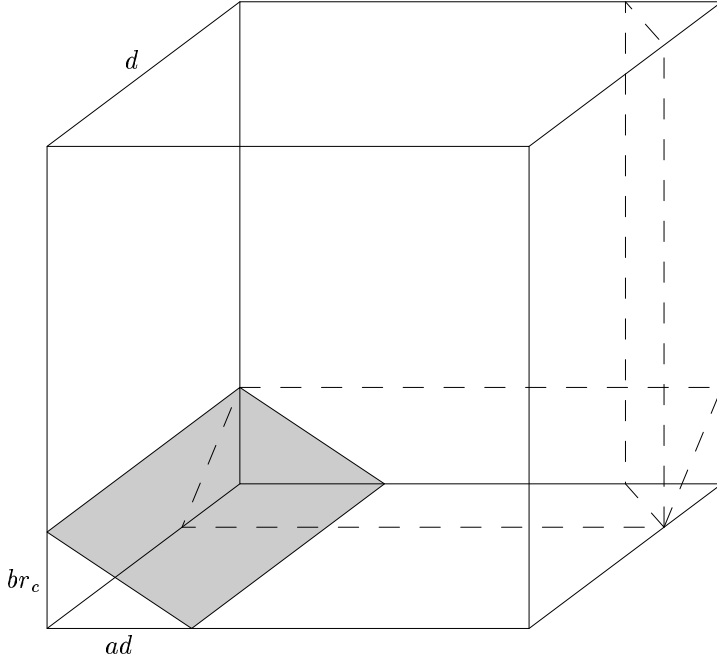
Figure 4.2: Geometry of RUC.

4.2.2   Geometrical properties

The channels inside the RUC model the pores in a porous medium. For single-phase flow, du Plessis and Roos (1994) developed an RUC model for sandstones. The RUC model presented here is adapted to two-phase flow. The cross-section of the channels can have different forms appropriate for the microstructure of the porous medium, e.g. triangular wedge like. The triangular wedge or corner can be open to the neighboring RUC or closed. This form is one of many: elliptical, rhombical and hypotrochoidal channels are also possible (van Brakel, 1975; Sisavath et al., 2000). Once a geometry is chosen for a given RUC, the geometrical parameters used in the flow equations can be determined.

The frontal pore area $\mathcal{A}_p$ of the RUC is given by (fig. 4.2):

$$\mathcal{A}_p \quad = \quad \frac{1}{2}\, adbr_c j \tag{4.1}$$

In this definition multiple channels are taken into account through the factor j, the number of channels or wedges inside an RUC. The factor a accounts for

the base length of the wedge relative to d, the RUC dimension. If the RUC channel is closed $b = 2$, or if open $b = 1$ (fig. 4.1). The critical radius for drainage (explained in section 4.3) is given by r_c.

The saturated "wetted" perimeter of a single pore corner is defined as:

$$\mathcal{P}_p = ad + (a^2d^2 + b^2r_c^2)^{1/2} \tag{4.2}$$

and the saturated wetted perimeter of an RUC is:

$$\mathcal{P} = \begin{cases} j(ad + (a^2d^2 + b^2r_c^2)^{1/2}) & : \text{ if } b = 2 \\ j(a^2d^2 + b^2r_c^2)^{1/2} & : \text{ if } b = 1 \end{cases} \tag{4.3}$$

Through trigonometric relations $\tan\alpha$ and $\sin\alpha$ are defined by:

$$\tan(\alpha) = \frac{r_c}{ad} \tag{4.4}$$

$$\sin(\alpha) = \frac{r_c}{(r_c^2 + a^2d^2)^{1/2}} \tag{4.5}$$

with α the half opening angle of the wedge. The pore volume $\mathcal{V}_p$ is defined from the RUC geometry as:

$$\mathcal{V}_p = 3d\mathcal{A}_p - \frac{j}{3}(a^2d^2br_c + b^2r_c^2ad) \tag{4.6}$$

$$= \mathcal{A}_p(3d - \frac{2}{3}(ad + br_c)) \tag{4.7}$$

As an approximation the flow length l_g inside the RUC is computed by requiring that the pore volume is equal to the frontal pore area times the flow length:

$$\mathcal{V}_p = l_g\mathcal{A}_p \tag{4.8}$$

$$l_g = \frac{\mathcal{V}_p}{\mathcal{A}_p} \tag{4.9}$$

$$= \frac{2\epsilon d^2}{abr_cj} \tag{4.10}$$

using the relation $\mathcal{V}_p = \epsilon d^3$ and equation (4.1). The above definition of l_g does not take into account changes in volumetric flow inside the different corners,

but is based on the ratio of the volume of a straight channel to the curved one inside the RUC.

Taking together equations (4.1), (4.6) and $\mathcal{V}_p = \epsilon d^3$:

$$d = \frac{br_c}{12\epsilon} \left((a^2 j^2 (2a-9)^2 - 48aj\epsilon)^{1/2} + aj(9-2a) \right) \tag{4.11}$$

In the above development r_c and ϵ are taken as the main structural parameters of the porous medium. These parameters in turn define the magnitude of the parameters d and α, together with a, b and j. With these, the geometry of an RUC is completely defined. The parameters r_c and ϵ are regarded as macroscopic parameters of the porous medium, and are directly measurable on the macroscopic scale.

4.3 Capillary Pressure Relationship

The relation between the pressure difference between the fluids and the liquid saturation is modeled similar to Mason and Morrow (1991), using the Mayer and Stowe-Princen (MSP) method (Princen, 1969a,b, 1970). The relationship does not take into account the effects of short range adhesion forces, but could be modified accordingly with the Augmented Young-Laplace equation (see section 2.2.2).

If a non-wetting fluid enters a pore filled with a wetting fluid, an interface between the two fluids is formed. This interface is called a main terminal meniscus (MTM). As soon as the two principal radii of the meniscus have the same magnitude, the non-wetting fluid enters the capillary. This radius is called the critical radius for drainage, r_c. During imhibition, when a wetting fluid fills a capillary, a possibly different critical radius corresponds to complete filling of the capillary with the wetting fluid. This radius corresponds to the situation that the liquid from the separate corners starts to touch each other. Both critical radii depend on the contact angle and the specific geometry of the pore. For the modeling of the capillary pressure saturation relationship, channel curvature in the longitudinal direction is not taken into account. The critical radius for drainage is expressed as:

$$r_c = -\frac{\gamma_{gl}}{p_{lc}} \tag{4.12}$$

In this expression assumption 11 (p. 35) was used, which implies that the contact angle $\theta = 0$. The critical liquid pressure for drainage p_{lc} is similar to

the air entry pressure in traditional soil physics modeling. Equation (4.12) is written without the factor 2 in the Young-Laplace equation for a spherical interface. This corresponds to $R_2 = \infty$ in equation (2.18). Effectively it is assumed that the gas liquid interface is approximately cylindrical at $r = r_c$ inside a pore, and that at gas entry, the pore drains abruptly. The use of equation (4.12) allows r_c to be calculated from the air entry pressure of a desaturation experiment. Thus r_c is defined based on a macroscopic measurement and as such a macroscopic measurable parameter. In effect, r_c denotes some kind of "average" critical radius for drainage.

4.3.1   Geometry of liquid inside a corner

In this section basic equations for the wetting fluid (liquid) inside a corner of a pore are derived. The following equations are derived for a single corner only (fig. 4.3) and still have to be assembled for the particular RUC in question. The fluid configuration has to obey the Concus-Finn conditions (Weislogel and Lichter, 1998) in order to yield a stable interface:

$$\theta < \frac{\pi}{2} - \alpha \tag{4.13}$$

with θ the contact angle and α the half opening angle of the corner. This condition states that liquid forms a stable interface only in certain combinations of corner opening half angle and contact angle. The length of the solid-liquid interface inside a corner is defined by (see fig. 4.3):

$$\mathcal{L}_{sl} = \frac{2r\cos(\theta + \alpha)}{\sin(\alpha)} \tag{4.14}$$

and with $\theta = 0$:

$$\mathcal{L}_{sl} = \frac{2}{\tan(\alpha)}\, r \tag{4.15}$$

$$= f_{\mathcal{L}_{sl}}\, r \tag{4.16}$$

Similarly, $\mathcal{L}_{gl}$ is defined as:

$$\mathcal{L}_{gl} = (\pi - 2\alpha - 2\theta)r \tag{4.17}$$

and with $\theta = 0$:

$$\mathcal{L}_{gl} = (\pi - 2\alpha)r \tag{4.18}$$

$$= f_{\mathcal{L}_{gl}}\, r \tag{4.19}$$
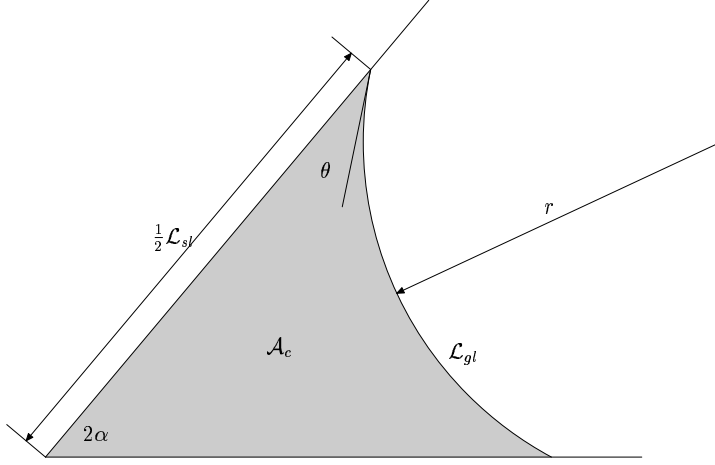
Figure 4.3: Geometry of interface between liquid and gas inside a corner; direction of flow is perpendicular to the paper.

The liquid filled area of a corner, $\mathcal{A}_c$, (fig. 4.3) given a radius of curvature of the gas-liquid interface, is defined by:

$$\mathcal{A}_c = r^2 \left[\frac{\cos^2(\theta + \alpha)\cos(\alpha)}{\sin(\alpha)} + \alpha + \theta - \frac{\pi}{2} + \frac{1}{2}\sin(2\theta + 2\alpha) \right] \qquad (4.20)$$

and, again, with $\theta = 0$:

$$\mathcal{A}_c = r^2 \frac{1 + (\alpha - \frac{\pi}{2})\tan(\alpha)}{\tan(\alpha)} \qquad (4.21)$$

$$= f_{\mathcal{A}} \, r^2 \qquad (4.22)$$

If the curvature of the gas liquid interface is approximately along r, i.e. R_1 in equation (2.13), the liquid pressure can be expressed as:

$$p_l = -\frac{\gamma_{gl}}{r} \qquad (4.23)$$

The liquid volume in a corner in the two-phase case is calculated as:

$$\mathcal{V}_c = \int_{l_g} \mathcal{A}_c \, dx \qquad (4.24)$$

And the liquid volume inside an RUC as:

$$\mathcal{V}_l = \int_{l_g} \frac{1}{2} \mathcal{A}_c bj \, dx \qquad (4.25)$$

$$= \quad \frac{1}{2}\, b j \mathcal{V}_c \tag{4.26}$$

The above definitions define the geometry related variables for an RUC. They will be used in the solution of the local RUC flow model in section 4.4 and in chapter 5 for the closure.

4.4   Flow Models

In order to find an approximate analytical solution for the closure problem, the resistance to flow in the RUC channels needs to be specified. Single-phase flow in micro channels was studied by e.g. MacLaine-Cross (1969), Ayyaswamy et al. (1974), Sisavath et al. (2000, 2001), Thompson and Fogler (1997), and Patzek and Kristensen (2001). The standard monograph on the subject is Shah and London (1978). Common to these approaches is the assumption of Stokes flow, which leads to a Poiseuille flow regime inside the channel for fully developed flow (Romero and Yost, 1996; Weislogel and Lichter, 1998). In two-phase flow in micro channels, the liquid is in part in contact with the solid surface, and in part with another fluid phase. Here the other fluid phase is a gas (air), which exerts no shear stress on the liquid (Ma et al., 1994; Hilfer, 1996). For slow flows, as studied here, the velocity profile is nearly instantaneously fully developed (Weislogel and Lichter, 1998), and curvature effects along the corner are not significant. This assumption introduces negligible error if the flow length is larger than $2-3$ times the hydraulic radius (Ruth and Ma, 1993).

How can such a simple flow model reflect the flow in porous media, where the pores are not smooth and converging-diverging? Erickson et al. (2002) showed by numerical calculations that the basic flow mechanism in capillary pressure driven flow does not change qualitatively in converging-diverging pores in an average sense. What does change are the values of some parameters, but the dynamics stay the same. Borhan and Rungta (1993) showed, by using a semi-analytic model for flow between periodically corrugated plates, that the flow equations can be scaled to the standard dynamic ones, but with another characteristic capillary penetration time. Lago and Araujo (2001) and Staples and Shaffer (2002), by experiments and by a morphological porous medium model, showed that these dynamics also hold in porous media. Lago and Araujo (2001) also observed the typical algebraic behavior of the capillary velocity against time. As slow, continuous flow is assumed, contact line pinning is assumed to play no significant role. Pinning is mostly important near the imhibition threshold, but there is no direct evidence that it is important in

corner flow (Schäffer and Wong, 2000). Lago and Araujo (2001) showed that pinning has influence in packings of glass beads, but that no such behavior can be observed in sandstones. It is assumed that this has to do with the micro structure of the pores in packings of glass beads. In these the wetting fluid has no continuous corners for flow, but instead has to follow converging-diverging flow paths. In sandstones the flow paths are more wedge like, as is assumed here. Weislogel and Lichter (1998) state that because the flow in a corner is predominantly parallel to the contact line, the normal velocity perpendicular to the contact line is small, and the discontinuity in the velocity at the contact line is not significantly influencing the flow (see assumption 12, p. 36).

Rewriting the momentum balance equations (eqs. 2.10) as (Shah and London, 1978):

$$\nabla^2 \mathbf{v}_l = \frac{1}{\mu} \nabla p_l \tag{4.27}$$

and:

$$\nabla^2 \mathbf{v}_l = \text{constant} \tag{4.28}$$

i.e. fully developed flow. Under the assumption of Poiseuille flow this leads to (Panton, 1984):

$$\mathbf{v}_{p,c} = -\frac{F_{p,c}}{\mu_l} \mathcal{A}_c \frac{\partial p_l}{\partial x} \tag{4.29}$$

with $F_{p,c}$ a resistance factor and the average pore or corner velocity defined as:

$$\mathbf{v}_{p,c} = \frac{1}{\mathcal{A}_c} \int_{\mathcal{A}_c} \mathbf{v}_l \; d\mathcal{A} \tag{4.30}$$

4.4.1 Single-phase flow

For single-phase flow, the magnitude of $\mathbf{v}_p$ does not change in axial direction. F_p is a constant, as is the pressure drop. Commonly the resistance factor for laminar flow in pipes is expressed as the product of the Fanning friction factor f and the Reynolds number Re (Shah and London, 1978):

$$f\text{Re} = \text{constant} \tag{4.31}$$

The definition of the Reynolds number for flow in the pores is:

$$\mathrm{Re} = \rho_l \left| \mathbf{v}_p \right| \frac{4 r_h}{\mu_l} \tag{4.32}$$

The Fanning friction factor is given by (Ma et al., 1994; Shah and London, 1978):

$$\mathrm{f} = \frac{2 r_h}{\rho_l |\mathbf{v}_p|^2} \frac{\partial p_l}{\partial x} \tag{4.33}$$

Combining equations (4.32) and (4.33) gives:

$$\mathrm{fRe} = \frac{8 r_h^2}{\mu_l \left| \mathbf{v}_p \right|} \frac{\partial p_l}{\partial x} \tag{4.34}$$

with the hydraulic radius r_h of a cross section of the pores inside an RUC defined by:

$$r_h = \frac{\mathcal{A}_p}{\mathcal{P}_p} \tag{4.35}$$

Combined, the above equations define the following equation for single phase flow in a pore:

$$\mathbf{v}_p = -\frac{8 r_h^2}{\mu_l \, \mathrm{fRe}} \frac{\partial p_l}{\partial x} \tag{4.36}$$

By comparing equations (4.29) and (4.36), the relation between fRe and F can be obtained:

$$F_p = \frac{8}{\mathrm{fRe}} \frac{r_h^2}{\mathcal{A}_p} \tag{4.37}$$

Numerical values for fRe are given in Shah and London (1978) for different pore geometries.

4.4.2 Two-phase flow

Capillary driven two-phase flow in a corner is described by a Poiseuille type equation, similar to a nonlinear diffusion equation (Dong and Chatzis, 1995; Romero and Yost, 1996; Weislogel and Lichter, 1998). This nonlinear partial differential equation is similar to the foam drainage equation (Verbist et al., 1996). In principle it can be transformed to an ordinary differential equation by a similarity transformation (Mayer et al., 1983). Weislogel and Lichter (1998) list classes of solutions for this equation with given boundary conditions. For instance, for a constant pressure boundary condition the speed of the advancing meniscus is proportional to $\sqrt{t}$. There are no general analytical solutions available for arbitrary initial and boundary conditions, but the dynamics were studied for a variety of conditions by Weislogel and Lichter (1998), Weislogel (2001), and Romero and Yost (1996). Solutions were established for planar and non-planar corner geometries. Apart from a solution for the dynamics of this equation, an approximation for the resistance factor is also required. The derivation of the resistance factors for two-phase flow in corners was studied by Ayyaswamy et al. (1974). Ransohoff and Radke (1988) used finite element calculations to derive the resistance factor. Zhou et al. (1997) developed analytical correlations, but their correlations can deviate substantially from the true solution. Weislogel and Lichter (1998) developed the method used here, by scaling of the flow equations. The corner flow problem is also widely studied in heat transfer in micro channels, e.g. in electronics cooling. These solutions are usually not applicable, because due to forced convection the shear stress at the gas-liquid interface is not negligible (Suh et al., 2001).

The general geometry of the flow is shown in figure 4.4. The governing equation (4.27) can be rewritten as:

$$\frac{\partial p_l}{\partial x} = \mu_l \left(\frac{\partial^2}{\partial y^2} \mathbf{v}_l + \frac{\partial^2}{\partial z^2} \mathbf{v}_l \right) \tag{4.38}$$

Scaling by $x^* = x/L$, $y^* = y/H$, $z^* = z/(H\tan(\alpha))$, $v^* = \mathbf{v}_l/v$, and $P^* = fHp_l/\gamma_{gl}$ (with starred quantities denoting dimensionless quantities), yields:

$$\frac{\gamma_{gl}}{HfL} \frac{\partial P^*}{\partial x^*} = \mu_l v \left(\frac{1}{H^2 \tan^2(\alpha)} \frac{\partial^2 v^*}{\partial y^{*2}} + \frac{1}{H^2} \frac{\partial^2 v^*}{\partial z^{*2}} \right) \tag{4.39}$$

with L a characteristic length scale along the pore, H a characteristic height of the liquid, α the half opening angle of the wedge, v a characteristic velocity,
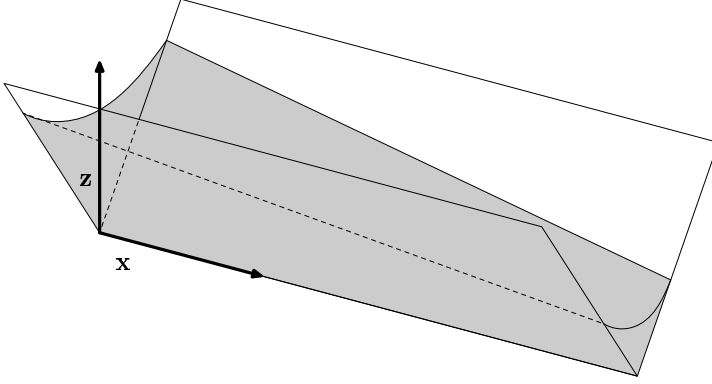
Figure 4.4: Geometry for two-phase corner flow in a wedge, gray area denotes fluid filled part.

and P^* scaled by $\frac{fH}{\gamma_{gl}}$ to take surface tension effects into account. The factor f is defined by (Weislogel and Lichter, 1998):

$$f = \frac{\sin \alpha}{\cos \theta - \sin \alpha} \tag{4.40}$$

Written as a balance between the left hand side and the right hand side, and dropping the differential terms, assumed $\mathcal{O}(1)$ (Weislogel, 2001), equation (4.39) becomes:

$$\frac{\gamma_{gl}}{HfL} \sim \mu_l v \left(\frac{1}{H^2 \tan^2(\alpha)} + \frac{1}{H^2} \right) = \frac{\mu_l v}{H^2 \sin^2(\alpha)} \tag{4.41}$$

Solving for v, this gives the velocity scale:

$$v = \frac{H}{L} \frac{\gamma_{gl} \sin^2(\alpha)}{\mu_l f} \tag{4.42}$$

This velocity scale is composed of the geometry dependent terms $\frac{H}{L} \frac{\sin^2(\alpha)}{f}$, and the balance between surface tension and viscosity. It is used to scale the resistance factor for two-phase flow. This simple analysis shows that surface tension, viscosity and geometry are the main determining factors for this type of flow.

Two-phase flow model

In this section the flow model for two-phase flow is developed. The model takes into account the change of liquid area available for flow along a pore coupled to the change of capillary pressure. The mass balance equation for quasi one-dimensional flow along a corner can be written as (Dong and Chatzis, 1995):

$$\frac{\partial}{\partial x}\mathbf{q}_c(x,t) = -\frac{\partial}{\partial t}\mathcal{A}_c(x,t) \tag{4.43}$$

with $\mathbf{q}_c(x,t) = \mathbf{v}_c\mathcal{A}_c$, the volumetric corner discharge.

The scaling factor of equation (4.42) is based on a two-dimensional flow description. In order to use it in the quasi one-dimensional Poiseuille equation (eq. (4.29)), it is adapted resulting in a dimensionless resistance factor $F_v\frac{\sin^2(\alpha)}{f^2 f_{\mathcal{A}}}$. Substituting this resistance factor in the flow equation (eq. (4.29)), the flow equation for a corner becomes:

$$\mathbf{v}_c = -\frac{F_v}{\mu_l}\frac{\sin^2(\alpha)}{f^2 f_{\mathcal{A}}}\mathcal{A}_c\frac{\partial p_l}{\partial x} \tag{4.44}$$

for Poiseuille type flow (Weislogel and Lichter, 1998). F_v is a dimensionless constant, defined as in Weislogel and Lichter (1998):

$$F_v = 1.6 \ ... \ 1.8 \approx 1.7 \tag{4.45}$$

Equation (4.44) is a scaled form of equation (4.29). The resistance factor F_c for two-phase flow from equation (4.29) can then be written as:

$$F_c = F_v\frac{\sin^2(\alpha)}{f^2 f_{\mathcal{A}}} \tag{4.46}$$

In steady state, equation (4.43) becomes $\frac{\partial}{\partial x}\mathbf{q}_c(x,t) = 0$ and can be analytically integrated together with equation (4.44). This leads to an expression of the liquid area in a corner:

$$\mathcal{A}_c(x) = (A_0^{3/2} + x\frac{(A_1^{3/2} - A_0^{3/2})}{l_g})^{2/3} \tag{4.47}$$

where the subscripts $_0$ and $_1$ denote the entrance and exit of the corner. The above equation can be integrated along the corners in a RUC, yielding an

expression for the volume of liquid, expressed in terms of liquid entrance and exit pressure. Using equation (4.25):

$$\mathcal{V}_l \quad = \quad \frac{3bjf_\mathcal{A}\gamma_{gl}^2 l_g(p_1^{-5} - p_0^{-5})}{10(p_1^{-3} - p_0^{-3})} \tag{4.48}$$

whereby equations (4.22) and (4.23) are used to express $\mathcal{A}_c$ in terms of p_l. With the definition of $n_l = \mathcal{V}_l/\mathcal{V}_p$ (eq. (2.40)):

$$n_l = \frac{3bjf_\mathcal{A}\gamma_{gl}^2 l_g(p_0^4 + p_1 p_0^3 + p_0^2 p_1^2 + p_0 p_1^3 + p_1^4)}{10\mathcal{V}_p(p_0^2 + p_0 p_1 + p_1^2)p_0^2 p_1^2} \tag{4.49}$$

The above expression for n_l will be used in chapter 6 in the calculations of the quasi steady momentum balance. If $p_0 = p_1 = p_a^l$:

$$n_l = \frac{bjf_\mathcal{A}\gamma_{gl}^2 l_g}{2\mathcal{V}_p p_a^{l\,2}} \tag{4.50}$$

In the closure (ch. 5), the following definition for the cross sectional average shear stress for a corner is used (Shah and London, 1978; Ma et al., 1994):

$$\tau_{\mathcal{S}_{sl}}(x) = -\frac{\partial p_l}{\partial x}\frac{\mathcal{A}_c}{\mathcal{L}_{sl}} \tag{4.51}$$

4.5   Velocity Relations

The flow model introduced in the last section describes the flow inside a pore. Due to the tortuosity of the liquid flow, the pore length average velocity is not equal to the volume averaged velocity (du Plessis and Masliyah, 1988). Figure 4.5 schematically shows this in 2-D. In order to have a certain volumetric discharge through the RUC, the microscale or pore velocity needs to be larger than the macroscale or volume average velocity. The following definitions are used to express the pore or corner average velocity in the volume average velocity:

$$\mathbf{v}_{ca} \quad = \quad \frac{1}{l_g}\int\limits_{l_g} \mathbf{v_c}\,dx \tag{4.52}$$

$$\mathbf{v}_D \quad = \quad \langle\mathbf{v}_l\rangle = \frac{\epsilon n_l dbj}{2l_g}\,\mathbf{v}_{ca} \tag{4.53}$$
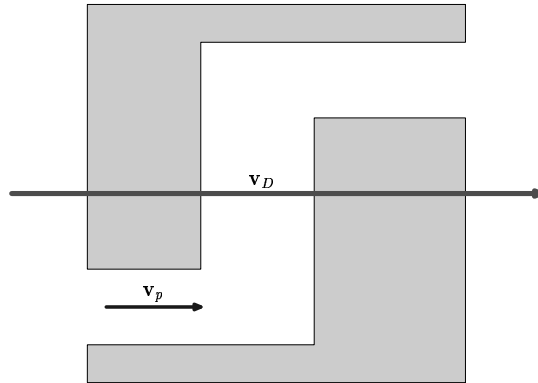
Figure 4.5: Schematic explanation of the difference between pore length average and volume average velocity ($\mathbf{v}_p$ pore velocity, $\mathbf{v}_D$ volume average velocity), note distorted scale of vectors.

For single-phase flow the analogous expression becomes:

$$\mathbf{v}_D = \langle \mathbf{v}_l \rangle = \frac{\epsilon dbj}{4l_g}\, \mathbf{v}_p \tag{4.54}$$

The definitions were derived by equating the volumetric flux through the pores to the volumetric flux through an RUC. The above relations will be used in chapter 5 for the closure modeling.

5 Closure Modeling

In chapter 3 the averaged equations were derived. Chapter 4 describes an RUC model, in which the microscopic flow processes are modeled. In this chapter equations (3.28) and (3.29) will be combined with the results from chapter 4. The closure problem in these equations, i.e. the integrals still containing microscopic quantities, will be solved and the microscopic quantities will be replaced by macroscopic quantities. Boundary and initial conditions are stated and the equations are formulated to be compatible with these conditions. For the solution of the closure problem, the quasi one-dimensional flow modeling inside the pores, adopted in chapter 4, implies that the RUC is aligned with $\mathbf{v}_D$. In chapter 6 the equations will be further analyzed.

In equations (3.29), three integral terms still contain microscopic parameters:

$$\frac{\mu_l}{\mathcal{V}_0}\nabla \cdot \int_{\mathcal{S}_{slg}} \boldsymbol{\nu}\mathbf{v}_l \; d\mathcal{S} + \frac{\mu_l}{\mathcal{V}_0}\int_{\mathcal{S}_{slg}} \boldsymbol{\nu} \cdot (\nabla\mathbf{v}_l) \; d\mathcal{S} - \frac{1}{\mathcal{V}_0}\int_{\mathcal{V}_0} \nabla p_l \; d\mathcal{V} \tag{5.1}$$

These terms are called: the divergence term, the viscous term and the pressure term. In the following sections these are reformulated term by term.

5.1 Closure of the Divergence Term

The divergence term models the influence of the flow on the gas-liquid interface. Whitaker (1986a,b) incorrectly stated that this term was zero, because he assumed a no-slip condition at the gas-liquid interface. Bousquet-Melou et al. (2002) derived a simplified closure for the divergence term for solidification problems. Their closure was based on a quasi no-slip condition, and the development followed here results in a similar macroscopic term as derived by Bousquet-Melou et al. (2002), although the specifics of the closure are different. In order to approximate the divergence term, the liquid velocity is split into

a part normal to the gas-liquid interface and a part tangent to the interface (Chen et al., 2000):

$$\mathbf{v}_l = v_{l_\nu}\boldsymbol{\nu} + v_{l_s}\mathbf{s} \tag{5.2}$$

with $\mathbf{s}$ a unit vector tangent to the interface. The divergence term becomes:

$$\frac{\mu_l}{\mathcal{V}_0}\nabla \cdot \int_{\mathcal{S}_{slg}} \boldsymbol{\nu}\mathbf{v}_l \, d\mathcal{S} \;\; = \;\; \frac{\mu_l}{\mathcal{V}_0}\nabla \cdot \int_{\mathcal{S}_{slg}} \boldsymbol{\nu}(v_{l_\nu}\boldsymbol{\nu} + v_{l_s}\mathbf{s}) \, d\mathcal{S} \tag{5.3}$$

The magnitude of v_{l_ν} is much smaller than the magnitude of v_{l_s}, because the flow is mainly tangent to the interface in the length direction of a corner. If the above products were written differently, the two tensors $\boldsymbol{\nu}\boldsymbol{\nu}$ and $\boldsymbol{\nu}\mathbf{s}$ would arise directly. The components of both tensors are usually of the same order of magnitude. Assuming that $v_{l_s}\mathbf{s}$ can be modeled by $\mathbf{v}_{ca}$, and dropping the smaller term containing v_{l_ν}:

$$\frac{\mu_l}{\mathcal{V}_0}\nabla \cdot \int_{\mathcal{S}_{slg}} \boldsymbol{\nu}\mathbf{v}_l \, d\mathcal{S} \;\; \approx \;\; \frac{\mu_l}{\mathcal{V}_0}\nabla \cdot \int_{\mathcal{S}_{slg}} \boldsymbol{\nu}\mathbf{v}_{ca} \, d\mathcal{S} \tag{5.4}$$

Probably $\mathbf{v}_{ca}$ in the above equation is an overestimation of the magnitude, because the integral is over the total solid-liquid-gas interface, and velocity at the solid-liquid interface is zero. The integral in equation (5.4) can be directly solved by taking $\mathbf{v}_{ca}$ out of the integral, because it is already an averaged quantity:

$$\frac{\mu_l}{\mathcal{V}_0}\nabla \cdot \int_{\mathcal{S}_{slg}} \boldsymbol{\nu}\mathbf{v}_l \, d\mathcal{S} \;\; \approx \;\; \frac{\mu_l}{\mathcal{V}_0}\nabla \cdot \int_{\mathcal{S}_{slg}} \boldsymbol{\nu} \, d\mathcal{S} \, \mathbf{v}_{ca} \tag{5.5}$$

Using the volume averaging rule (Crapiste et al., 1986):

$$\frac{1}{\mathcal{V}_0}\int_{\mathcal{S}_{sgl}} \boldsymbol{\nu} \, d\mathcal{S} = -\nabla(\epsilon n_l) \tag{5.6}$$

equation 5.5 becomes:

$$\frac{\mu_l}{\mathcal{V}_0}\nabla \cdot \int_{\mathcal{S}_{slg}} \boldsymbol{\nu}\mathbf{v}_l \, d\mathcal{S} \;\; \approx \;\; -\mu_l\nabla \cdot (\nabla(\epsilon n_l)\,\mathbf{v}_{ca}) \tag{5.7}$$

Using equation (4.53):

$$\frac{\mu_l}{\mathcal{V}_0}\nabla\cdot\int\limits_{\mathcal{S}_{slg}}\boldsymbol{\nu}\mathbf{v}_l\,d\mathcal{S} \quad\approx\quad -\frac{2\mu_l l_g}{dbj}\nabla\cdot[(\nabla n_l)\frac{1}{n_l}\,\mathbf{v}_D] \tag{5.8}$$

In this derivation only the larger term in the integral was taken into account. There is considerable uncertainty if the above derivation is accurate, but during the order of magnitude analysis in section 6.2, it will be shown that the divergence term is small and is not expected to influence the flow significantly. If the smaller term containing v_{l_ν} was retained, a dynamic term would result (see also section 5.2.2). Equation (5.8) is similar to one of the closure terms derived by Bousquet-Melou et al. (2002) and Goyeau et al. (1997).

5.2 Closure of the Viscous Term

The viscous term describes the viscous dissipation inside the pore due to the flow of liquid and the momentum change due to the change of gas-liquid interfacial area:

$$\frac{\mu_l}{\mathcal{V}_0}\int\limits_{\mathcal{S}_{slg}}\boldsymbol{\nu}\cdot(\nabla\mathbf{v}_l)\,d\mathcal{S} \quad=\quad \frac{\mu_l}{\mathcal{V}_0}\int\limits_{\mathcal{S}_{sl}}\boldsymbol{\nu}\cdot(\nabla\mathbf{v}_l)\,d\mathcal{S} + \frac{\mu_l}{\mathcal{V}_0}\int\limits_{\mathcal{S}_{gl}}\boldsymbol{\nu}\cdot(\nabla\mathbf{v}_l)\,d\mathcal{S} \tag{5.9}$$

The integral over the solid-liquid interfacial area and the integral over the gas-liquid interfacial area in equation (5.9) are treated separately in the following sections. All shear stress acts along the solid-liquid interface, as no shear stress is assumed to act on the gas-liquid interface (eqs. (3.3), (3.4)) (Suh et al., 2001). However due to the change of gas-liquid surface area and liquid volume, the gas-liquid surface area term is non-zero.

5.2.1 The solid-liquid interfacial area term

The microscopic Poiseuille flow model from section 4.4.2 is used here to derive a volume averaged expression for the momentum dissipated through friction along the surface of the solid phase inside the RUC:

$$\begin{aligned}\frac{\mu_l}{\mathcal{V}_0}\int\limits_{\mathcal{S}_{sl}}\boldsymbol{\nu}\cdot(\nabla\mathbf{v}_l)\,d\mathcal{S} &= \frac{\mu_l}{\mathcal{V}_0}\int\limits_{\mathcal{S}_{sl}}\frac{\partial\mathbf{v}_l}{\partial\boldsymbol{\nu}}\,d\mathcal{S} \\ &= \frac{\mu_l}{\mathcal{V}_0}\int\limits_{l_g}\int\limits_{\mathcal{L}_{sl}}\frac{\partial\mathbf{v}_l}{\partial\boldsymbol{\nu}}\,d\mathcal{L}\,dx_c\end{aligned} \tag{5.10}$$

whereby $\frac{\partial}{\partial \boldsymbol{\nu}}$ is the directional derivative in the direction of $\boldsymbol{\nu}$ with dimension length^{-1}. With $\tau_{sl} = -\frac{1}{\mathcal{L}_{sl}} \int\limits_{\mathcal{L}_{sl}} \mu \frac{\partial}{\partial \boldsymbol{\nu}} \mathbf{v}_l \, d\mathcal{L}$ (Shah and London, 1978):

$$\frac{\mu_l}{\mathcal{V}_0} \int\limits_{\mathcal{S}_{sl}} \boldsymbol{\nu} \cdot (\nabla \mathbf{v}_l) \, d\mathcal{S} \quad = \quad -\frac{1}{\mathcal{V}_0} \int\limits_{l_g} \tau_{sl} \mathcal{L}_{sl} \, dx_c$$

using equations (4.51), (4.29), (4.52) and (4.53):

$$\frac{\mu_l}{\mathcal{V}_0} \int\limits_{\mathcal{S}_{sl}} \boldsymbol{\nu} \cdot (\nabla \mathbf{v}_l) \, d\mathcal{S} \quad = \quad -\frac{1}{\mathcal{V}_0} \int\limits_{l_g} -\frac{\partial p_l}{\partial x_c} \, \mathcal{A}_c \, dx_c$$

$$= \quad -\frac{\mu_l}{F \mathcal{V}_0} \int\limits_{l_g} \mathbf{v}_c \, dx_c$$

$$= \quad -\frac{\mu_l l_g}{F \mathcal{V}_0} \, \mathbf{v}_{ca}$$

$$= \quad -\frac{2 \mu_l l_g^2}{\epsilon n_l d F \mathcal{V}_0 bj} \, \mathbf{v}_D \tag{5.11}$$

For two-phase flow equation (5.11) with equation (4.46) becomes:

$$\frac{\mu_l}{\mathcal{V}_0} \int\limits_{\mathcal{S}_{sl}} \boldsymbol{\nu} \cdot (\nabla \mathbf{v}_l) \, d\mathcal{S} = -\frac{2 \mu_l \, f^2 \, f_{\mathcal{A}} \, l_g^2}{\epsilon n_l \, d \, F_v \sin^2(\alpha) \, \mathcal{V}_0 bj} \, \mathbf{v}_D \tag{5.12}$$

And for single-phase flow the above equation with equations (4.37) and (4.54) becomes:

$$\frac{\mu_l}{\mathcal{V}_0} \int\limits_{\mathcal{S}_{sl}} \boldsymbol{\nu} \cdot (\nabla \mathbf{v}_l) \, d\mathcal{S} = -\frac{\mu_l \, \text{fRe} \, \mathcal{A}_p \, l_g^2}{2 \epsilon \, d \, r_h^2 \, \mathcal{V}_0 bj} \, \mathbf{v}_D \tag{5.13}$$

The form of the solid-liquid interfacial area term for single-phase flow in equation (5.13) is different from the expression developed by du Plessis and Masliyah (1988). They choose to express this term directly as a function of wetted solid surface area, and not in terms of the hydraulic radius as in equation (5.13). In principle these two formulations are compatible and can be expressed in each other. Here the choice is for the hydraulic radius form, because it connects better with the two-phase form of the equations.

5.2.2 The gas-liquid interfacial area term

The gas-liquid interfacial area term describes the change of momentum due to the change of gas-liquid surface area during unsteady flow. In most descriptions of unsaturated flow this term is ignored (Whitaker, 1986b). Pride and Flekkøy (1999) described the influence of the change of interfacial area on unsaturated flow in the fixed contact line regime, and concluded that it is highly nonlinear. Kralchevsky et al. (1994) derived expressions for the situation of no shear stress along the interface and normal motion to the interface. The boundary conditions at the interface used here (eqs. (3.3), (3.4)) are relative simple compared to the full stress balance (Hilfer, 1996). If the surface tension was space dependent or surfactants were assumed to be present at the interface, different boundary conditions would result (Lopez and Hirsa, 1998). Analog to the solid-liquid term (eq. (5.10)):

$$\frac{\mu_l}{\mathcal{V}_0} \int\limits_{\mathcal{S}_{gl}} \boldsymbol{\nu} \cdot (\nabla \mathbf{v}_l) \, d\mathcal{S} \quad = \quad \frac{\mu_l}{\mathcal{V}_0} \int\limits_{\mathcal{S}_{gl}} \frac{\partial \mathbf{v}_l}{\partial \boldsymbol{\nu}} \, d\mathcal{S} \tag{5.14}$$

Using the decomposition of the velocity in the surface (eq. (5.2)):

$$\frac{\mu_l}{\mathcal{V}_0} \int\limits_{\mathcal{S}_{gl}} \boldsymbol{\nu} \cdot (\nabla \mathbf{v}_l) \, d\mathcal{S} \quad = \quad \frac{\mu_l}{\mathcal{V}_0} \int\limits_{\mathcal{S}_{gl}} \frac{\partial}{\partial \boldsymbol{\nu}} (v_{l_\nu} \boldsymbol{\nu} + v_{l_s} \mathbf{s}) \, d\mathcal{S}$$

$$= \quad \frac{\mu_l}{\mathcal{V}_0} \int\limits_{\mathcal{S}_{gl}} \frac{\partial}{\partial \boldsymbol{\nu}} (v_{l_\nu} \boldsymbol{\nu}) + \frac{\partial}{\partial \boldsymbol{\nu}} (v_{l_s} \mathbf{s}) \, d\mathcal{S} \tag{5.15}$$

The two terms in the integral cancel for a stationary interface. However, if a surfactant was present, this would not necessarily be the case (Bisperink, 1997; Lopez and Hirsa, 1998). For a non-stationary interface undergoing dilatation it is assumed that the dilatation is mainly in the direction of $\boldsymbol{\nu}$ and that $\boldsymbol{\nu}$ is (nearly) perpendicular to the length direction of the corner. Dropping the second term because of the last assumption:

$$\frac{\mu_l}{\mathcal{V}_0} \int\limits_{\mathcal{S}_{gl}} \boldsymbol{\nu} \cdot (\nabla \mathbf{v}_l) \, d\mathcal{S} \quad \approx \quad \frac{\mu_l}{\mathcal{V}_0} \int\limits_{\mathcal{S}_{gl}} \frac{\partial}{\partial \boldsymbol{\nu}} (v_{l_\nu} \boldsymbol{\nu}) \, d\mathcal{S}$$

$$\approx \quad \frac{\mu_l}{\mathcal{V}_0} \int\limits_{l_g} \int\limits_{\mathcal{L}_{gl}} \frac{\partial}{\partial \boldsymbol{\nu}} (v_{l_\nu} \boldsymbol{\nu}) \, d\mathcal{L} \, dx_c \tag{5.16}$$

The factor v_{l_ν} is related to the change of the radius of the gas-liquid interface (Chen et al., 2000). It describes a "source of surface area" due to normal
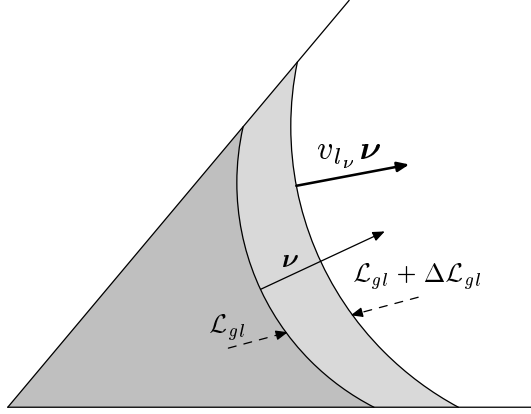
Figure 5.1: Schematic view of surface expansion, $\mathcal{L}_{gl}$ is unexpanded cross sectional surface and $\mathcal{L}_{gl} + \Delta\mathcal{L}_{gl}$ expanded cross sectional surface; vectors indicate direction of $\boldsymbol{\nu}$ and $v_{l_\nu}\boldsymbol{\nu}$.

flow to the surface. Figure 5.1 shows the directions of $\boldsymbol{\nu}$ and the change of the gas-liquid interface in a two-dimensional cross section. Chen et al. (2000) expressed v_{l_ν} as:

$$v_{l_\nu} = -\frac{\partial r}{\partial t} \tag{5.17}$$

The corner cross sectional contribution is modeled as:

$$\int_{\mathcal{L}_{gl}} \frac{\partial}{\partial \boldsymbol{\nu}} (v_{l_\nu}\boldsymbol{\nu}) \, d\mathcal{L} \quad \approx \quad -\mathbf{N}\frac{\partial f_{\mathcal{L}_{gl}} r}{\partial t} \tag{5.18}$$

whereby the factor $f_{\mathcal{L}_{gl}}$ accounts for the length of $\mathcal{L}_{gl}$, and $\mathbf{N}$ is a unit vector in the direction of $\mathbf{v}_D$. Using equations (5.18) and (4.19) in equation (5.16):

$$\frac{\mu_l}{\mathcal{V}_0} \int_{\mathcal{S}_{gl}} \boldsymbol{\nu} \cdot (\nabla\mathbf{v}_l) \, d\mathcal{S} \quad \approx \quad -\frac{\mu_l}{\mathcal{V}_0}\mathbf{N} \int_{l_g} \frac{\partial \mathcal{L}_{gl}}{\partial t} \, dx_c \tag{5.19}$$

The above integral containing $\int_{l_g} \frac{\partial \mathcal{L}_{gl}}{\partial t} \, dx_c$ describes the change of liquid gas surface area inside an averaging volume, and could be worked out in terms of surface area. We choose to work in terms of the corner cross sectional area of liquid, $\mathcal{A}_c$. This results in a nonlinear relation in terms of liquid volume

(see eq. 4.24). The advantage is that no surface area is introduced in the macroscopic equations. If it were introduced, surface area would be another variable to be specified and measured (criterion IV, p. 29). Expressing $\mathcal{L}_{gl}$ in $\mathcal{A}_c$ (eqs. (4.19), (4.22)) and simplifying:

$$\frac{\mu_l}{\mathcal{V}_0} \int\limits_{\mathcal{S}_{gl}} \boldsymbol{\nu} \cdot (\nabla \mathbf{v}_l) \, d\mathcal{S} \quad \approx \quad -\frac{\mu_l}{\mathcal{V}_0} \mathbf{N} \int\limits_{l_g} \frac{f_{\mathcal{L}_{gl}}}{\sqrt{f_{\mathcal{A}}}} \frac{\partial \sqrt{\mathcal{A}_c}}{\partial t} \, dx_c \tag{5.20}$$

$\mathcal{A}_c$ is split in an average part and the deviations (analogous to eq. (2.48), but in one dimension along the pore only):

$$\mathcal{A}_c = \langle \mathcal{A}_c \rangle + \dot{\mathcal{A}}_c \tag{5.21}$$

After substitution of equation (5.21), equation (5.20) becomes:

$$\frac{\mu_l}{\mathcal{V}_0} \int\limits_{\mathcal{S}_{gl}} \boldsymbol{\nu} \cdot (\nabla \mathbf{v}_l) \, d\mathcal{S} \quad \approx \quad -\frac{\mu_l}{\mathcal{V}_0} \mathbf{N} \int\limits_{l_g} \frac{f_{\mathcal{L}_{gl}}}{\sqrt{f_{\mathcal{A}}}} \frac{\partial \sqrt{\langle \mathcal{A}_c \rangle + \dot{\mathcal{A}}_c}}{\partial t} \, dx_c \tag{5.22}$$

Changing temporal differentiation and spatial integration, because l_g is independent of time:

$$\frac{\mu_l}{\mathcal{V}_0} \int\limits_{\mathcal{S}_{gl}} \boldsymbol{\nu} \cdot (\nabla \mathbf{v}_l) \, d\mathcal{S} \quad \approx \quad -\frac{\mu_l}{\mathcal{V}_0} \mathbf{N} \frac{f_{\mathcal{L}_{gl}}}{\sqrt{f_{\mathcal{A}}}} \frac{\partial}{\partial t} \int\limits_{l_g} \sqrt{\langle \mathcal{A}_c \rangle + \dot{\mathcal{A}}_c} \, dx_c \tag{5.23}$$

Expanding the square root term in a series:

$$\frac{\mu_l}{\mathcal{V}_0} \int\limits_{\mathcal{S}_{gl}} \boldsymbol{\nu} \cdot (\nabla \mathbf{v}_l) \, d\mathcal{S}$$
$$\approx \quad -\frac{\mu_l}{\mathcal{V}_0} \mathbf{N} \frac{f_{\mathcal{L}_{gl}}}{\sqrt{f_{\mathcal{A}}}} \frac{\partial}{\partial t} \left[\sqrt{\langle \mathcal{A}_c \rangle} \int\limits_{l_g} (1 + \frac{1}{2} \frac{\dot{\mathcal{A}}_c}{\langle \mathcal{A}_c \rangle} - \frac{1}{8} \frac{\dot{\mathcal{A}}_c^2}{\langle \mathcal{A}_c \rangle^2} + \ldots) \, dx_c \right] \tag{5.24}$$

Integrating the first two terms:

$$\frac{\mu_l}{\mathcal{V}_0} \int\limits_{\mathcal{S}_{gl}} \boldsymbol{\nu} \cdot (\nabla \mathbf{v}_l) \, d\mathcal{S}$$
$$\approx \quad -\frac{\mu_l}{\mathcal{V}_0} \mathbf{N} \frac{f_{\mathcal{L}_{gl}}}{\sqrt{f_{\mathcal{A}}}} \frac{\partial}{\partial t} \left[\sqrt{\langle \mathcal{A}_c \rangle} \left(l_g + 0 + \int\limits_{l_g} (-\frac{1}{8} \frac{\dot{\mathcal{A}}_c^2}{\langle \mathcal{A}_c \rangle^2} + \ldots) \, dx_c \right) \right] \tag{5.25}$$

Dropping higher order terms, which in essence is a linearization:

$$\frac{\mu_l}{\mathcal{V}_0} \int\limits_{\mathcal{S}_{gl}} \boldsymbol{\nu} \cdot (\nabla \mathbf{v}_l) \, d\mathcal{S} \quad \approx \quad -\frac{\mu_l}{\mathcal{V}_0} \mathbf{N} \frac{f_{\mathcal{L}_{gl}}}{\sqrt{f_{\mathcal{A}}}} \frac{\partial}{\partial t} \left[\sqrt{\langle \mathcal{A}_c \rangle} l_g \right] \tag{5.26}$$

Using $\langle \mathcal{A}_c \rangle = 2\mathcal{V}_l/(l_g bj)$:

$$\frac{\mu_l}{\mathcal{V}_0} \int\limits_{\mathcal{S}_{gl}} \boldsymbol{\nu} \cdot (\nabla \mathbf{v}_l) \, d\mathcal{S} \quad \approx \quad -\frac{\mu_l}{\mathcal{V}_0} \mathbf{N} \frac{f_{\mathcal{L}_{gl}}}{\sqrt{f_{\mathcal{A}}}} \frac{\partial}{\partial t} \left[\sqrt{\frac{2\mathcal{V}_l}{l_g bj}} \, l_g \right] \tag{5.27}$$

Using eqs. (2.39) and (2.40):

$$\frac{\mu_l}{\mathcal{V}_0} \int\limits_{\mathcal{S}_{gl}} \boldsymbol{\nu} \cdot (\nabla \mathbf{v}_l) \, d\mathcal{S} \quad \approx \quad -\frac{\mu_l}{\mathcal{V}_0} \mathbf{N} \frac{f_{\mathcal{L}_{gl}}}{\sqrt{f_{\mathcal{A}}}} \frac{\partial}{\partial t} \left[\sqrt{\frac{2\epsilon n_l \mathcal{V}_0 l_g}{bj}} \right]$$

$$\approx \quad -\frac{\mu_l}{\sqrt{2}\mathcal{V}_0} \mathbf{N} \frac{f_{\mathcal{L}_{gl}}}{\sqrt{f_{\mathcal{A}}}} \sqrt{\mathcal{V}_0} \, \sqrt{l_g} \frac{1}{\sqrt{\epsilon n_l bj}} \frac{\partial \epsilon n_l}{\partial t} \tag{5.28}$$

As a result of the above closure, the left hand side of equation (5.9), combining equations (5.12), and (5.28) becomes:

$$\frac{\mu_l}{\mathcal{V}_0} \int\limits_{\mathcal{S}_{slg}} \boldsymbol{\nu} \cdot (\nabla \mathbf{v}_l) \, d\mathcal{S} \quad = \quad -\frac{2\mu_l \, f^2 \, f_{\mathcal{A}} \, l_g^2}{\epsilon n_l \, d \, F_v \sin^2(\alpha) \, \mathcal{V}_0 bj} \, \mathbf{v}_D$$

$$-\mathbf{N} \frac{\mu_l}{\sqrt{2}\mathcal{V}_0} \frac{f_{\mathcal{L}_{gl}}}{\sqrt{f_{\mathcal{A}}}} \sqrt{\mathcal{V}_0} \, \sqrt{l_g} \frac{1}{\sqrt{\epsilon n_l bj}} \frac{\partial \epsilon n_l}{\partial t} \tag{5.29}$$

These terms model the viscous effects in two-phase flow. The first term is due to the shear stress along the solid-liquid surface and the second term describes effects due to surface dilatation in unsteady flow.

5.3   Closure of the Pressure Term

In this section the liquid pressure term (eq. 3.22) is rewritten using the RUC model from chapter 4. The liquid pressure is defined in the liquid only, and as

such averaging is done in the liquid phase:

$$\langle \nabla p_l \rangle^l = \frac{1}{\mathcal{V}_l} \int_{\mathcal{V}_l} \nabla p_l \, d\mathcal{V} \tag{5.30}$$

$$= \frac{1}{\mathcal{V}_l} \int_{l_g} \int_{\mathcal{A}_c} \mathbf{N} \frac{l_g}{d} \frac{\partial p_l}{\partial x_c} \, d\mathcal{S} \, dx_c \tag{5.31}$$

with $\mathbf{N}$ a unit vector. A change of coordinate system in the direction of the corner was done. This change of coordinate system in a corner was approximated by:

$$\nabla p_l = \frac{\partial \mathbf{x}_c}{\partial \mathbf{x}} \frac{\partial p_l}{\partial x_c} \approx \mathbf{N} \frac{\Delta x_c}{\Delta x} \frac{\partial p_l}{\partial x_c} = \mathbf{N} \frac{l_g}{d} \frac{\partial p_l}{\partial x_c} \tag{5.32}$$

whereby the gradient is in the direction along the pore and $\frac{\partial x_c}{\partial x}$ is the Jacobian. Due to the assumptions made, p_l is constant at any cross section in a pore, and can be directly integrated over $\mathcal{A}_c$:

$$\langle \nabla p_l \rangle^l = \mathbf{N} \frac{l_g}{\mathcal{V}_l d} \int_{l_g} \mathcal{A}_c \frac{\partial p_l}{\partial x_c} \, dx_c \tag{5.33}$$

Using eqs. (4.22) and (4.23):

$$\langle \nabla p_l \rangle^l = \mathbf{N} \frac{f_{\mathcal{A}} \gamma_{gl}^2 l_g}{\mathcal{V}_l d} \int_{l_g} \frac{1}{p_l^2} \frac{\partial p_l}{\partial x_c} \, dx_c \tag{5.34}$$

$$= \mathbf{N} \frac{f_{\mathcal{A}} \gamma_{gl}^2 l_g}{\mathcal{V}_l d} \int_{l_g} -\frac{\partial p_l^{-1}}{\partial x_c} \, dx_c \tag{5.35}$$

The above expression can be directly integrated along the length direction of the corner:

$$\langle \nabla p_l \rangle^l = -\mathbf{N} \frac{f_{\mathcal{A}} \gamma_{gl}^2 l_g}{\mathcal{V}_l d} \left(\frac{1}{p_1} - \frac{1}{p_0} \right) \tag{5.36}$$

This expression is further used for the liquid pressure term. It can be written in more familiar notation as:

$$\langle \nabla p_l \rangle^l = \mathbf{N} \frac{f_{\mathcal{A}} \gamma_{gl}^2 l_g}{\mathcal{V}_l} \frac{1}{p_0 p_1} \frac{p_1 - p_0}{d} \tag{5.37}$$

In order to be compatible with the rest of the momentum balance, the expression for the liquid pressure term needs to be written in a form which is valid over $\mathcal{V}_0$ and not only $\mathcal{V}_l$. Use is made of the volume averaging rule $\langle \mathbf{\Psi} \rangle = \epsilon n_l \langle \mathbf{\Psi} \rangle^i$ (Crapiste et al., 1986). The above equation was averaged along one corner. In order to assemble it for the RUC model, taking into account the number of pores in an RUC, j, and factor b:

$$\frac{1}{\mathcal{V}_0} \int_{\mathcal{V}_0} \nabla p_l \, d\mathcal{V} \quad = \quad -\mathbf{N} \epsilon n_l \frac{f_\mathcal{A} \gamma_{gl}^2 l_g b j}{2 \mathcal{V}_l d} \left(\frac{1}{p_1} - \frac{1}{p_0} \right) \tag{5.38}$$

5.4 Boundary and Initial Conditions on the Macroscale

The boundary conditions which arise for the pressure on the macroscale are simply p_0 and p_1. The time dependent terms entering the closure also require additional initial conditions, which have no analog in the traditional Buckingham-Darcy type equations. The boundary and initial conditions are given by:

$$n_l(t = t_0) \quad = \quad n_l^0 \tag{5.39}$$

$$n_l(x = x_0, x_1) \quad = \quad n_{l_{x_{0,1}}} \tag{5.40}$$

$$p_{0,1}(t) \quad = \quad p_{0,1} \tag{5.41}$$

$$\mathbf{v}_D(x = x_0, x_1) \quad = \quad \mathbf{v}_{D_{x_{0,1}}} \tag{5.42}$$

5.5 The Total Averaged Equations

In this section the combined averaged equations are given in their final form. These equations are valid on the macroscopic scale and contain only macroscopic variables. In this form they are further analyzed and used in chapter 6. Rewriting equation (3.28) using equation (4.53) gives the macroscopic mass balance equation:

$$\nabla \cdot \mathbf{v}_D \quad = \quad -\frac{\partial \epsilon n_l}{\partial t} \tag{5.43}$$

The momentum balance equation (eq. (3.29)) becomes, using equations (4.53), (5.8), (5.29), (5.38) and (5.8):

$$-\epsilon n_l \rho_l \mathbf{g} + \mu_l \left[-\nabla(\nabla \cdot \mathbf{v}_D) + \nabla \times (\nabla \times \mathbf{v}_D) \right]$$
$$-\epsilon n_l \frac{f_{\mathcal{A}} \gamma_{gl}^2 l_g bj}{2\mathcal{V}_l d} \mathbf{N} (\frac{1}{p_1} - \frac{1}{p_0}) = -\frac{2\mu_l \; f^2 \; f_{\mathcal{A}} \; l_g^2}{\epsilon n_l \; d \; F_v \sin^2(\alpha) \; \mathcal{V}_0 bj} \; \mathbf{v}_D$$
$$-\frac{\mu_l}{\sqrt{2}\mathcal{V}_0} \frac{f_{\mathcal{L}_{gl}}}{\sqrt{f_{\mathcal{A}}}} \sqrt{\mathcal{V}_0} \; \sqrt{l_g} \frac{1}{\sqrt{\epsilon n_l bj}} \; \mathbf{N} \; \frac{\partial \epsilon n_l}{\partial t}$$
$$-\frac{2\mu_l l_g}{dbj} \; \nabla \cdot [(\nabla n_l) \frac{1}{n_l} \mathbf{v}_D] \tag{5.44}$$

The above equations contain microscopic geometric parameters. These can be eliminated by using the RUC relations from chapter 4. Using a simpler form with:

$$-\epsilon n_l \rho_l \mathbf{g} + \mu_l \left[-\nabla(\nabla \cdot \mathbf{v}_D) + \nabla \times (\nabla \times \mathbf{v}_D) \right]$$
$$-c1 \; \mathbf{N} (\frac{1}{p_1} - \frac{1}{p_0})$$
$$= \; -\frac{c2}{n_l} \mathbf{v}_D - \frac{c3}{n_l^{1/2}} \mathbf{N} \frac{\partial \epsilon n_l}{\partial t} - c4 \; \nabla \cdot [(\nabla n_l) \frac{1}{n_l} \mathbf{v}_D] \tag{5.45}$$

With $c1$, $c2$, $c3$ and $c4$ given by:

$$c1 \;\; = \;\; \frac{f_{\mathcal{A}} \gamma_{gl}^2 l_g bj}{2d^4} \tag{5.46}$$

$$c2 \;\; = \;\; \frac{2\mu_l \; f^2 \; f_{\mathcal{A}} \; l_g^2}{\epsilon \; d^4 \; F_v \sin^2(\alpha) \; bj} \tag{5.47}$$

$$c3 \;\; = \;\; \frac{\mu_l f_{\mathcal{L}_{gl}} l_g^{1/2}}{\sqrt{2} d^{3/2} f_{\mathcal{A}}^{1/2} \epsilon^{1/2} b^{1/2} j^{1/2}} \tag{5.48}$$

$$c4 \;\; = \;\; \frac{2\mu_l l_g}{dbj} \tag{5.49}$$

The mass balance (eq. (5.43)) could be used to further rewrite equation (5.45), and terms containing $\frac{\partial \epsilon n_l}{\partial t}$ would arise. This is not done here in order to facilitate the analysis in chapter 6. Equations (5.45) will be further analyzed in chapter 6, where they are compared to the Buckingham-Darcy type equations and to an experiment.

For single-phase flow and standard averaging of the pressure term (du Plessis and Diedericks, 1997), the momentum balance becomes:

$$-\epsilon \rho_l \mathbf{g} + \epsilon \nabla \langle p_l \rangle^l + \mu_l \nabla \times (\nabla \times \mathbf{v}_D) \quad = \quad -\frac{\mu_l \ \text{fRe} \ \mathcal{A}_p \ l_g^2}{2\epsilon \ d^4 \ r_h^2 bj} \ \mathbf{v}_D \qquad (5.50)$$

whereby it is assumed that in single-phase flow an average liquid pressure is defined.

There are still microscopic geometric parameters left in the averaged momentum equations: a, b, j. The handling of these will be explained in chapter 6. The parameters f, $f_{\mathcal{A}}$, l_g, d, $\sin \alpha$, and $f_{\mathcal{L}_{gl}}$ are determined using the expressions from chapter 4, using the macroscopic parameters ϵ and r_c or p_{lc}.

5.6   Discussion

Starting from the pore scale equations (eqs. (2.38)), and using the assumptions of section 3.2, macroscale equations were derived. The main assumptions were: relative slow flow with no inertial effects, quasi steady-state flow at the pore scale, no dynamic contact line effects, and capillarity as the main driving force. The equations were written with the fraction of liquid inside the pores, n_l, as a main variable. Macroscopic surface area was expressed in terms of n_l also, yielding equations (5.45). The pressure term was directly integrated and $\mathbf{N}$ was added to express the direction of the macroscopic pressure gradient. In essence this integration was along one space dimension only. The main difference between equations (5.45) and the traditional Buckingham-Darcy type equations is in the pressure term. Due to the direct integration of the microscopic pressure gradient, no macroscopic pressure gradient arises directly. The integrated pressure term is not really an volume averaged term, but a macroscopic term describing the influence of a difference in liquid pressure across an RUC. The other terms in equations (5.45) are volume averaged terms, comparable to the traditional equations and volume averaging work by Whitaker (1986b). The integrated pressure term is a nonlocal term, in contrast with the traditional equations, and depends on the averaging length scale through the distance between p_0 and p_1. No factor like the conductivity arises directly, but instead factors arising from the RUC model account for the conductivity. If p_0 (or p_1) tend to become very negative, flow still can occur and is driven by the other less negative pressure. In the traditional equations, the gradient of liquid pressure would then tend to become very large, and the conductivity would

tend to become extremely small, resulting in a behavior of the equations critically dependent on the conductivity parameterization (Fuentes et al., 1992). The proposed equations also contain dynamic terms which were derived using closure assumptions. These are not present in the traditional equations, and are often modeled heuristically (Stauffer, 1977). Due to the exactly defined RUC, the order of magnitude of these macroscopic terms can be estimated (sec. 6.3.4).

6 Comparison of the Macroscale Equations with the Buckingham-Darcy Equation

6.1 Introduction

The goal of this chapter is to analyze and compare the equations derived in chapter 5 with the traditional Buckingham-Darcy (BD) type equations and the dynamic capillary pressure model used by Hassanizadeh et al. (2002). Furthermore a numerical comparison will be made with an experiment by Stauffer (1977). First an order of magnitude analysis is conducted on equations (5.45), followed by analytical approximations to compare the structure of these equations to the BD approach. Then a numerical simulation of an experiment is done on the basis of a data set from Stauffer (1977). In this chapter analysis is only conducted with respect to drainage, implying a contact angle $\theta = 0$ (assumption 11, p. 35).

6.2 Order of Magnitude Analysis of the Averaged Equation

Equations (5.45) are the full macroscale equations for the momentum balance in unsaturated flow. In this section they are made dimensionless using the notation in table 6.1. Because n_l is already dimensionless, n_l^* is defined as a place-holder of $\mathcal{O}(1)$. p_1 and p_0 are not variables in the momentum balance equations. They are treated as "constant" boundary conditions, and written as P and $P + \Delta P$. Using the above notation yields for the mass balance equation (eq. 5.43):

$$\frac{\epsilon N_l}{T} \frac{\partial n_l^*}{\partial t^*} = -\frac{V}{L} \frac{\partial v^*}{\partial x^*} \tag{6.1}$$

$$
\begin{array}{ll}
x^* = \frac{x}{L} & z^* = \frac{z}{L} \\
t^* = \frac{t}{T} = \frac{tV}{\epsilon N_l L} & n_l^* = \frac{n_l}{N_l} \\
\mathbf{g} = g\nabla \mathbf{z} & v^* = \frac{\mathbf{v}_D}{V}
\end{array}
$$

Table 6.1: Notation for variables in dimensionless equations.

Dropping the differential terms, which are of $\mathcal{O}(1)$, the following time scale can be estimated:

$$
T = \frac{\epsilon N_l L}{V} \tag{6.2}
$$

This estimated time scale is already used in table 6.1. The dimensionless momentum balance equation becomes by normalizing with respect to the pressure term:

$$
\begin{aligned}
1 \;=\; & -\frac{c2\,V}{N_l c1(\frac{1}{P+\Delta P} - \frac{1}{P})}\, v^* - \frac{c3\,V}{L N_l^{1/2} c1\left(\frac{1}{P+\Delta P} - \frac{1}{P}\right)}\, \frac{\partial n_l^*}{\partial t^*} \\
& +\frac{\epsilon N_l \rho_l g}{c1\left(\frac{1}{P+\Delta P} - \frac{1}{P}\right)}\, \frac{\partial}{\partial z^*}\, z^* - \mu_l \frac{V}{L^2 c1\left(\frac{1}{P+\Delta P} - \frac{1}{P}\right)} \\
& * \left[-\frac{\partial}{\partial x^*}\left(\frac{\partial}{\partial x^*} \cdot v^*\right) + \frac{\partial}{\partial x^*} \times \left(\frac{\partial}{\partial x^*} \times v^*\right) \right] \\
& -\frac{c4\,V}{c1\,Ld(\frac{1}{P+\Delta P} - \frac{1}{P})}\, \frac{\partial}{\partial z^*} \cdot \left[\frac{\partial n_l^*}{\partial z^*}\, \frac{1}{n_l^*}\, v_d^* \right]
\end{aligned} \tag{6.3}
$$

whereby the terms were normalized with the factor $(c1\frac{d}{L}(\frac{1}{P+\Delta P} - \frac{1}{P}))^{-1}$, yielding on the left hand side a term coming from $\mathbf{N}$ of magnitude unity. To estimate the order of magnitude of the other terms, table 6.2 lists the magnitudes used. These values were taken from the data of experiment IIa by Stauffer (1977). p_{lc} corresponds to an air entry value of $h = -0.32$ m. To estimate $c1$, $c2$, $c3$, and $c4$, the RUC relations from chapter 4 are employed. If the above values are used in equation (6.3):

$$
\begin{aligned}
1 \;\approx\; & \mathbf{1.6 * 10^{-1}}\, v_D^* - \mathbf{1.6 * 10^{-5}}\, \frac{\partial n_l^*}{\partial t^*} + \mathbf{1.0 * 10^{0}}\, \frac{\partial}{\partial z^*}\, z^* \\
& -\mathbf{1.6 * 10^{-7}} \left[\frac{\partial}{\partial x^*}\left(\frac{\partial}{\partial x^*} \cdot v_D^*\right) - \frac{\partial}{\partial x^*} \times \left(\frac{\partial}{\partial x^*} \times v_D^*\right) \right] \\
& +\mathbf{1.7 * 10^{-7}}\, \frac{\partial}{\partial z^*} \cdot \left[\frac{\partial n_l^*}{\partial z^*}\, \frac{1}{n_l^*}\, v_d^* \right]
\end{aligned} \tag{6.4}
$$

$$
\begin{array}{rrlrrl}
\epsilon & = & 0.336 & \mathrm{m^3/m^3} & \gamma_{gl} = & 0.07 & \mathrm{kg/s^2} \\
\rho_l & = & 998 & \mathrm{kg/m^3} & g = & 9.81 & \mathrm{m/s^2} \\
L & = & 0.02 & \mathrm{m} & V = & 5*10^{-5} & \mathrm{m/s} \\
\mu_l & = & 0.001 & \mathrm{kg/ms} & P = & -5.9*10^3 & \mathrm{kg/ms^2} \\
p_{lc} & = & -3.1*10^3 & \mathrm{kg/ms^2} & \Delta P = & -200 & \mathrm{kg/ms^2} \\
N_l & = & 0.24 & - & a = & 1 & - \\
j & = & 2 & - & b = & 2 & -
\end{array}
$$

Table 6.2: Magnitude of quantities used in scaling equations (6.3) and in simulations.

From equation (6.4) it can be easily seen that the most important terms are the term coming from **N** on the left hand side, which stands for the pressure term, the gravity term and the velocity term. Keeping only these three terms would lead to a BD like description of the flow equations. The order of magnitude of these terms is consistent with traditional unsaturated flow modeling, where in Darcy's law only gravitational and pressure effects are used to describe flow velocity. It is not surprising that the dynamic terms are small, as they are not widely used and, in general, good agreement with experiments is obtained without them.

6.3   Further Analysis

As explained in section 3.4.2, it is assumed that tensiometers directly measure $p_{0,1}$ and not $\langle p_l \rangle^l$. With these two measurements the pressure term in equations (5.45) can be directly evaluated. One important property of equations (5.45):

$$
\begin{aligned}
-\epsilon n_l \rho_l \mathbf{g} &+ \mu_l \left[-\nabla(\nabla \cdot \mathbf{v}_D) + \nabla \times (\nabla \times \mathbf{v}_D) \right] \\
&- c1 \, \mathbf{N}(\frac{1}{p_1} - \frac{1}{p_0}) \\
= \quad & -\frac{c2}{n_l} \, \mathbf{v}_D - \frac{c3}{n_l^{1/2}} \, \mathbf{N} \, \frac{\partial \epsilon n_l}{\partial t} - c4 \, \nabla \cdot [(\nabla n_l) \frac{1}{n_l} \mathbf{v}_D]
\end{aligned}
$$

is that if p_0 or p_1 tends to very large negative values (i.e. the porous medium becomes dry), and a wetting or drying front develops, flow can still happen and is driven by the other pressure. This behavior is analogous to the behavior of the corner flow equation and allows "autonomous" spreading in dry soils. It may seem paradoxical at first sight that the liquid flow can be written

depending on $\frac{1}{p_1} - \frac{1}{p_0}$ and not depending on $\nabla \langle p_l \rangle^l$, but the following example should clarify this: If a soil is dry, the infiltration is controlled by the pressure in the water phase behind the wetting front. This front moves and is not directly dependent on the fact that "no water" is present in the dry soil. If the soil is already moist, the wetter part (large $\frac{1}{p_{0,1}}$) of the soil "controls" the movement of the liquid to a larger degree than the drier part (small $\frac{1}{p_{0,1}}$). This is in contrast to the BD equations, where $\nabla \langle p_l \rangle^l$ tends to become extremely large and the constitutive relation $k_r(\langle p_l \rangle^l)$ must become extremely small in order to keep the spreading of the liquid phase within limits. It must be kept in mind that both the BD equation and equation (5.45) are strictly not valid near a saturation front, because the volume averaging length scale constraints are not satisfied.

In order to get a better understanding of the averaged momentum balance equations, the relatively small terms are dropped and an analysis is conducted for one-dimensional flow. One-dimensional flow is chosen, because it is most relevant for pressure cell and column experiments, and it allows simplification of the averaged momentum balance equations. In one-dimensional form, equations (5.45) become:

$$
-\epsilon n_l \rho_l g - \mu_l \frac{\partial}{\partial z} \left[\frac{\partial}{\partial z} v_D \right] - c1 \left(\frac{1}{p_1} - \frac{1}{p_0} \right)
$$
$$
= -\frac{c2}{n_l} v_D - \frac{\epsilon c3}{n_l^{1/2}} \frac{\partial n_l}{\partial t} - c4 \frac{\partial}{\partial z} \left[\frac{\partial n_l}{\partial z} \frac{1}{n_l} v_D \right] \tag{6.5}
$$

Dropping the relatively small term containing $c4$:

$$
-\epsilon n_l \rho_l g - c1 \left(\frac{1}{p_1} - \frac{1}{p_0} \right) - \mu_l \frac{\partial}{\partial z} \left[\frac{\partial}{\partial z} v_D \right]
$$
$$
= -\frac{c2}{n_l} v_D - \frac{\epsilon c3}{n_l^{1/2}} \frac{\partial n_l}{\partial t} \tag{6.6}
$$

Substituting the averaged mass balance (eq. (5.43)) in the divergence term and solving for v_D:

$$
v_D = \frac{c1 n_l}{c2} \left(\frac{1}{p_1} - \frac{1}{p_0} \right) + \frac{\epsilon n_l^2}{c2} \rho_l g - \frac{\mu_l \epsilon n_l}{c2} \frac{\partial}{\partial z} \frac{\partial n_l}{\partial t}
$$
$$
- \frac{c3 \, \epsilon n_l^{1/2}}{c2} \frac{\partial n_l}{\partial t} \tag{6.7}
$$

The above equation has two dynamic terms: $-\frac{\mu_l \epsilon n_l}{c2} \frac{\partial}{\partial z} \frac{\partial n_l}{\partial t}$ and $-\frac{c3 \; \epsilon n_l^{1/2}}{c2} \frac{\partial n_l}{\partial t}$. These two terms are further analyzed in section 6.3.4. Here, these terms are dropped because of their relative small magnitude:

$$v_D \;\; = \;\; \frac{c1 \; n_l}{c2} \left(\frac{1}{p_1} - \frac{1}{p_0} \right) + \frac{\epsilon n_l^2}{c2} \rho_l g \qquad (6.8)$$

Equation (6.8) is not a differential equation. It can be described as an algebraic equation, relating v_D to the boundary pressures p_0 and p_1. This equation is length scale dependent through the pressure term. Implicit in this term is that the distance between p_0 and p_1 must be given. It is illustrative to compare equation (6.8) to the one-dimensional BD type equation:

$$v_D = -\frac{k_D k_r(\langle p_l \rangle^l)}{\rho_l g} \frac{\partial \langle p_l \rangle^l}{\partial z} + k_D k_r(\langle p_l \rangle^l) \qquad (6.9)$$

Equation (6.8) can be rearranged to yield:

$$\mathbf{v}_D = -\frac{c1 n_l d}{c2 p_1 p_0} \frac{p_1 - p_0}{d} + \frac{\epsilon n_l^2}{c2} \rho_l g \qquad (6.10)$$

In order to approximately compare equations (6.9) and (6.10), the following approximations are used:

$$\lim_{p_{0,1} \to p_a^l, d \to 0} \frac{p_1 - p_0}{d} = \frac{\partial p_a^l}{\partial z} \qquad (6.11)$$

and:

$$\lim_{p_{0,1} \to p_a^l} n_l(p_0, p_1) = n_l(p_a^l) \qquad (6.12)$$

whereby n_l is defined by equation (4.49) and p_a^l is an "average" liquid pressure. These approximations are similar to the approximations used by Whitaker (1986a) to define pressure measurements. In effect Whitaker (1986a) assumed that pressure measurements are point measurements, and that two of these point measurements allow the calculation of $\nabla \langle p_l \rangle^l$. The assumption of point measurements is at odds with the typical dimensions of a tensiometer, which are in the order of an averaging volume. Equation (6.10) becomes with approximations (6.11) and (6.12):

$$v_D = -\frac{c1 \; n_l d}{c2 \; p_a^{l \; 2}} \frac{\partial}{\partial z} p_a^l + \frac{\epsilon n_l^2}{c2} \rho_l g \qquad (6.13)$$

Using for n_l equation(4.50) and equation (5.46) for $c1$:

$$v_D = -\frac{\epsilon n_l^2}{c2} \frac{\partial}{\partial z} p_a^l + \frac{\epsilon n_l^2}{c2} \rho_l g \tag{6.14}$$

Comparing equations (6.9) and (6.14), it is possible to identify the functional form of $k(\langle p_l \rangle^l)$ as:

$$\frac{k_D k_r(\langle p_l \rangle^l)}{\rho_l g} \approx \frac{\epsilon n_l^2}{c2} = \frac{F_v f_{\mathcal{A}} b^3 \gamma_{gl}^4 j^3 \sin^2(\alpha)}{8\mu_l d^2 f^2} \left(\frac{1}{p_a^l}\right)^4 \tag{6.15}$$

whereby equations (4.50) and (5.47) where used. This functional form is similar to a Brooks-Corey expression for k_r (Stauffer, 1977):

$$k_r \sim \left(\frac{1}{p_a^l}\right)^{3+2\lambda} \tag{6.16}$$

with λ the Brooks-Corey coefficient given as $\lambda = 2/3$.

6.3.1   Stationary solution

In this section the behavior of equation (6.7) is analyzed for the situation that the velocity is zero and a static pressure distribution develops in the porous medium. The BD equation predicts a linear pressure profile versus height above the saturated-unsaturated interface:

$$\frac{\partial \langle p_l \rangle^l}{\partial z} = -\rho_l g \tag{6.17}$$

which can be directly integrated:

$$\frac{\langle p_l \rangle^l}{\rho_l g} = -z \tag{6.18}$$

However Gray and Hassanizadeh (1991a, p. 1850) in their article "Paradoxes and Realities in Unsaturated Flow Theory", predicted that in unsaturated flow the above statement is only approximately correct. They give two reasons for this. The first reason is that the density of water is not truly constant. This effect is not taken into account here, as it is assumed that the density is constant (assumption 1, p. 34). The second reason is related to the capillary
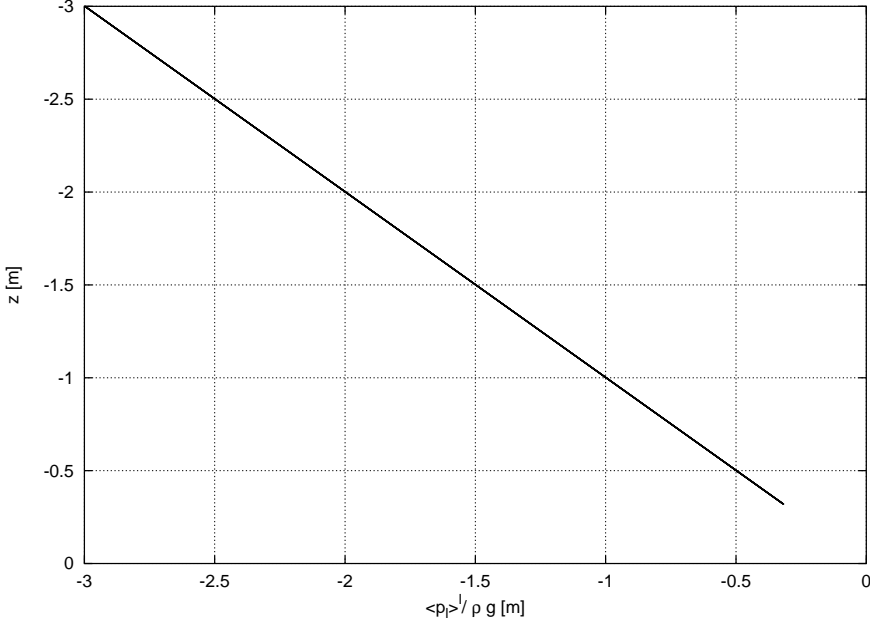
Figure 6.1: $\langle p_l \rangle^l / \rho_l g$ vs. z (eq. (6.20)).

forces in the porous medium. Gray and Hassanizadeh (1991a) assume that
the capillary forces "hold" an extra amount of water in the porous medium,
and that because of this the pressure profile is not given by equation (6.18).
If $v_D = 0$, equation (6.7) or (6.8) becomes:

$$0 = \frac{c1 n_l}{c2}\left(\frac{1}{p_1} - \frac{1}{p_0}\right) + \frac{\epsilon n_l^2}{c2}\rho_l g \tag{6.19}$$

When using the RUC relations for $c1$, $c2$ and n_l from chapter 4, the above
equation becomes:

$$\frac{p_1 - p_0}{d} = -\rho_l g \frac{3\,(p_0^4 + p_1 p_0^3 + p_0^2 p_1^2 + p_0 p_1^3 + p_1^4)}{5\,(p_0^2 + p_0 p_1 + p_1^2) p_0 p_1} \tag{6.20}$$

Figure 6.1 shows the pressure profile predicted by equation (6.20), calculated
for a water table ≈ 3 m deep in a soil. This figure shows that the predicted
pressure profile is virtually identical to the profile predicted by equation (6.18).
However a careful analysis of the relative difference:

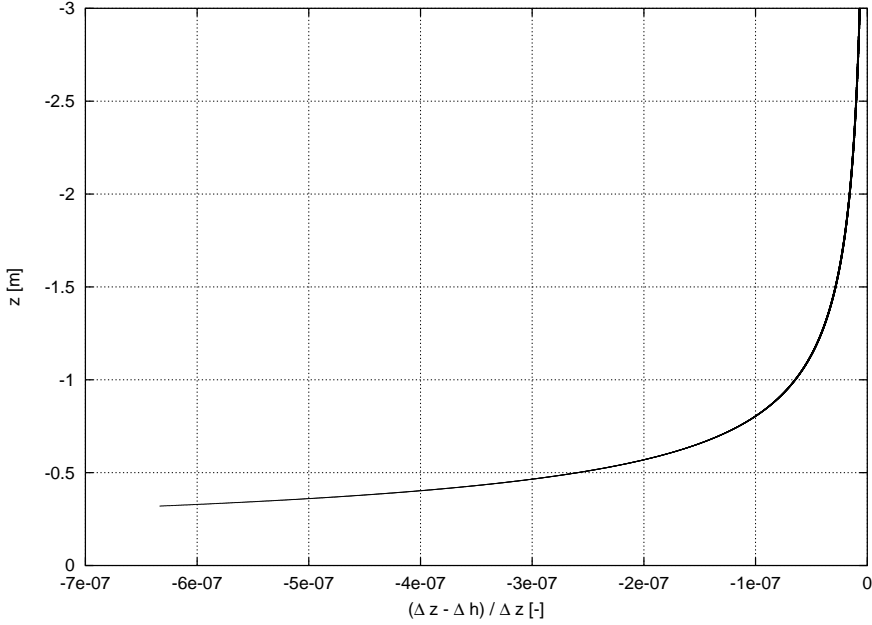$$\frac{\Delta z - \Delta \frac{p_{0,1}}{\rho g}}{\Delta z} \tag{6.21}$$

Figure 6.2: Relative difference of stationary pressure profile; eq. (6.21) vs. z.

shows that the pressure profile predicted by equation (6.20) is not exactly a straight line. Figure 6.2 shows the relative difference (eq. (6.21)) as a function of z. It is obvious that the deviations from the linear profile are quite small and can be ignored for practical purposes. Nonetheless, figure 6.2 shows that the predicted profile is less than hydrostatic, as conjectured by Gray and Hassanizadeh (1991a). In effect more liquid is held in the porous medium than predicted by equation (6.17). At larger water contents (less negative liquid pressures) this effect is more pronounced. To the authors knowledge equation (6.20) is the first equation proposed for unsaturated porous media which shows this behavior consistent with the work of Gray and Hassanizadeh (1991a). An explanation for the deviation from the hydrostatic pressure profile is that the gravity term is defined in terms of average liquid content, whereas the pressure term is based on areal average liquid pressures per unit volume.

6.3.2 Comparison of the averaged pressure term

As shown in appendix A, using the traditional averaging of the pressure term yields (Whitaker, 1986b):

$$\langle \nabla p_l \rangle = \epsilon n_l \nabla \langle p_l \rangle^l$$

or in one-dimensional form:

$$\langle \frac{\partial p_l}{\partial z} \rangle = \epsilon n_l \frac{\partial}{\partial z} \langle p_l \rangle^l \tag{6.22}$$

The averaged pressure terms in equation (6.22) and equation (6.7) can be compared directly:

$$\epsilon n_l \frac{\partial}{\partial z} \langle p_l \rangle^l \quad : \quad -c1 \left(\frac{1}{p_1} - \frac{1}{p_0} \right) \tag{6.23}$$

$$: \quad \frac{c1 d}{p_0 p_1} \frac{p_1 - p_0}{d} \tag{6.24}$$

Using equations (4.50) and (5.46), and approximations (6.11) and (6.12):

$$\epsilon n_l \frac{\partial}{\partial z} \langle p_l \rangle^l \quad : \quad \epsilon n_l \frac{\partial}{\partial z} p_a^l \tag{6.25}$$

The above relation shows that the traditional averaging of the pressure term is similar to the method introduced here, if approximations (6.11) and (6.12) are used. If during the development of the averaged pressure term in section 5.3 it was assumed that the sum of all corner liquid areas $\mathcal{A}_{cs}$ is independent of liquid pressure, the following averaging would result:

$$
\begin{aligned}
\langle \nabla p_l \rangle^l &= \frac{1}{\mathcal{V}_l} \int_{\mathcal{V}_l} \nabla p_l \, d\mathcal{V} \\
&= \frac{1}{\mathcal{V}_l} \int_{l_g} \int_{\mathcal{A}_{cs}} \mathbf{N} \frac{l_g}{d} \frac{\partial p_l}{\partial x_c} \, d\mathcal{S} \, dx_c \\
&= \mathbf{N} \frac{l_g}{d\mathcal{V}_l} \int_{l_g} \mathcal{A}_{cs} \frac{\partial p_l}{\partial x_c} \, dx_c \\
&= \mathbf{N} \frac{\mathcal{A}_{cs} l_g}{\mathcal{V}_l} \frac{p_1 - p_0}{d} \\
&= \mathbf{N} \frac{p_1 - p_0}{d}
\end{aligned}
\tag{6.26}
$$

whereby equation (5.32) was used and $\mathcal{A}_{cs}$ is defined analogous to equation (4.8) as $\mathcal{A}_{cs} = \frac{\mathcal{V}_l}{l_g}$. For one-dimensional flow, equation (6.22) on the left hand side and equation (6.26) on the right hand side:

$$\frac{\partial}{\partial z}\langle p_l\rangle^l : \frac{p_1 - p_0}{d} \tag{6.27}$$

If the fluid area $\mathcal{A}_{cs}$ is constant along the corners in an RUC, the geometric transformation multiplier $\frac{l_g}{d}$ directly cancels and does not enter the averaged equations as in the averaging of the pressure term in section 5.3 for unsaturated flow (Ma and Ruth, 1993).

The factor $\frac{l_g}{d}$ in the nonlocal form of the pressure term is similar to the aerosity factor proposed by Ma and Ruth (1993). If change in cross-sectional liquid area had not been taken into account during the averaging, the newly proposed result would be even more like the traditional averaged pressure term, however, with the important difference that the newly proposed term is nonlocal, whereas the traditional term is local.

6.3.3   Estimation of the saturated hydraulic conductivity

The RUC geometric relations developed in chapter 4 allow a direct estimation of the saturated hydraulic conductivity. It can be evaluated using equation 5.50 as:

$$k_d = \frac{2\epsilon^2 d^4 r_h^2 bj\rho g}{\mu_l \mathrm{fRe}\mathcal{A}_p l_g^2} \tag{6.28}$$

fRe is given in Shah and London (1978) as:

$$\mathrm{fRe} \approx 12.3 \tag{6.29}$$

Using the values from table 6.2, and the RUC relations from chapter 4:

$$k_d = 1.3 * 10^{-4}\mathrm{m/s} \tag{6.30}$$

This value can be directly compared to the average value measured by Stauffer (1977) for his experiment II as $2.1*10^{-4}$ m/s. The simple RUC and flow model of chapter 4 together with the closure for saturated flow in section 5.2 provides an estimate of k_D only using the macroscopic variables ϵ, p_{lc}, and the properties μ_l, ρ_l, g, and an estimate of fRe from Shah and London (1978). The estimate of k_D is quite accurate, considered that only ϵ and p_{lc} were used as porous medium parameters. This estimate compares in accuracy with more standard methods (Carman, 1956).

6.3.4 Comparison of the dynamic terms with Stauffer's model

Equation (6.7) contains two time dynamic terms: one with the divergence of the velocity, and the other with the derivative of the liquid content. Both originate from the microscopic viscous term. Most two-phase flow equations have no or one dynamic term. In his dissertation Stauffer (1977) proposed a model for a dynamic capillary pressure. This dynamic model was proposed in order to model rapid changes in water content in his experiments. He conjectured that the pressure in the Buckingham-Darcy equation is a dynamic pressure and that it can be expressed as:

$$\langle p_c \rangle_d^l - \langle p_c \rangle_s^l = -\tau \frac{\partial n_l}{\partial t} \tag{6.31}$$

whereby subscript $_d$ indicates a dynamic pressure and subscript $_s$ indicates a static pressure and τ a dimensionless proportionality factor. In terms of the liquid pressure:

$$\langle p_l \rangle_d^l - \langle p_l \rangle_s^l = \tau \frac{\partial n_l}{\partial t} \tag{6.32}$$

with $\langle p_l \rangle_s^l$ the static volume average liquid pressure and $\langle p_l \rangle_d^l$ the dynamic volume average liquid pressure. Stauffer (1977) indicated that τ could depend on water content, but did not elaborate further on this. The term $\frac{\partial n_l}{\partial t}$ is also called a capillary relaxation factor. If equation (6.32) is used in the standard BD equation (eq. (6.9)):

$$\mathbf{v}_D = -\frac{k_D k_r(\langle p_l \rangle_d^l)}{\rho_l g} \left[\frac{\partial}{\partial z} \langle p_l \rangle_s^l + \frac{\partial}{\partial z} \left(\tau \frac{\partial n_l}{\partial t} \right) \right] + k_D k_r(\langle p_l \rangle_d^l) \tag{6.33}$$

The dynamic term was introduced ad hoc in Stauffer's dissertation, although he tried to find physical explanations in terms of dynamic contact angles (see Stauffer, 1977, p. 130). It is shown here that a dynamic term of the same form as the second term on the right hand side of equation (6.33) can be directly derived from the Brinkman term (Brinkman, 1947, 1949) without the introduction of a dynamic pressure. In section 3.4.2, the viscous term was averaged, yielding a sum of terms, containing $\mu_l \nabla^2 \langle \mathbf{v}_l \rangle$. In the beginning of section 6.3 (p. 78) this term was rewritten for one-dimensional flow together with the mass balance as:

$$-\frac{\mu_l \epsilon n_l}{c2} \frac{\partial}{\partial z} \frac{\partial n_l}{\partial t} \tag{6.34}$$

The dynamic term in the dynamic BD equation (eq. (6.33)) and equation (6.34) have the same mathematical form. Stauffer (1977) assumed that τ was constant, and with this assumption the order of magnitude of the factor in front of the differential can be directly compared:

$$\frac{k_D k_r(\langle p_l \rangle_d^l)}{\rho_l g}\tau \quad : \quad \frac{\mu_l \epsilon n_l}{c2} \tag{6.35}$$

Stauffer speculated that τ could depend on water content, but took it as a constant defined by[1]:

$$\tau = \frac{p_{lc}^2 \alpha}{k_D \rho_l g \lambda} \tag{6.36}$$

with α a constant, k_D the saturated hydraulic conductivity, and λ the Brooks-Corey exponent (see Stauffer, 1977, p. 128). Simplifying relation (6.35) and using equation (6.36) and $k_D k_r(\langle p_l \rangle_d^l) = k_D n_l^{3+2/\lambda}$ (Stauffer, 1977):

$$\frac{n_l^{3+2/\lambda} p_{lc}^2 \alpha}{\rho_l^2 g^2 \lambda} \quad : \quad \frac{\mu_l \epsilon n_l}{c2} \tag{6.37}$$

using numerical values for all variables (tab. 6.2) and $\alpha \approx 0.03$, $\lambda \approx 6$ (Stauffer, 1977):

$$5 * 10^{-4} n_l^{3\frac{1}{3}} \quad : \quad 5 * 10^{-10} n_l \tag{6.38}$$

As is to be expected, Stauffer's (1977) dynamic term has a much larger multiplier than the dynamic term derived from the Brinkman term, which will be explained later. If the Brinkman term was large, the length scale constraints of volume averaging would be violated, and volume averaged equations would not apply to the problem at hand (Whitaker, 1986a). Both terms depend on n_l, although the exponent is different. Figure 6.3 shows the behavior of both terms dependent on n_l. At low n_l, both terms can have an equal magnitude due to the power of n_l on the left hand side of relation (6.38).

Stauffer's (1977) assessment of the dynamic term is based on his column experiments. The experimental geometry had multiple tensiometers at distances

---

[1]In Stauffer (1978) a slightly different definition of τ is used:

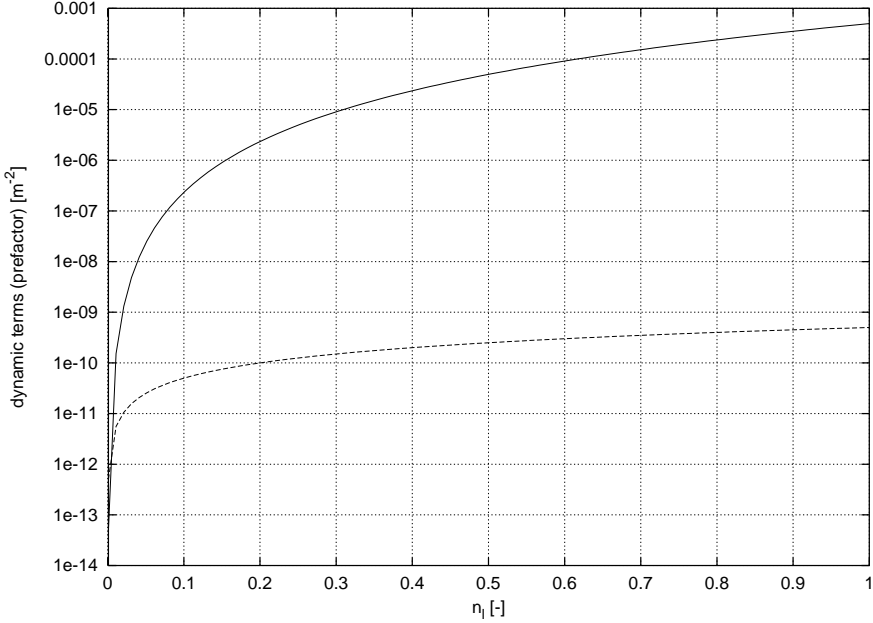$$\tau = \epsilon\,\tau \text{(Stauffer, 1978)}$$

Figure 6.3: Prefactors of dynamic terms, eq. (6.38) vs. n_l; solid line left hand side of eq. (6.38), dashed line right hand side of eq. (6.38).

of ≈ 10 cm, and in between water content measurement locations (fig. 6.5). The water content measurement and tensiometers were thus not at the same locations but at ≈ 5 cm distances. The time interval of the water content measurements was in the order of minutes for repeated measurements at the same location. This raises the question if these measurements can be the basis for an assessment of the local dynamic terms. The experimental setup implies a dependence of $\frac{\partial n_l}{\partial t}$ on the distance of the tensiometer locations and the measurement frequency, but it is difficult to derive from these experiments a local dependence of $\langle p_l \rangle^l$ on $\frac{\partial \epsilon n_l}{\partial t}$. Another issue related to the estimation of the dynamic term of Stauffer (1977) is related to the saturation front. Stauffer (1977) used measurements close to the front for estimation, but it is questionable if his flow equation parameterizations are valid near the saturation front.

The second dynamic term in equation (6.7):

$$- \frac{c3 \, \epsilon n_l^{1/2}}{c2} \, \frac{\partial n_l}{\partial t} \tag{6.39}$$
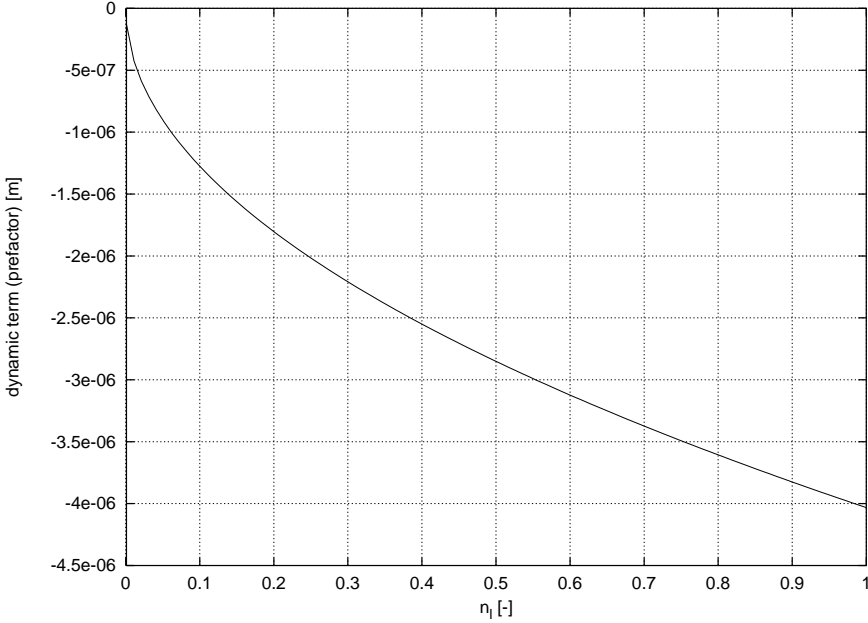
Figure 6.4: Prefactor of dynamic term, eq. (6.39) vs. n_l.

comes into the equations due to the deformation of gas-liquid interface on the microscopic scale. This term is a novel term describing dynamic effects in unsaturated flow in porous media. It depends only on the change of liquid saturation in time and is not dependent on spatial gradients. Figure 6.4 shows the factor before the differential against n_l. In effect it can be seen as a hysteresis term. During imbibition it reduces the volume average velocity, whereas during drainage it enlarges the volume average velocity. This effect is due to the change in liquid saturation in an averaging volume. Equation (6.39) can not be directly compared to Stauffer's dynamic term, because it has a different mathematical form.

One dynamic term was discarded in the closure in section 5.1, because it was assumed to be very small. The discarded term would might have a mathematical form similar to Stauffer's term, however it would be much smaller.

Both the dynamic terms in equation (6.7) and the dynamic term from Stauffer (1977) originate from the volume averaged stress tensor. In the work of Hassanizadeh and Gray (1980), from thermodynamics, they proposed that the volume average stress tensor could depend on a multitude of variables, and as such the dynamic terms used in this dissertation do not contradict the work

of Hassanizadeh and Gray (1980). It is not expected that the dynamic terms normally play an important role in flow in unsaturated porous media, however near a saturation front these terms could become important.

6.4 Comparison with Experiment

After the analytical analysis in the previous sections, in this section the numerical solution of equation (6.8) is compared to an experiment by Stauffer (1977). Equation (6.8) is chosen because it does not contain the dynamic terms and the other comparably small term. If a numerical solution of equation (6.7) with the dynamic terms was the goal, a relation between $p_{0,1}$ and n_l had to be found, whereby $n_l = n_l(p_{0,1}(t), t)$. In section 4.4.2 an expression for n_l (eq. (4.49)) was found, based on quasi-steady flow in a corner. In principle a dynamic expression for n_l could be found, but this would make the local flow model much more involved. As the order of magnitude analysis in section 6.2 already indicated, it is not expected that dynamic terms play an important role in unsaturated flow as studied here. This is the reason why a quasi-steady calculation procedure is used. Stauffer (1977) used the same experiment to estimate his proposed dynamic term (see section 6.3.4 for a discussion).

6.4.1 Description of experiment

The porous medium employed by Stauffer is unconsolidated sand with an average porosity of 0.336. The mean particle diameter of the sand is approximately $3 * 10^{-4}$ m. It is assumed that the liquid (water) is completely wetting the sand and that the contact angle $\theta = 0$. The experimental unit consists of a vertical sand column in a cylinder of diameter 0.045 m and length 0.638 m. At the top of the column there is no liquid inflow or outflow and atmospheric pressure, while the bottom of the column drains in a reservoir with a constant level. Figure 6.5 shows schematically the geometry of the experiment.

To conduct an experiment, the sand column is completely saturated and then allowed to drain freely. The liquid pressure is measured with tensiometers along the column and water content is measured with a gamma ray absorption technique. Additionally the air pressure is measured throughout the column in order to detect effects of pressure variation in the gas phase and its possible influence on the liquid movement. The outflow is collected and weighted on a digital scale. Here the data from experiment IIa are used to compare with
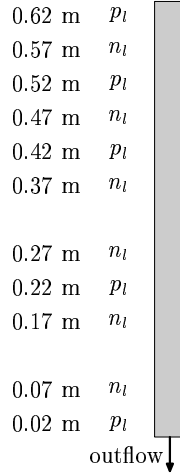
0.62 m	p_l
0.57 m	n_l
0.52 m	p_l
0.47 m	n_l
0.42 m	p_l
0.37 m	n_l
0.27 m	n_l
0.22 m	p_l
0.17 m	n_l
0.07 m	n_l
0.02 m	p_l

outflow

Figure 6.5: Geometry of experimental setup (exp. IIa, Stauffer (1977)), showing locations of measurements, distances are from bottom of column.

the numerical simulation. This experiment was chosen because the data set was the most complete. An important property of this experiment is the high speed of the saturation front when drainage starts. The speed was up to 180 m/d or $2.15 * 10^{-3}$ m/s. The movement of the front controls to a large degree the outflow dynamics. Data relating to the parameters in the experiment are given in table 6.2.

6.4.2   Calculations

For the simulations we use the following discretised form of equation (6.8):

$$\mathbf{v}_D^{i+1/2} \quad = \quad \frac{c1}{c2} \frac{d}{\Delta x} n_l^{i+1/2} \left(\frac{1}{p^{i+1}} - \frac{1}{p^i} \right) + \frac{\epsilon \rho_l g}{c2} n_l^{i+1/2^2} \tag{6.40}$$

whereby the superscript containing i indicates the node location and $\frac{d}{\Delta x}$ is a discretisation factor to adjust the length scale implicit in the equations through $p_{0,1}$ to the numerical discretisation step Δx. This discretisation factor was used to asses the effect of different discretisation length scales on the simulations. It was found that 2 cm is a reasonable length scale, concerning the tradeoff between calculation time and change of the predicted outflow between different

run nr.	$\dfrac{p_{lc}}{\rho_l g}$	a	b	j	calculated outflow (g)
1	-0.32	1	1	1	266.29
2	-0.32	1	2	1	252.63
3	-0.32	1	1	2	253.65
4	-0.32	1	2	2	245.52
5	-0.32	0.7	1	1	284.07
6	-0.32	0.7	2	1	263.73
7	-0.32	0.7	1	2	267.01
8	-0.32	0.7	2	2	252.02
measured in experiment:	-0.32	-	-	-	273.79

Table 6.3: Combinations of parameters used in simulations and calculated outflow (g) at the end of the experiment.

discretisation lengths. The mass balance is explicitly discretised in time as:

$$\frac{\mathbf{v}_D^{i+1/2} - \mathbf{v}_D^{i-1/2}}{\Delta x} \quad = \quad -\epsilon \frac{n_{l\,t+\Delta t}^{i} - n_{l\,t}^{i}}{\Delta t} \tag{6.41}$$

whereby Δt is the time step. Parameters $c1$ and $c2$ were calculated from the data of experiment IIa by Stauffer (1977) using the RUC relations from chapter 4 (see also table 6.3). The system of equations (6.40) and (6.41) is set up for the whole column and solved sequentially. The simulations were run with explicit time stepping, the time step was adjusted dynamically by a Courant number criterion. The simulation code is written in the XLisp-Stat programming language (Tierney, 1990). As equation (6.40) is only valid for unsaturated flow, the position of the saturated-unsaturated interface was dynamically tracked. Nodes which became unsaturated were added to the simulation domain. Effectively, only the unsaturated part of the domain is simulated by equations (6.40) and (6.41), and the position of the interface between saturated and unsaturated flow is used as a bottom boundary condition for the simulation. The top boundary condition is given by a no-flow condition. The parameters $c1$ and $c2$ contain the geometric parameters a, b and j defined in chapter 4. In order to asses their importance, simulations were done for different values of these parameters. Table 6.3 lists the combinations and shows the simulated outflow compared to the measured outflow at the end of the experiment.
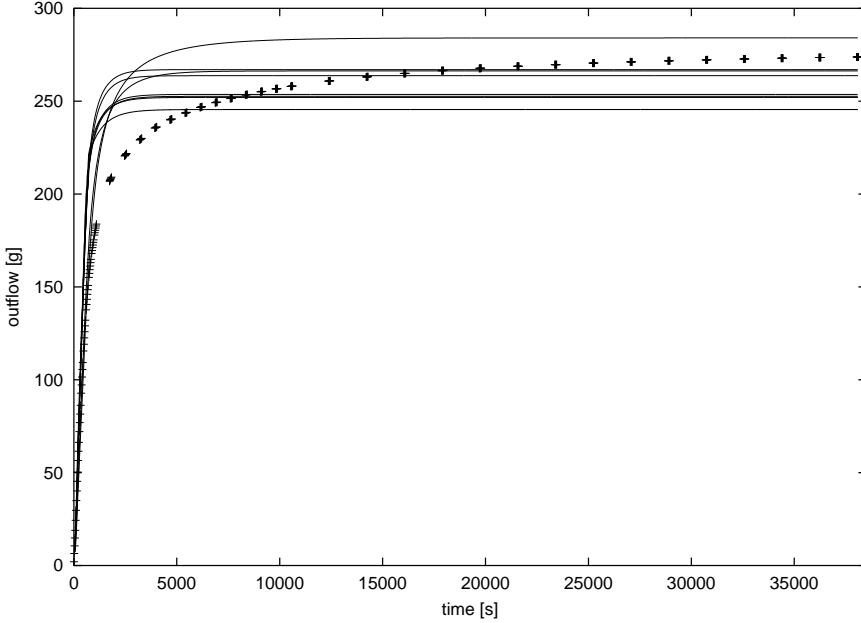
Figure 6.6: Measured outflow (cross symbols) and simulations with parameter combinations from table 6.3 (lines) vs. time.

6.4.3   Calculation results

Figure 6.6 shows the simulated outflow for all combinations of parameters in table 6.3, together with the measured outflow. It can be seen directly that the choice of parameters a, b, j influences the outflow curves, but that all parameter combinations give a reasonable description of the outflow. It is clear that through optimization a better fit could be obtained, but this was not the goal. It is shown that the parameter range allows satisfactory simulation of the outflow. For these simulations the only parameters which need to be measured for a specific porous medium are ϵ and p_{lc}, and these were directly taken from the data of Stauffer (1977). No other parameters were needed, except the fluid properties μ_l, γ_{gl} and ρ_l. In view of this the simulation results are quite satisfactory. After about 2000 s the simulated outflow increases more than the measured outflow. This indicates that the resistance parameterization or the simple Young-Laplace model for the liquid pressure overestimate the unsaturated hydraulic conductivity. Figure 6.7 shows profiles of n_l at different time steps during the simulation for run number 1 and a measured saturation profile at ≈ 22000 s. The profiles show the typical behavior expected from
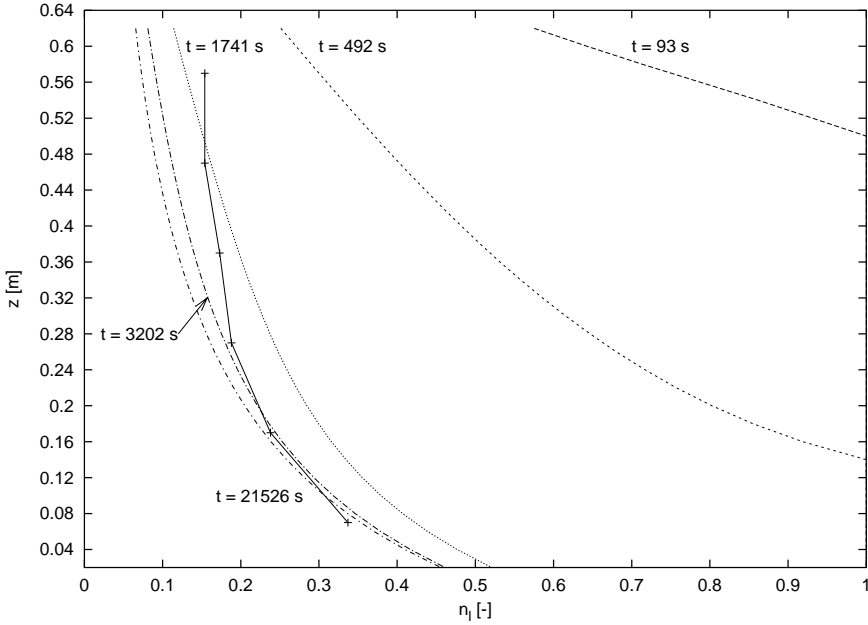
Figure 6.7: Simulated profiles of saturation for run nr. 1; line with + signs: measured profile at ≈ 22000 s.

saturation profiles in drainage, although the simulation results over predict the drainage in the top of the column. At the end of the experiment, the predicted outflow is close to the measured outflow. The largest deviation of the simulated outflow from the measured outflow was for run nr. 4, with about 10% deviation (table 6.3). Run nr. 7 predicted the total outflow best, with a deviation of only $\approx 2\%$. Overall the simulated behavior of equation (6.8) shows the behavior of the saturation and outflow in reasonable agreement with the measured data. At the end of the simulations predicted pressure profiles were close to hydrostatic, as expected from the outflow curves. The measured pressure profiles of Stauffer (1977) show no hydrostatic profile at the end of the experiment, although during the experiment a nearly hydrostatic pressure profile was measured.

7 Discussion, Recommendations and Conclusions

In this chapter a discussion of equations (5.45) and the mass balance equation (5.43) derived in chapter 5 is given. Together with the comparison in chapter 6, strengths and weaknesses of the above equations are discussed. First the general properties and the averaged pressure term are discussed, followed by a discussion of the dynamic terms. Then the drawbacks are explained and recommendations for possible extensions are given. Finally recommendations and general conclusions will be stated.

7.1 Discussion

In section 5.5 equations (5.45) were proposed as the averaged momentum balance equations on the macroscale. These equations differ from the traditional volume averaged equations in the pressure term, the dynamic terms and in the form chosen for the Brinkman term. In chapter 6 these were simplified to one-dimensional form (eq. (6.5)) and relatively small terms were neglected. The resulting equation (6.8) was compared to the traditional Buckingham-Darcy equation and to an experiment. The simplified one-dimensional form of the averaged equations (6.8) is in an algebraic equation. This is the result of the direct integration of the pressure term and effectively removes the spatial derivative from this term. The fact that the momentum balance equations become nonlocal is caused by the direct effect of the boundary conditions on the flow. A similar effect of the boundary conditions is also observed in upscaling from the core to larger scales, e.g. in renormalization calculations in unsaturated flow (Hoffmann, 2000a). The relation between liquid saturation and boundary pressures was established for quasi-steady flow only, which implies that the combination of equations (5.45)and (4.49) can only be solved for quasi-steady flow. The volume averaged mass balance equation derived in

this dissertation is identical to the traditional volume averaged mass balance equation.

Naturally the question arises: Can the averaged momentum balance equations be called "truly"volume averaged equations? Two views are possible:

- Yes, because each term in the equations is averaged over an averaging volume.

- No, because the averaged pressure term contains area averaged pressures. These quantities are therefor not truly volume averaged quantities. Moreover this term is nonlocal and length scale dependent. In the traditional equations the length scale does not enter directly into the equations.

Another point of discussion is whether equations (5.45) are truly three-dimensional equations. The mathematical notation is in three-dimensional vector form, but the pressure term and one dynamic term were averaged along a corner inside a Representative Unit Cell along one dimension only. On the macroscale these terms contain a unit vector, which is a notational help in making these terms three-dimensional.

7.1.1   Pressure term

As already explained in chapter 6, the pressure term has a different form than the traditional volume averaged pressure term. This is the main difference between equations (5.45) and the traditional volume averaged equations. The precise form of this difference is due to the interpretation of the pressure measurement made by tensiometers and in pressure cells. Hassanizadeh and Gray (1979a) state that *"The average value of a microscopic quantity must be the same function that is most widely observed and measured in a field situation or in the laboratory"* (Criterion IV (p. 29)). Here the pressure measurement is interpreted as an area average measurement and not a volume average measurement. If this interpretation is valid, the principle of areal averaging of the pressure term developed in section 5.3 is valid. The areal averaging directly uses equation (4.23) to express liquid area in liquid pressure. This is a simplification of reality. A better representation of the relation between liquid area in a corner and liquid pressure could improve the averaged pressure term greatly. Extensions could include a more realistic pore geometry, taking into account surface roughness, or using a relation derived from measurements. In effect

the relation between liquid area in a corner and and liquid pressure could be seen as a constitutive relation.

The form of the averaged pressure term shows that the flow of liquid in unsaturated porous media can be written proportional to $\frac{1}{p_1} - \frac{1}{p_0}$. In principle the flow is still driven by the gradients in liquid pressure, but due to the nonlinear coupling between capillary forces and liquid pressure gradient, the apparent driving force is proportional to $\frac{1}{p_1} - \frac{1}{p_0}$. This form reduces the need to introduce the highly nonlinear $k_r(\langle p_l \rangle^l)$ relationship (eqs. (6.15) and (6.16)) which is used in the traditional models for flow in unsaturated porous media. A related property is that the difference $\frac{1}{p_1} - \frac{1}{p_0}$ becomes smaller as $p_{0,1}$ become more negative, i.e. the porous medium becomes drier. This reduces the effective driving force for flow and accounts for part of the nonlinearities in unsaturated flow.

The result obtained by averaging the pressure term is similar to the result that would be obtained with the "control volume method" used in fluid mechanics (Panton, 1984). In this method the forces acting on a control volume are calculated by summing the forces around the perimeter surface of the control volume. In effect a similar method has been used by Hassanizadeh et al. (2002) in their pore network simulation model. They calculated the areal average liquid pressure at the entry and exit planes of their pore network and related this to the volume average static capillary pressure. Hassanizadeh et al. (2002, p. 50) state: "a natural definition of the macroscopic capillary pressure is given by the pressure difference associated with the boundary fluid reservoirs". The result is a nonlocal definition of the capillary pressure term, which depends on the averaging length scale (the pore network length scale). In their work Hassanizadeh et al. (2002) apparently did not directly take into account the length scale dependence of their nonlocal definition of capillary pressure.

The nonlocal pressure definition avoids the need to presuppose that liquid flow is driven by the gradient of the average liquid pressure (Whitaker, 1986b). By its definition the pressure term of section 5.3 represents a static liquid pressure, although the pressure at the entry and exit planes can depend on time. The areal average pressure definition avoids the need to use a dynamic liquid pressure to account for dynamic effects.

7.1.2 Dynamic terms

The two dynamic terms in equation (5.45) containing $\frac{\partial \epsilon n_l}{\partial t}$ describe the effect of volume averaging on the flow dynamics. On the microscale equations (2.38)

describe steady flow, but due to a change in liquid saturation in the averaging volume, the dynamic terms directly enter the macroscopic mass and momentum balance equations. In the momentum balance equations these terms originate from the microscopic viscous term and they act as a "momentum sink". The first dynamic term $\mu\epsilon\frac{\partial}{\partial x}\frac{\partial n_l}{\partial t}$ is part of the macroscopic Brinkman term. As shown in the order of magnitude analysis in section 6.2, it is relatively small and not expected to influence flow in unsaturated porous media significantly. The remarkable property of this term is that it has the same mathematical form as the dynamic term proposed by Stauffer (1977), as shown in section 6.3.4.

The second dynamic term $\frac{\epsilon\,c3}{n_l^{1/2}}\frac{\partial n_l}{\partial t}$ does not depend on the spatial derivative, but on the temporal derivative only. It was derived from the surface dilatation through direct integration and linearisation in section 5.2. It is a novel term in the momentum balance for two-phase flow. Basically it describes the effect of advection of liquid into the averaging volume and damps the dynamics. It could be interpreted as a hysteresis term. This hysteresis is then only due to the flow dynamics and has nothing to do with the traditional hysteresis effect which is explained in terms of the ink bottle effect and contact angle hysteresis. The interesting aspect is that the factor $\frac{\epsilon\,c3}{n_l^{1/2}}$ becomes large as n_l becomes small. But at small n_l, $\frac{\partial n_l}{\partial t}$ is small, except near a steep wetting front. Such a steep wetting fronts can be observed during infiltration of water into a dry soil. But near such a steep wetting front the volume averaging length scale constraints are not valid and thus the averaged equations are not valid. However it must be remarked that the form of the second dynamic term is based on assumptions and as such is not the result of a strict mathematical derivation.

In section 6.4 the dynamic terms were not included in the simulations because they are relatively small. An improved dynamic closure incoorperating the dynamic terms in the relationship $n_l(p_0, p_1, t)$ would be needed to do this. However it is expected that the total influence of the dynamic terms is not important in unsaturated flow in sand-like porous media. These terms could play a role close to a wetting front, but then the volume averaging length scale constraints are not satisfied.

7.1.3   Representative Unit Cell model

The RUC model proposed in chapter 4 encompasses a concrete geometric specification, in contrast to the abstract Representative Elementary Volume (REV)

model. The geometric specification allows the development of a microscale flow model and avoids the need to parameterize the closure relations as is done in the traditional volume averaging procedure. Both the REV and RUC are an abstraction of a real porous medium. The flow model used in the RUC is based on a Poiseuille assumption and simplifies the description of the flow. It uses a resistance factor and a scaling proposed by Weislogel and Lichter (1998). Although the geometric specification of the RUC is relative simple, apparently the wedge like corner geometry captures the most important geometry and topology related aspects of a real porous medium (sand). With this, unsaturated flow can be modeled, needing only the porosity and the air entry value as porous medium parameters. The microscopic geometric parameters a, b and j influence the flow dynamics and there is no direct way to determine them a priori. They could be used as tuning parameters, together with the constant resistance factor F_v. As shown in chapter 6, the exact choice of a, b and j influences the flow dynamics, but the total outflow predicted is relative insensitive to their precise value.

7.1.4 Constitutive relations

In the Buckingham-Darcy (BD) equation two constitutive relations are needed to describe the relations between relative hydraulic conductivity and liquid saturation $k_r(S)$ or volume average pressure $k_r(\langle p_l \rangle^l)$, and volume average pressure and saturation $S(\langle p_l \rangle^l)$. Equations (5.45) or (6.8) have no direct analog to $k_r(S)$ or $k_r(\langle p_l \rangle^l)$. In effect during the averaging of the pressure term the two-dimensional Young-Laplace equation (eq. 4.23) served as a constitutive relation. Together with the averaging of the viscous term an analog to the $k_r(\langle p_l \rangle^l)$ relation was proposed in chapter 6 (eq. 6.15). The use of the two-dimensional Young-Laplace equation is a simplification. The constitutive relation $S(\langle p_l \rangle^l)$ was implicitly accounted for through the use of the Young-Laplace equation for liquid area in a corner. This proposed relation is only valid for unsaturated flow, and the switching to saturated flow is discontinuous. When solving the BD equation together with the volume averaged mass balance a related difficulty arises. In this case the constitutive relation $S(\langle p_l \rangle^l)$ needs to be inverted to $\langle p_l \rangle^l(S)$. This relation is not unique for $S = 1$, and difficulties arise in determining exactly the location of the saturated-unsaturated interface in a porous medium. The relation between liquid saturation and the boundary pressures (eq. (4.49)) could be seen as a constitutive relation. However it is based on the microscopic flow model of section 4.4.2 and as such a direct result of averaging.

7.2   Recommendations and Possible Extensions

The first recommendation is to test the averaged momentum equations with other data sets. In chapter 6 simulations were done for one experiment, and reasonable agreement between simulations and measured values was obtained. Additional tests could show whether the developed model is capable of simulating unsaturated flow in a wide range of sand-like porous media.

In the averaging process from microscale to macroscale several simplifications were made. A number of these simplifications are addressed here and some new possible extensions are suggested:

1. The relation between corner liquid area $\mathcal{A}_c$ and averaged pressure $p_{0,1}$ is based on the Young-Laplace equation. This simple relation could be replaced by a more realistic parameterization, either based on a relation accounting for more physics through introducing adhesive forces and surface roughness, or a more realistic pore geometry. This extension is relatively easy to implement in the current flow model, because it would modify only the pressure term and the microscale flow model.

2. At low saturations, vapor diffusion plays an important role in the movement of the liquid phase through evaporation and condensation. In order to take this effect into account, an equation for the movement of the liquid vapor should be introduced and coupled to the momentum and mass balance equations. This extension implies that the averaging needs to be redone, as no transport across the gas-liquid interface was assumed. Additionally momentum and mass balance equations would arise for the vapor and gas phase, making the total transport model much more complicated.

3. The Representative Unit Cell (RUC) model is an abstraction of reality. It appears that the RUC model covers the most important geometry related aspects of a simple porous medium (sand). Extensions could include taking into account channel curvature in the flow model. A non-planar corner geometry could improve the modeling of the corner liquid area and pressure relation. In principle the RUC model could be extended much more and made more complicated. But this would contradict the goal of the RUC model in using it as a simple model for a porous medium.

4. Through the volume averaging procedure, dynamic terms were introduced in the mass and momentum balance equations. All spatial vari-

ables are spatially averaged, but the time dependent terms depend on a "microscopic"time scale. Temporal averaging of the equations could result in an improved modeling of the dynamic terms and a temporal scale better fitting the spatial scale (Ishii, 1975). This process of combining temporal and spatial averaging gives rise to new closure problems and raises the issue of the commutativity of the two different averaging processes (Pedras and de Lemos, 2000). An extension in this direction would involve substantial theoretical work.

5. It would be interesting to directly compare the RUC model to pore network modeling simulations. Moreover, the corner flow model developed in chapter 4 could be used in advanced pore network models with angular pores for a more realistic porous medium representation than the circular tube models commonly employed in pore network modeling.

7.3 Conclusions

– Through the use of volume averaging and direct integration macroscopic momentum and mass balance equations were derived from the microscopic momentum and mass balance equations. As a result a novel form of the macroscopic pressure term is proposed.

– The apparent driving force for liquid flow in unsaturated porous media is $\frac{1}{p_1} - \frac{1}{p_0}$. This is a result of the nonlinear coupling between capillary forces and liquid pressure gradient.

– A geometric representation of a porous medium (sand) called a Representative Unit Cell model was developed and used in the closure problem generated by the volume averaging. The simple RUC model appears to be capable of modeling the important characteristics of a porous medium for unsaturated flow.

– In this work two dynamic terms were derived by simplifications of the flow dynamics in an RUC. They remain to be tested quantitatively and still have considerable uncertainty concerning their exact form and/or magnitude.

– Comparison of the newly proposed equations with the Buckingham-Darcy equation shows that, using reasonable assumptions, the newly

proposed equations can be written in a form similar to the Buckingham-Darcy equation. However the newly proposed equations are nonlocal and have an apparent nonlinear driving force.

– A numerical solution of the newly proposed equations was compared to an outflow experiment and satisfactory agreement between experiment and calculations was observed.

A   Traditional Form of the Volume Averaged Pressure Term

In this appendix the traditional form of the volume averaged pressure term (Whitaker, 1986a,b; Ma and Ruth, 1993) is presented. As stated in chapters 3 and 5, the liquid pressure is averaged over the liquid phase only, as the macroscopic pressure measurement is an intrinsic liquid phase measurement. The derivation of Ma and Ruth (1993) is followed, adjusted for the two-phase case:

$$\langle \nabla p_l \rangle^l \;\; = \;\; \frac{1}{\mathcal{V}_l} \int\limits_{\mathcal{V}_l} \nabla p_l d\mathcal{V} \tag{A.1}$$

$$= \;\; \nabla \langle p_l \rangle^l + \frac{1}{\mathcal{V}_l} \int\limits_{\mathcal{S}_{slg}} \nu \, \dot{p}_l \, d\mathcal{S} \tag{A.2}$$

$$= \;\; \nabla \langle p_l \rangle^l + \frac{1}{\epsilon n_l \mathcal{V}_0} \int\limits_{\mathcal{S}_{slg}} \nu p_l \, d\mathcal{S} + \frac{\langle p_l \rangle^l}{\epsilon n_l} \nabla(\epsilon n_l) \tag{A.3}$$

whereby the integral containing $\dot{p}_l$ was rewritten using equation 2.2 in Ma and Ruth (1993). The integral term in the above equation is normally assumed to be small and dropped:

$$= \;\; \nabla \langle p_l \rangle^l + \frac{\langle p_l \rangle^l}{\epsilon n_l} \nabla(\epsilon n_l) \tag{A.4}$$

The last term in the above equation is a Brinkman (1949, 1947) like term, and required to be small in order to satisfy the volume averaging length scale constraints. It is proportional to $\langle p_l \rangle^l$, and this requires an absolute definition of pressure. A relative definition of liquid pressure, as adopted in chapter 2 of this dissertation is not possible. If this was done, it would depend on

the chosen pressure reference level. Dropping the term and using the volume averaging rule ([Crapiste et al., 1986](#)) $\langle \mathbf{\Psi} \rangle = \epsilon n_l \langle \mathbf{\Psi} \rangle^i$:

$$\langle \nabla p_l \rangle \quad = \quad \epsilon n_l \nabla \langle p_l \rangle^l \tag{A.5}$$

Equation ([A.5](#)) is used in most volume averaging descriptions of unsaturated flow.

Summary

This dissertation describes modeling of unsaturated flow in porous media. The fluid phases considered are a wetting liquid and a gas. In practice one can think of a sandy soil, partially saturated with water, partially with air.

Starting from the description of fluid flow through individual pores, an equation for flow of a liquid in a porous medium in the presence of a gas is derived. This flow is directly influenced by phase interfaces, e.g. solid-liquid or gas-liquid. By explicitly including these pore scale phenomena in a continuum description of fluid transport in porous media, a consistent theoretical description of fluid flow on the macroscale is obtained.

Chapter 2 provides an overview and gives a historical perspective of the study of flow in porous media. Single-phase and two-phase flow at the pore scale are described, basic equations introduced, and concepts of the different flow mechanisms explained. Thereafter different methods for upscaling to a continuum description of flow in porous media are introduced and the basics of volume averaging explained.

Chapter 3 describes the development of upscaled unsaturated flow equations in porous media. The main assumptions are listed and the starting equations on the pore scale and the boundary and initial conditions are stated. These equations are volume averaged and the closure problem is developed. The approach taken here is based on the closure scheme developed by du Plessis and Masliyah (1988), augmented with additional boundary conditions which are introduced due to fluid-fluid interfaces.

Chapter 4 describes the development of a Representative Unit Cell (RUC) model for the closure of the volume averaged equations derived in chapter 3.

In chapter 5 the volume averaged equations derived in chapter 3 are combined with the results from chapter 4. The closure problem in these equations is solved and microscopic quantities are replaced by macroscopic quantities. Boundary and initial conditions are stated and the equations are formulated to be compatible with these conditions.

Chapter 6 analyzes and compares the equations derived in chapter 5 with the

traditional Buckingham-Darcy (BD) type equations and the dynamic capillary pressure model used by Hassanizadeh et al. (2002). Furthermore a numerical comparison is made with an experiment by Stauffer (1977).

In chapter 7 a discussion of the upscaled equations is given. Together with the comparison in chapter 6, strengths and weaknesses of the above equations are discussed. First the general properties and the averaged pressure term are discussed, followed by a discussion of the dynamic terms. Then the drawbacks are explained and recommendations for possible extensions are given.

The main recommendations are: a) To test the averaged momentum equations with other data sets; b) To improve the relation between corner liquid area and averaged pressure; c) To include vapor diffusion at low saturations; d) To improve the Representative Unit Cell (RUC) model; e) To include temporal averaging in the upscaling procedure; f) To directly compare the RUC model to pore network modeling simulations.

The main results are: a) Macroscopic momentum and mass balance equations were derived from the microscopic momentum and mass balance equations; b) The apparent driving force for liquid flow in unsaturated porous media is $\frac{1}{p_1} - \frac{1}{p_0}$. This is a result of the nonlinear coupling between capillary forces and liquid pressure gradient; c) A geometric representation of a porous medium (sand) called a Representative Unit Cell model was developed and used in the closure problem generated by the volume averaging. The simple RUC model appears to be capable of modeling the important characteristics of a porous medium for unsaturated flow; d) Two dynamic terms were derived by simplifications of the flow dynamics in an RUC. They remain to be tested quantitatively; e) Comparison of the newly proposed equations with the Buckingham-Darcy equation shows that, using reasonable assumptions, the newly proposed equations can be written in a form similar to the Buckingham-Darcy equation. However the newly proposed equations are nonlocal and have an apparent nonlinear driving force; f) Comparison of the newly proposed equations to an outflow experiment shows satisfactory agreement between experiment and calculations.

Samenvatting

Dit proefschrift beschrijft het modelleren van onverzadigde stroming in poreuze media. De beschreven vloeistoffen zijn een benattende vloeistof en een gas. In de praktijk kan men denken aan zand, gedeeltelijk verzadigd met water, gedeeltelijk verzadigd met lucht.

Uitgaande van de beschrijving van vloeistofstroming door individuele poriën, wordt een vergelijking voor de stroming van een vloeistof in de aanwezigheid van een gas afgeleid. Deze stroming wordt mede bepaald door grensvlakken, bijvoorbeeld vast-vloeibaar of gas-vloeibaar. Door expliciet deze poriëschaal verschijnselen in een continuüm beschrijving van vloeistof stroming door poreuze media mee te nemen, wordt een consistente theoretische beschrijving op de macroschaal verkregen.

Hoofdstuk 2 geeft een overzicht en een korte geschiedenis van het onderzoek naar stroming in poreuze media. Een- en twee-fase stroming op poriëschaal wordt beschreven, de basis vergelijkingen worden geïntroduceerd, en de concepten van de verschillende stromingsmechanismen worden verklaard. Daarna worden verschillende methodes voor het opschalen naar een continuüm beschrijving van vloeistof stroming in poreuze media beschreven evenals de basismethode van volume middeling.

Hoofdstuk 3 beschrijft de ontwikkeling van nieuwe opgeschaalde onverzadigde stromingsvergelijkingen in poreuze media. De hoofdaannames worden beschreven en de initiële en randvoorwaarden worden vastgesteld. Deze nieuwe vergelijkingen worden volume gemiddeld en het sluitingsprobleem wordt ontwikkeld. De benadering die hier gekozen is, is gebaseerd op het sluitingsschema zoals ontwikkeld door du Plessis and Masliyah (1988), aangevuld met additionele randvoorwaarden door de aanwezigheid van vloeistof-vloeistof grensvlakken.

Hoofdstuk 4 beschrijft de ontwikkeling van een "Representative Unit Cell (RUC)" model voor de sluiting van de volume gemiddelde vergelijkingen, afgeleid in hoofdstuk 3.

In hoofdstuk 5 worden de volume gemiddelde vergelijkingen van hoofdstuk 3 samengevoegd met de resultaten van hoofdstuk 4. Het sluitingsprobleem

in deze vergelijkingen wordt opgelost en microscopische grootheden worden vervangen door macroscopische grootheden. Rand- en initiële voorwaarden worden opgesteld, en de vergelijkingen worden compatibel met deze geformuleerd.

Hoofdstuk 6 analyseert en vergelijkt de vergelijkingen afgeleid in hoofdstuk 5 met de traditionele Buckingham-Darcy (BD) type vergelijkingen en het dynamische capillaire druk model zoals gebruikt door Hassanizadeh et al. (2002). Verder wordt een numerieke oplossing van de vergelijkingen vergeleken met een experiment van Stauffer (1977).

In hoofdstuk 7 wordt een discussie van de opgeschaalde vergelijkingen gegeven. Samen met de uitkomsten van hoofdstuk 6, worden sterkte en zwakte punten van de bovengenoemde vergelijkingen besproken. Eerst worden de algemene eigenschappen en de gemiddelde drukterm besproken, gevolgd door een discussie van de dynamische termen. Daarna worden mogelijke nadelen verklaard en aanbevelingen voor mogelijke uitbreidingen gegeven.

De belangrijkste aanbevelingen zijn: a) Het testen van de gemiddelde momentum vergelijkingen met andere data sets; b) Het verbeteren van de relatie tussen corner liquid area en gemiddelde druk; c) Het meenemen van waterdamp diffusie bij lage verzadigingen; d) Het verbeteren van het "Representative Unit Cell" (RUC) model; e) Het toevoegen van tijdmiddeling in de opschalings-procedure; f) Het direct vergelijken van het RUC model met porië netwerk modellen.

De belangrijkste resultaten zijn: a) Macroscopische momentum en massa balans vergelijkingen zijn afgeleid van microscopische momentum en massa balans vergelijkingen; b) De schijnbaar veroorzakende kracht for vloeistof stroming in onverzadigde poreuze media is $\frac{1}{p_1} - \frac{1}{p_0}$. Dit is het gevolg van de niet-lineaire koppeling tussen capilaire krachten en de drukgradient in de vloeistof; c) Een geometrische representatie van een poreus medium (zand), genoemd "Representative Unit Cell" model is ontwikkeld en gebruikt in het sluitingsprobleem bij de volume middeling. Het eenvoudige RUC model lijkt goed in staat de belangrijke eigenschappen van een poreus medium voor onverzadigde stroming te modelleren; d) Twee dynamische termen zijn afgeleid door vereenvoudigingen van de stromingsdynamica in een RUC. Deze moeten nog kwantitatief getest worden; e) Een vergelijking van de nieuw voorgestelde vergelijkingen met de Buckingham-Darcy vergelijking laat zien, dat gebruik makende van redelijke aannames, de nieuw voorgestelde vergelijkingen in een vorm kunnen worden geschreven, die lijkt op de Buckingham-Darcy vergelijking. Echter, de nieuw voorgestelde vergelijkingen zijn niet lokaal en hebben een schijnbaar niet lineaire veroorzakende kracht; f) Vergelijking van de nieuw voorgestelde vergelijkingen met een uitstroom experiment laat redelijke overeenkomst tussen

experiment en berekeningen zien.

Bibliography

Adler, P. M. and Brenner, H., 1988. Multiphase flow in porous media. *Ann. Rev. Fluid Mech.*, 20:35 – 59.

Alemán, M. A., Ramamohan, T. R., and Slattery, J. C., 1989. The difference between stedy-state and unsteady-state relative permeabilities. *Transport in Porous Media*, 4(5):449 – 493.

Anderson, T. B. and Jackson, R., 1967. A fluid mechanical description of fluidized beds. *Ind. & Eng. Chem. Fund.*, 6(4):527 – 539.

Ayyaswamy, P. S., Catton, I., and Edwards, D. K., 1974. Capillary flow in triangular grooves. *Trans. ASME, Journal of Applied Mechanics*, pp. 332 – 336.

Bachmann, J., Horton, R., Grant, S. A., and van der Ploeg, R. R., 2002. Temperature dependence of water retention curves for wettable and water-repellent soils. *Soil Sci. Soc. Amer. J.*, 66(1):44 – 52.

Bear, J., 1988. *Dynamics of Fluids in Porous Media*. Dover, Mineola, N.Y. ISBN 0-486-65675-6.

Bear, J. and Bachmat, Y., 1990. *Introduction to Modelling of Transport Phenomena in Porous Media*, volume 4 of *Theory and Applications of Transport in Porous Media series*. Kluwer Academic Publishers, Dordrecht, The Netherlands. ISBN 0-7923-0557-4.

Bear, J. and Bensabat, J., 1989. Advective fluxes in multiphase porous media under nonisothermal conditions. *Transport in Porous Media*, 4(5):423 – 448.

Bear, J. and Nitao, J. J., 1993. Infiltration and contaminant transport in the vadose zone (nonisothermal); part 1: Conceptual and mathematical models. Technical Report UCRL-JC-111742 pt 1 PREPRINT, Lawrence Livermore National Laboratory, USA. This paper was prepared for submittal to Water Resources Research, but never appeared.

Bird, R. B., Stewart, W. E., and Lightfoot, E. N., 1960. *Transport Phenomena*. Wiley, New York.

Bisperink, C. G. J., 1997. *The Influence of Spreading Particles on the Stability of Thin Liquid Films*. Ph.D. thesis, Wageningen Agricultural University, Wageningen, The Netherlands.

Blake, T. R. and Garg, S. K., 1976. On the species transport equation for flow in porous media. *Water Resources Research*, 12(4):748 – 750.

Borhan, A. and Rungta, K. K., 1993. Lucas-Washburn kinetics for capillary penetration between periodically corrugated plates. *J. of Colloid and Interface Science*, 155(2):438 – 443.

Bousquet-Melou, P., Goyeau, B., Quintard, M., Fichot, F., and Gobin, D., 2002. Average momentum equation for interdendritic flow in a solidifying columnar mushy zone. *Int. J. of Heat and Mass Transfer*, 45(17):3651 – 3665.

Bowen, R. M., 1984. Porous media model formulations by the theory of mixtures. In J. Bear and M. Y. Corapcioglu, editors, *Fundamentals of Transport Phenomena in Porous Media*, volume 82 of *NATO Advanced Study Institutes series*, pp. 63 – 119. Martinus Nijhoff Publishers, Dordrecht, The Netherlands. ISBN 90-247-2982-3.

Brinkman, H. C., 1947. A calculation of the viscous force exerted by a flowing fluid on a dense swarm of particles. *Appl. Sci. Res.*, A 1:27 – 34.

Brinkman, H. C., 1949. Problems of fluid flow through swarms of particles and through macromolecules in solution. *Research (London)*, 2:190 – 194.

Brodkey, R. S. and Hershey, H. S., 1988. *Transport Phenomena - A Unified Approach*. McGraw-Hill Chemical Engineering Series. McGraw-Hill, New York. ISBN 0-07-100152-2.

Buckingham, E., 1907. Studies on the movement of soil moisture. Bulletin 38, U. S. Department of Agriculture – Bureau of Soils, Washington.

Buckley, S. E. and Leverett, M. C., 1942. Mechanism of fluid displacement in sands. *Trans. American Institute of Mining Engineers*, 146:107 – 116.

Carman, P. C., 1956. *Flow of Gases Through Porous Media*. Butterworths, London.

Chen, K. P., Saric, W., and Stone, H., 2000. On the deviatoric normal stress on a slip surface. *Physics of Fluids*, 12(12):3280 – 3281.

Corey, A. T., 1994. *Mechanics of Inmiscible Fluids in Porous Media*. Water Resources Publications, Fort Collins, Colorado, third edition. ISBN 0-918334-83-7. Revised edition of: Mechanics of Heterogeneous Fluids in Porous Media.

Crapiste, G. H., Rotstein, E., and Whitaker, S., 1986. A general closure scheme for the method of volume averaging. *Chemical Engineering Science*, 41(2):227 – 235.

Cushman, J. H., editor, 1990a. *Dynamics of Fluids in Hierarchical Porous Media*. Academic Press, London. ISBN 0-12-200260-1.

Cushman, J. H., 1990b. An introduction to hierarchical porous media. In J. H. Cushman, editor, *Dynamics of Fluids in Hierarchical Porous Media*, chapter I, pp. 1 – 6. Academic Press, London. ISBN 0-12-200260-1.

Dahle, H. K., Celia, M. A., Hassanizadeh, S. M., and Hvistendahl Karlsen, K., 2002. A total pressure-saturation formulation of two-phase flow incorporating dynamic effects in the capillary-pressure-saturation relationship. In S. M. Hassanizadeh, R. J. Schotting, W. G. Gray, and G. F. Pinder, editors, *Computational Methods in Water Resources, Volume 2*, number 47 in Developments in Water Science, pp. 1067 – 1074. Elsevier, Amsterdam.

Darcy, H., 1856. *Les Fontaines Publiques de la Ville de Dijon*. Victor Dalmont, Paris.

de Gennes, P. G., 1985. Wetting: Statics and dynamics. *Reviews of Modern Physics*, 57(3):827 – 863.

Diedericks, G. P. J., 1999. *Pore-Scale Modelling of Transport Phenomena in Homogeneous Porous Media*. Ph.D. thesis, University of Stellenbosch, Stellenbosch, South Africa.

Diedericks, G. P. J. and du Plessis, J. P., 1997. Modelling of flow through homogeneous foams. *Mathematical Engineering in Industry*, 6(2):133 – 154.

Dong, M. and Chatzis, I., 1995. The imhibition and flow of a wetting liquid along the corners of a square capillary tube. *J. of Colloid and Interface Science*, 172(2):278 – 288.

Dracos, T., 1991. Multiphase flow in porous media. In J. Bear and J.-M. Buchlin, editors, *Modelling and Applications of Transport Phenomena in Porous Media*, volume 5 of *Theory and Applications of Transport in Porous Media*, lecture series presented at the von Karman Institute for Fluid Dynamics, Rhode-Saint-Genèse, Belgium, nov. 30 - dec. 4, 1987 ch. 2, pp. 195 – 220. Kluwer, Dordrecht. ISBN 0-7923-1443-3.

Drew, D. A., 1983. Mathematical modeling of two phase flow. *Ann. Rev. of Fluid Mech.*, 15:261 – 291.

du Plessis, J. P., 1992. High reynolds number flow through granular porous media. In T. F. Russel, R. E. Ewing, C. A. Brebbia, and G. F. Pinder, editors, *Computational Methods in Water Resources IX*, volume 2 Math. Mod. in Water Resources, pp. 180 – 186. Proc. of the ninth Int. Conf. on Comp. Meth. in Water Res., held at the Univ. of Colorado, Denver, USA, June, 1992, Computational Mechanics Publications, Southampton, Boston. ISBN 1-85312-198-3.

du Plessis, J. P., 1994. Analytical quantification of coefficients in the Ergun equation for fluid friction in a packed bed. *Transport in Porous Media*, 16(2):189 – 207.

du Plessis, J. P., editor, 1997. *Fluid Transport in Porous Media*, volume 13 of *Advances in Fluid Mechanics*. Computational Mechanics Publications, Southampton. ISBN 1-85312-429-X.

du Plessis, J. P. and Diedericks, G. P. J., 1997. Pore-scale modelling of interstitial transport phenomena. In P. du Plessis, editor, *Fluid Transport in Porous Media*, volume 13 of *Advances in Fluid Mechanics*, chapter 2, pp. 61 – 104. Computational Mechanics Publications. ISBN 1-85312-429-X.

du Plessis, J. P. and Masliyah, J. H., 1988. Mathematical modelling of flow through consolidated isotropic porous media. *Transport in Porous Media*, 3(2):145 – 161.

du Plessis, J. P. and Masliyah, J. H., 1991. Flow through isotropic granular porous media. *Transport in Porous Media*, 6(3):207 – 221.

du Plessis, J. P. and Roos, L. I., 1994. Predicting the hydrodynamic permeability of sandstone with a pore-scale model. *Journal of Geophysical Research*, 99(B10):19,771 – 19,776.

Dussan V., E. B., 1979. On the spreading of liquids on solid surfaces: Static and dynamic contact lines. *Ann. Rev. Fluid Mech.*, 11:371 – 400.

Ene, H. I., 1990. Application of the homogenization method to transport in porous media. In J. H. Cushman, editor, *Dynamics of Fluids in Hierarchical Porous Media*, chapter VIII, pp. 223 – 241. Academic Press, London. ISBN 0-12-200260-1.

Erickson, D., Li, D., and Park, C. B., 2002. Numerical simulation of capillary-driven flows in nonuniform cross-sectional capillaries. *J. of Colloid and Interface Science*, 250(2):422 – 430.

Fourie, J. G., 2000. *The Mathematical Modelling of Heat Transfer and Fluid Flow in Cellular Metallic Foams*. Ph.D. thesis, University of Stellenbosch, Stellenbosch, South Africa.

Fuentes, C., Haverkamp, R., and Parlange, J.-Y., 1992. Parameter constraints on closed-form soilwater relationships. *J. of Hydrology*, 134(1 - 4):117 – 142.

Goyeau, B., Benihaddadene, T., Gobin, D., and Quintard, M., 1997. Averaged momentum equation for flow through a nonhomogenenous *(sic)* structure. *Transport in Porous Media*, 28(1):19 – 50.

Grant, S. A. and Salehzadeh, A., 1996. Calculation of temperature effects on wetting coefficients of porous solids and their capillary pressure functions. *Water Resources Research*, 32(2):261 – 270.

Gray, W. G., 1975. A derivation of the equations for multi-phase transport. *Chem. Eng. Sci.*, 30(3):229 – 233.

Gray, W. G. and Hassanizadeh, S. M., 1991a. Paradoxes and realities in unsaturated flow theory. *Water Resources Research*, 27(8):1847 – 1854.

Gray, W. G. and Hassanizadeh, S. M., 1991b. Unsaturated flow theory including interfacial phenomena. *Water Resources Research*, 27(8):1855 – 1863.

Gray, W. G. and Lee, P. C. Y., 1977. On the theorems for local volume averaging of multiphase systems. *Int. J. Multiphase Flow*, 3:333 – 340.

Gray, W. G., Leijnse, A., Kolar, R. L., and Blain, C. A., 1993. *Mathematical Tools for Changing Spatial Scales in the Analysis of Physical Systems*. CRC Press, Boca Raton. ISBN 0-8493-8934-8.

Hager, J. and Whitaker, S., 2000. Vapor-liquid jump conditions within a porous medium: Results for mass and energy. *Transport in Porous Media*, 40(1):73 – 111.

Hager, J. and Whitaker, S., 2002a. Reply to the comment by S. J. Kowalski. *Transport in Porous Media*, 46(1):103 – 105.

Hager, J. and Whitaker, S., 2002b. The thermodynamic significance of the local volume averaged temperature. *Transport in Porous Media*, 46(1):19 – 35.

Haines, W. B., 1927. Studies in the physical properties of soils – iv a further contribution to the theory of capillary phenomena in soil. *J. of Agricultural Science*, 17:264 – 290.

Hassanizadeh, M. and Gray, W. G., 1979a. General conservation equations for multiphase systems: 1. averaging procedure. *Advances in Water Resources*, 2(3):131 – 144.

Hassanizadeh, M. and Gray, W. G., 1979b. General conservation equations for multiphase systems: 2. mass, momenta, energy, and entropy equations. *Advances in Water Resources*, 2(4):191 – 203.

Hassanizadeh, M. and Gray, W. G., 1980. General conservation equations for multiphase systems: 3. constitutive theory for porous media flow. *Advances in Water Resources*, 3(1):25 – 40.

Hassanizadeh, S. M., Celia, M. A., and Dahle, H. K., 2002. Dynamic effect in the capillary pressure-saturation relationship and its impacts on unsaturated flow. *Vadose Zone Journal*, 1(1):38 – 57.

Hassanizadeh, S. M. and Gray, W. G., 1993. Thermodynamic basis of capillary pressure in porous media. *Water Resources Research*, 29(10):3389 – 3405.

Hassanizadeh, S. M. and Gray, W. G., 1997. Recent advances in theories of two-phase flow in porous media. In P. du Plessis, editor, *Fluid Transport in Porous Media*, volume 13 of *Advances in Fluid Mechanics*, chapter 3, pp. 104 – 160. Computational Mechanics Publications. ISBN 1-85312-429-X.

Hassanizadeh, S. M., Miller, C. T., and Parlange, M. B., editors, 2001. *Advances in Water Resources – Special Issue Pore Scale Modeling*, volume 24. Elsevier.

Helmig, R., 1997. *Multiphase Flow and Transport Processes in the Subsurface – a Contribution to the Modeling of Hydrosystems.* Springer, Berlin. ISBN 3-540-62703-0.

Hilfer, R., 1996. Transport and Relaxation Phenomena in Porous Media. *Advances in Chemical Physics*, 92:299 – 424.

Hilfer, R. and Øren, P. E., 1996. Dimensional Analysis of Pore Scale and Field Scale Immiscible Displacement. *Transport in Porous Media*, 22(1):53 – 72.

Hoffmann, M. R., 2000a. Fast real space renormalization for two-phase porous media flow. In J. M. Crolet, editor, *Computational Methods for Flow and Transport in Porous Media*, volume 17 of *Theory and Applications of Transport in Porous Media*, pp. 83 – 91. Kluwer, Dordrecht. ISBN 0-7923-6263-2.

Hoffmann, M. R., 2000b. Volume averaged equations for two-phase flow in porous media. In L. R. Bently, J. F. Sykes, C. A. Brebbia, and C. F. Pinder, editors, *Computational Methods in Water Resources XII*, volume 1, pp. 225 – 230. Balkema, Dordrecht. ISBN 90-5809-125-4.

Hornung, U., editor, 1997. *Homogenization and Porous Media*, volume 6 of *Interdisciplinary Applied Mathematics*. Springer Verlag. ISBN 0-387-94786-8.

Hsu, C. T. and Cheng, P., 1988. Closure schemes of the macroscopic energy equation for convective heat transfer in porous media. *Int. Comm. Heat Mass Transfer*, 15:689 – 703.

Hubbert, M. K., 1956. Darcy law and the field equations for the flow of underground fluids. *Trans. Am. Inst. Metal. Eng.*, 207:222 – 239.

Ishii, M., 1975. *Thermo-Fluid Dynamic Theory of Two-Phase Flow.* Eyrolles, Paris.

Kaviany, M., 1995. *Principles of Heat Transfer in Porous Media.* Mechanical Engineering Series. Springer, New York, second edition. ISBN 0-387-94550-4.

Knackstedt, M. A. and du Plessis, J. P., 1996. Simple Permeability Model for Natural Granular Media. *Geophysical Research Letters*, 23(13):1609 – 1612.

Koorevaar, P., Menelik, G., and Dirksen, C., 1983. *Elements of Soil Physics.* Developments in Soil Science (13). Elsevier, Amsterdam, third edition. ISBN 0-444-42242-0.

Kowalski, S. J., 2000. Comment on 'vapor-liquid jump conditions within a porous medium: Results for mass and energy' by J. Hager and S. Whitaker. *Transport in Porous Media*, 40(1):113.

Kralchevsky, P. A., Eriksson, J. C., and Ljunggren, S., 1994. Theory of curved interfaces and membranes: Mechanical and themodynamical approaches. *Adv. in Colloid and Interface Science*, 48:19 – 59.

Lago, M. and Araujo, M., 2001. Capillary rise in porous media. *J. of Colloid and Interface Science*, 234(1):35 –43.

Leverett, M. C., 1941. Capillary behaviour in porous solids. *Trans. American Institute of Mining Engineers*, 142:152 – 169.

Lopez, J. M. and Hirsa, A., 1998. Direct determination of the dependence of the surface shear and dilatational viscosities on the thermodynamic state of the interface: Theoretical foundations. *J. of Colloid and Interface Science*, 206(1):231 – 239.

Lucas, R., 1918. Ueber das Zeitgesetz des kapillaren Aufstiegs von Flüssigkeiten. *Kolloid-Zeitschrift*, 23(1):15 – 22.

Ma, H. and Ruth, D. W., 1993. The microscopic analysis of high Forchheimer number flow in porous media. *Transport in Porous Media*, 13(2):139 – 160.

Ma, H. B., Peterson, G. P., and Lu, X. J., 1994. The influence of vapour-liquid interactions on the liquid pressure drop in triangular microgrooves. *Int. J. Heat Mass Transfer*, 37(15):2211 – 2219.

MacLaine-Cross, I. L., 1969. An approximate method for calculating heat transfer and pressure drop in ducts with laminar flow. *J. of Heat Transfer (Trans. ASME)*, 91:171 – 173.

Mason, G. and Morrow, N. R., 1991. Capillary behaviour of a Perfectly Wetting Liquid in Irregular Triangular Tubes. *J. of Colloid and Interface Science*, 141(1):262 – 274.

Mayer, F. J., McGrath, J. F., and Steele, J. W., 1983. A class of similarity solutions for the nonlinear thermal conduction problem. *J. Phys. A: Math. Gen.*, 16:3393 – 3400.

Miller, E. E. and Miller, R. D., 1956. Physical Theory for Capillary Flow Phenomena. *Journal of Applied Physics*, 27(4):324 – 332.

Montillet, A., Comiti, J., and Legrand, J., 1992. Determination of structural parameters of metallic foams from permeametry measurements. *J. of Materials Science*, 27:4460 – 4464.

Morrow, N. R., 1970. Physics and thermodynamics of capillary action in porous media. *Industrial and Engineering Chemistry*, 62(6):32 – 56.

Narasimhan, T. N., 1980a. Letters to the editor: On 'general conservation equations for multiphase systems: 1. averaging procedure' by M. Hassanizadeh and W. G. Gray. *Advances in Water Resources*, 3:143 – 144.

Narasimhan, T. N., 1980b. A note on volume averaging. *Advances in Water Resources*, 3:135 – 139.

Nitao, J. J. and Bear, J., 1996. Potentials and their role in transport in porous media. *Water Resources Research*, 32(2):225 – 250.

Nitsche, L. C. and Brenner, H., 1989. Eulerian kinematics of flow through spatially periodic models of porous media. *Arch. Rational Mech. Anal.*, 107:225 – 292.

Panton, R. L., 1984. *Incompressible Flow*. John Wiley & Sons, Inc., New York. ISBN 0-471-89765-5.

Patzek, T. W. and Kristensen, J. G., 2001. Shape factor correlations of hydraulic conductance in noncircular capillaries II. two-phase creeping flow. *J. of Colloid and Interface Science*, 236(2):305 – 317.

Payatakes, A. C., Tien, C., and Turian, R. M., 1973. A new model for granular porous media: Part I. Model formulation. *American Institute of Chemical Engineers Journal*, 19(1):58 – 67.

Pedras, M. H. J. and de Lemos, M. J. S., 2000. On the definition of turbulent kinetic energy for flow in porous media. *Int. Comm. Heat Mass Transfer*, 27(2):211 – 220.

Pellicer, J., Manzanares, J. A., and Mafé, 1995. The physical description of elementary description of elemantary surface phenomena: Thermodynamics versus mechanics. *American J. of Physics*, 63(6):542 – 547.

Pride, S. R. and Flekkøy, E. G., 1999. Two-phase flow through porous media in the fixed-contact-line regime. *Physical Review E*, 60(4):4285 – 4299.

Princen, H. M., 1969a. Capillary phenomena in assemblies of parallel cylinders; I. Capillary rise between two cylinders. *J. of Colloid and Interface Science*, 30(1):69 – 75.

Princen, H. M., 1969b. Capillary phenomena in assemblies of parallel cylinders; II. Capillary rise in systems with more than two cylinders. *J. of Colloid and Interface Science*, 30(3):359 – 371.

Princen, H. M., 1970. Capillary phenomena in assemblies of parallel cylinders; III. Liquid columns between horizontal parallel cylinders. *J. of Colloid and Interface Science*, 34(2):171 – 184.

Probstein, R. F., 1989. *Physicochemical Hydrodynamics: An Introduction*. Butterworths, Stoneham, MA.

Pullan, A. J., 1990. The quasilinear approximation for unsaturated porous media flow. *Water Resources Research*, 26(6):1219 – 1234.

Quintard, M. and Whitaker, S., 1990. Two-Phase Flow in Heterogeneous Porous Media II: Numerical Experiments for Flow Perpendicular to a Stratified System. *Transport in Porous Media*, 5(5):429 – 472.

Quintard, M. and Whitaker, S., 1994. Two-phase flow in heterogeneous porous media V: Geometrical results for two-dimensional systems. *Transport in Porous Media*, 15(2):183 – 196.

Ransohoff, T. C. and Radke, E., 1988. Laminar flow of a wetting liquid along the corners of a predominantly gas-occupied noncircular pore. *Journal of Colloid and Interface Science*, 121(2):392 – 401.

Richards, L. A., 1931. Capillary conduction of liquids through porous medium. *Physics*, 1:318 – 333.

Roberts, A. P. and Knackstedt, M. A., 1996. Structure-property correlations in model composite materials. *Physical Review E*, 54(3):2313 – 2328.

Romero, L. A. and Yost, F. G., 1996. Flow in an open channel capillary. *J. Fluid Mech.*, 322:109 – 129.

Ruan, H. and Illangasekare, T. H., 1999. Estimation of relative hydraulic conductivity based on a sheet flow model. *J. of Hydrology*, 219(1 - 2):83 – 93.

Ruth, D. W. and Ma, H., 1993. Numerical analysis of viscous, incompressible flow in a diverging-converging ruc. *Transport in Porous Media*, 13(2):161 – 177.

Sáez, A. E., Carbonell, R. G., and Levec, J., 1986. The hydrodynamics of trickling flow in packed beds; part I: Conduit models. *American Institute of Chemical Engineers Journal*, 32(3):353 – 368.

Schäffer, E. and Wong, P., 2000. Contact line dynamics near the pinning threshold: A capillary rise and fall experiment. *Physical Review E*, 61(5):5257 – 5277.

Scovazzo, P., Illangasekare, T. H., Hoehn, A., and Todd, P., 2001. Modeling of two-phase flow in membranes and porous media in microgravity as applied to plant irrigation in space. *Water Resources Research*, 37(5):1231 – 1243.

Shah, R. K. and London, A. L., 1978. *Laminar Flow Forced Convection in Ducts – A Source Book for Compact Heat Exchanger Analytical Data*, volume Supplement 1 of *Advances in Heat Transfer*. Academic Press, New York. ISBN 0-12-020051-1.

Sherwood, D., 1971. *Introductory Chemical Thermodynamics*. Longman, London. ISBN 0582 44208 7.

Sisavath, S., Jing, X. D., and Zimmerman, R. W., 2000. Effect of pore shape on the hydraulic conductivity of pores in sedimentary rocks. *Physics and Chemistry of the Earth (A)*, 25(2):163–168.

Sisavath, S., Jing, X. D., and Zimmerman, R. W., 2001. Laminar flow through irregularly-shaped pores in sedimentary rocks. *Transport in Porous Media*, 45(1):41 − 62.

Slattery, J. C., 1967. Flow of viscoelastic fluids through porous media. *AIChE J.*, 13(6):1066 − 1071.

Slattery, J. C., 1969. Single-phase flow through porous media. *AIChE J.*, 15(6):866 − 872.

Smit, G. J. F. and du Plessis, J. P., 2000. Pore-scale modelling of peculiarities of non-newtonian flow in porous media. In *Proceedings of NHTC'00, 34th National Heat Transfer Conference Pittsburgh, Pennsylvania August 20-22, 2000*, pp. 1 − 8. ASME. Published on CDROM.

Staples, T. L. and Shaffer, D. A., 2002. Wicking flow in irregular capillaries. *Colloids and Surfaces A*, 204(1 − 3):239 − 250.

Stauffer, F., 1977. *Einfluss der Kapillaren Zone auf Instationaere Drainagevorgaenge*. Diss. ETH Nr. 5931, Eidgenoessische Technische Hochschule Zuerich, Zuerich, Switzerland.

Stauffer, F., 1978. Time dependence of the relations between capillary pressure, water content and conductivity during drainage of porous media. In *Proceedings of the International IAHR Symposium on Scale Effects in Porous Media, Thessanoliki, Greece, Aug. 27 − Sep. 1, 1978*, pp. 3.35 − 3.52. International Association of Hydraulic Engineering and Research (IAHR), Madrid, Spain.

Suh, J.-S., Greif, R., and Grigoropoulos, C. P., 2001. Friction in micro-channel flows of a liquid and vapor in trapezoidal and sinusoidal grooves. *Int. J. Heat Mass Transfer*, 44(16):3101 − 3109.

Thompson, K. E. and Fogler, H. S., 1997. Modeling flow in disordered packed beds from pore-scale fluid mechanics. *AIChE J.*, 43(6):1377 − 1389.

Tierney, L., 1990. *Lisp-Stat: An Object-Oriented Environment for Statistical Computing and Dynamic Graphics*. John Wiley & Sons, New York. ISBN 0-471-50916-7.

Tosun, I. and Willis, M. S., 1980. Generalized proof of the modified averaging theorem. *Chem. Eng. Sci.*, 35:1462 − 1463.

Tuller, M. and Or, D., 2001. Hydraulic conductivity of variably saturated porous media: Film and corner flow in angular pore space. *Water Resources Research*, 37(5):1257 − 1276.

Tuller, M., Or, D., and Dudley, L. M., 1999. Adsorption and capillary condensation in porous media: Liquid retention and interfacial configurations in angular pores. *Water Resources Research*, 35(7):1949 − 1964.

van Brakel, J., 1975. Pore Space Models for Transport Phenomena in Porous Media. Review and Evaluation with Special Emphasis on Capillary Liquid Transport. *Powder Technology*, 11:205 − 236.

van Genuchten, M. T., 1980. A Closed-form Equation for Predicting the Hydraulic Conductivity of Unsaturated Soils. *Soil Sci. Soc. Amer. J.*, 44:892 − 898.

Verbist, G., Weaire, D., and Kraynik, A. M., 1996. The foam drainage equation. *J. Phys.: Condens. Matter*, 8(21):3715 − 3731.

Wang, C.-Y. and Beckermann, C., 1993. A two-phase mixture model of liquid-gas flow and heat transfer in capillary porous media − I. Formulation. *Int. J. Heat Mass Transfer*, 36(11):2747 − 2758.

Washburn, E. W., 1921. The Dynamics of Capillary Flow. *Physical Review, Second Series*, 17(3):273 – 283.

Weislogel, M. M., 2001. Capillary flow in interior corners: The infinite column. *Physics of Fluids*, 13(11):3101 – 3107.

Weislogel, M. M. and Lichter, S., 1998. Capillary flow in an interior corner. *J. of Fluid Mechanics*, 373:349 – 378.

Whitaker, S., 1966. The equations of motion in porous media. *Chem. Eng. Sci.*, 21:291 – 300.

Whitaker, S., 1967. Diffusion and dispersion in porous media. *AIChE J.*, 13(3):420 – 427.

Whitaker, S., 1969. Advances in theory of fluid motion in porous media. *Ind. & Eng. Chem.*, 61(12):14 – 28.

Whitaker, S., 1977. Simultaneous heat, mass, and momentum transfer in porous media: A theory of drying. *Advances in Heat Transfer*, 13:119 – 203.

Whitaker, S., 1980. Heat and Mass Transfer in Granular Porous Media. In A. S. Mujumdar, editor, *Advances in Drying*, volume 1, chapter 2, pp. 23 – 61. Hemisphere, Washington. ISBN 0-89116-185-6.

Whitaker, S., 1985. A simple geometrical derivation of the spatial averaging theorem. *Chemical Engineering Education*, 19:18 – 52.

Whitaker, S., 1986a. Flow in porous media I: A theoretical derivation of Darcy's law. *Transport in Porous Media*, 1(1):3 – 25.

Whitaker, S., 1986b. Flow in porous media II: The governing equations for immiscible, two-phase flow. *Transport in Porous Media*, 1(2):105 – 125.

Zhou, D., Blunt, M., and Orr, Jr., F. M., 1997. Hydrocarbon drainage along corners of noncircular capillaries. *J. of Colloid and Interface Science*, 187(1):11 – 21.

Nawoord

Met veel plezier heb ik de afgelopen jaren bij Wageningen Universiteit gewerkt. Onderzoek is leuk, en het werken op een universiteit bevalt mij goed. Bij het tot stand komen van dit proefschrift waren veel mensen belangrijk, hetzij door mijn constante vragen te beantwoorden hetzij door organisatorisch te helpen. Ten eerste wil ik Toon Leijnse, mijn promotor, bedanken. Toon, je hebt mij veel geholpen doordat ik altijd met jou kon praten en je altijd begreep waar ik het over had. Ook jouw ervaring als onderzoeker en persoon was waardevol gedurende dit onderzoek.

Verder wil ik Reinder Feddes bedanken voor het mogelijk maken van dit onderzoek. Na mijn terugkeer uit Grenoble heb jij geregeld dat ik dit onderzoek bij de vakgroep kon doen.

Peter Troch, mijn copromotor, heeft mij de mogelijkheid geboden in een aanstelling als onderzoeker, naast mijn officiële werk, verder te werken aan mijn proefschrift.

Tijdens een congres in Frankrijk leerde ik Prieur du Plessis kennen. Hij vertelde een boeiend verhaal over zijn RUC modellen, en direct ontstond er de gedachte een keer op bezoek in Stellenbosch te gaan. Tijdens mijn verblijf in Stellenbosch werd ik gastvrij ontvangen en kon gebruik maken van de faciliteiten van het Departement Toegepaste Wiskunde van de Universiteit van Stellenbosch. Ook de collegas van Prieur: Francois, Hardus, Linda en Maretha, en zijn familie zorgden voor een plezierig verblijf. Prieur, bedankt voor de discussies over 'volume averaging' en de braai.

When I was visiting the University of Notre Dame to meet Toon, Bill Gray and his wife Genny offered a friendly welcome and a home to stay during the visit.

De groep onderzoekers in Delft, waar ik vaak contact mee heb: Majid, Ruud, Marco, Saskia, Cor, Hans, Anke Jannie en Twan, zorgde voor een stroom nieuwe ideeën en kritiek op mijn onderzoek.

En op de vakgroep natuurlijk Annemarie en Henny, die mij bij alle vragen konden helpen. In de bibliotheek hielpen vooral Magda en Lenie bij het vergaren

van literatuur.

Tenslotte waren de collega's van de gang naast de hydraulicahal natuurlijk heel belangrijk: ten eerste Lies en Paul, de paranimfen, die altijd open stonden voor vragen en ideeën; maar ook Annemiek, Ben, Remko, Margje, Rafal, Wubbo, Anton en Jan.

Laura en Kaai hielpen mij het onderzoek te relativeren. Laura, bedankt voor alles wat je hebt gedaan.

    Marc

Curriculum Vitae

Marc Rene Hoffmann was born on October 27th 1967 in Aachen, Germany. In 1989 he started the study "Bodem, Water, Atmosfeer" ("Soil, Water, Atmosphere") at Wageningen Agricultural University (now Wageningen University). He graduated in 1994 with the degree of ir. with distinction. His two main thesis works were in the areas of meteorology and soil physics. After a short period as a consulting engineer, he obtained a scholarship to do research in soil physics at the university "Joseph Fourier" in Grenoble, France. In September 1996 he started the research described in this dissertation at the department of water resources, Wageningen University.

Currently Marc is doing research and supervising students in hydraulics related subjects, including flow in porous media and ecohydraulics, at Wageningen University.